UNI BASEL

SNI SWISS NANOSCIENCE INSTITUTE
EINE INITIATIVE DER UNIVERSITÄT BASEL UND DES KANTONS AARGAU

Molecular and carbon-based electronic systems

Lecture 7: Graphene

structure, fabrication, characterization

Examples: nanogaps, QHE

Vorlesung Uni Basel, FS2017

- graphene structure
- fabrication and CVD growth
- characterization: Raman spectroscopy

Examples

- graphene electroburning for molecular junctions
- Quantum Hall Effect

graphene structure: honeycomb lattice

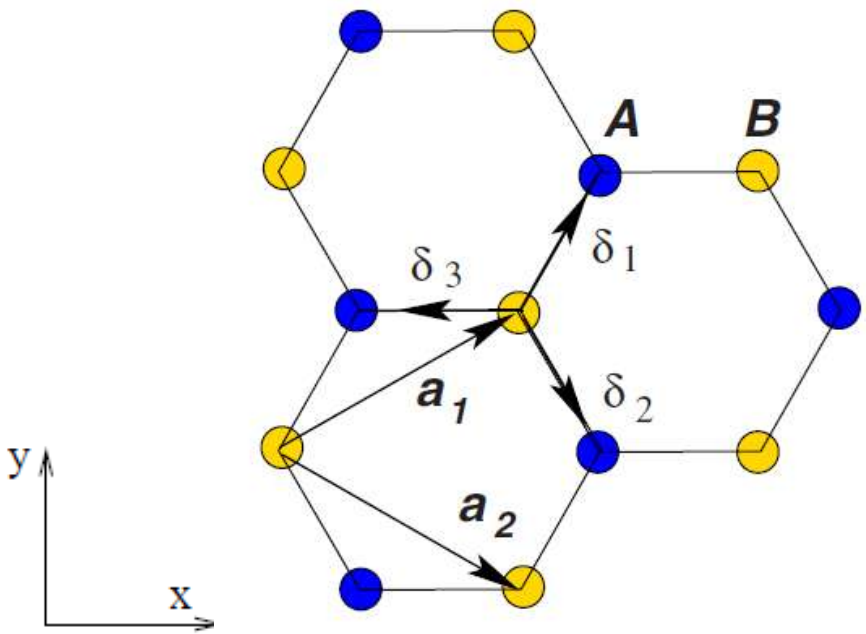

*vectors connecting a site on the **A sublattice** with a nearest neighbor (nn) on the **B sublattice***
C-C bond: a≈ 0.142nm

$$\boldsymbol{\delta}_1 = \frac{a}{2}(1, \sqrt{3}) \quad \boldsymbol{\delta}_2 = \frac{a}{2}(1, -\sqrt{3})$$

$$\delta_3 = -a(1,0)$$

six second nearest neighbors

$$\delta_1' = \pm \boldsymbol{a}_1, \; \delta_2' = \pm \boldsymbol{a}_2, \; \delta_3' = \pm(\boldsymbol{a}_2 - \boldsymbol{a}_1)$$

basis vectors of the triangular Bravais lattice (2 atoms basis)

$$\boldsymbol{a}_1 = \frac{a}{2}(3, \sqrt{3}), \quad \boldsymbol{a}_2 = \frac{a}{2}(3, -\sqrt{3})$$

density of C atoms
A_{uc}= $\sqrt{3}\cdot 3\cdot a/2$ = 0.051nm^2

$$n_C = 2/A_{uc} = 39 \text{ nm}^{-2} = 3.9 \times 10^{15} \text{ cm}^{-2}$$

density of π electrons
1 π e / C atom not involved in σ bond

$$n_\pi = n_C = 3.9 \times 10^{15} \text{ cm}^{-2}$$

Goerbig et al., Castro Neto et al., Rev. Mod. Phys 2009

graphene structure: reciprocal lattice

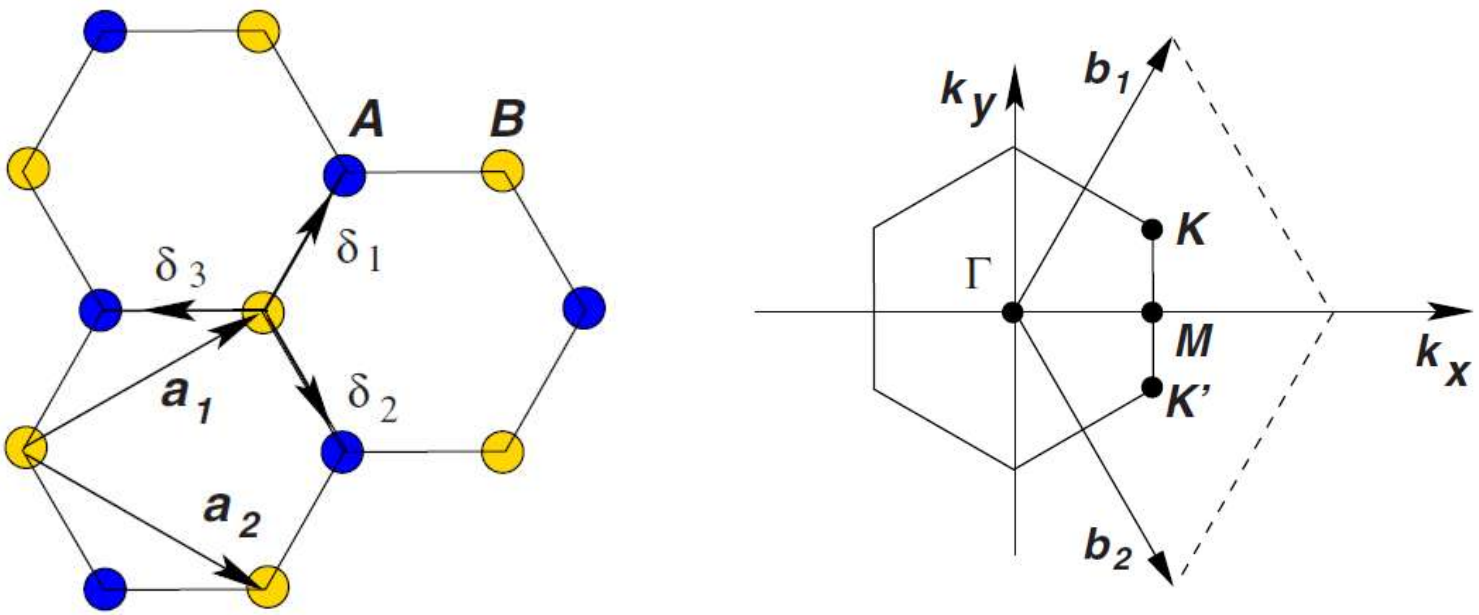

Honeycomb lattice and its corresponding Brillouin zone

reciprocal lattice basis vectors

$$\boldsymbol{b}_1 = \frac{2\pi}{3a}(1, \sqrt{3}) \qquad \boldsymbol{b}_2 = \frac{2\pi}{3a}(1, -\sqrt{3})$$

corners (6) of 1st BZ: K and K' (not equivalent), Dirac points

$$\boldsymbol{K} = \left(\frac{2\pi}{3a}, \frac{2\pi}{3\sqrt{3}a}\right) \qquad \boldsymbol{K}' = \left(\frac{2\pi}{3a}, -\frac{2\pi}{3\sqrt{3}a}\right)$$

⇨ *important points for electronic properties (low-energy excitations)*

Castro Neto et al., Rev. Mod. Phys 2009

graphene electronic structure

Tight-binding Hamiltonian for electrons in graphene

$$H = -t \sum_{\langle i,j\rangle,\sigma} (a^{\dagger}_{\sigma,i} b_{\sigma,j} + \text{H.c.}) - t' \sum_{\langle\langle i,j\rangle\rangle,\sigma} (a^{\dagger}_{\sigma,i} a_{\sigma,j} + b^{\dagger}_{\sigma,i} b_{\sigma,j} + \text{H.c.})$$

$a_{i,\sigma}$ $(a^{\dagger}_{i,\sigma})$ anihilates (creates) an electron with spin σ $(\sigma = \uparrow, \downarrow)$ on site $\mathbf{R_i}$ on sublattice **A**
*similar def. for sublattice **B***

t nearest-neighbor hopping energy, $t \approx 2.8$eV

t' next nearest-neighbor hopping energy, $0.02t < t' < 0.2t$
hopping in the same sublattice

Energy bands (Wallace, 1947)

$$E_{\pm}(\mathbf{k}) = \pm t\sqrt{3 + f(\mathbf{k})} - t' f(\mathbf{k})$$

+ upper band (π *), - lower band (π)

$$f(\mathbf{k}) = 2\cos(\sqrt{3}k_y a) + 4\cos\left(\frac{\sqrt{3}}{2}k_y a\right)\cos\left(\frac{3}{2}k_x a\right)$$

- symmetric spectrum if $t' = 0$
- electron-hole symmetry broken for $t' \neq 0$

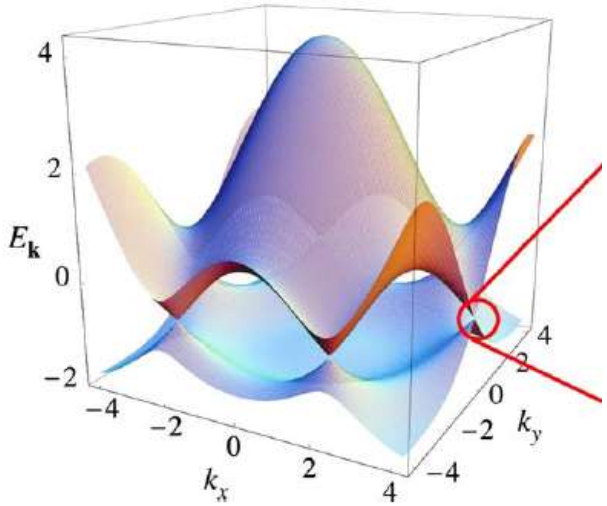

energy spectrum in units of t *for finite values of t and t, with t=2.7 eV and t=−0.2t*

Castro Neto et al., Rev. Mod. Phys 2009

graphene electronic structure

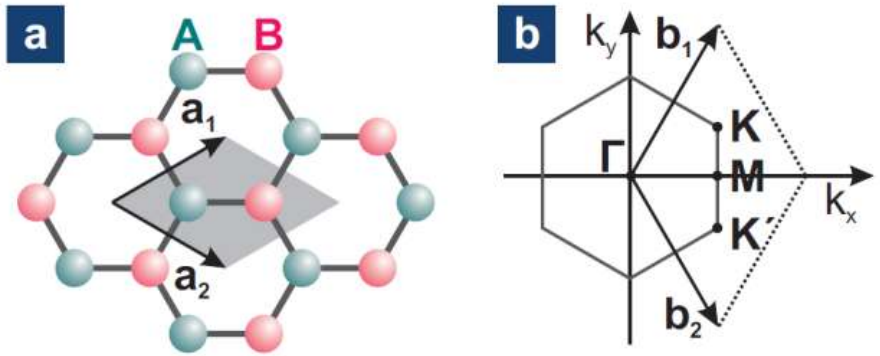

a) graphene honeycomb lattice *with the two triangular sublattices* ***sublattice A,***

b) graphene Brillouin zone *in momentum space*

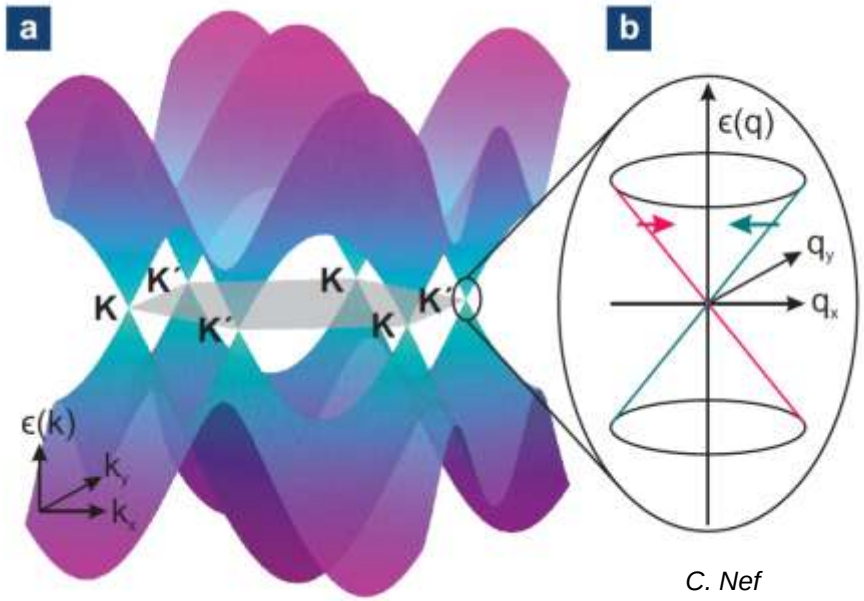

C. Nef

$E_{\pm}(q)$ band structure close to one of the Dirac points (at the K or K' point in the BZ): **linear**

Expand full band structure close to **K** (or **K'**)
k = K + q*, with* **|q|** « **|K|**

$$E_{\pm}(\mathbf{q}) \approx \pm v_F|\mathbf{q}| + O[(q/K)^2]$$

q momentum measured relatively to Dirac point
v_F Fermi velocity, $v_F = 3ta/2 \approx 10^6$ m/s

- Valence band filled, fermi energy at E=0
- Zero band-gap semiconductor
  vanishing DOS metal
- Two non-equivalent 'valleys', K and K', *pseudo-spin*

Castro Neto et al., Rev. Mod. Phys 2009

graphene field-effect device

charge carrier density n

[n] = m^{-2}

$$C = \frac{Q}{V_g} = \frac{\epsilon_0 \epsilon A}{d}$$

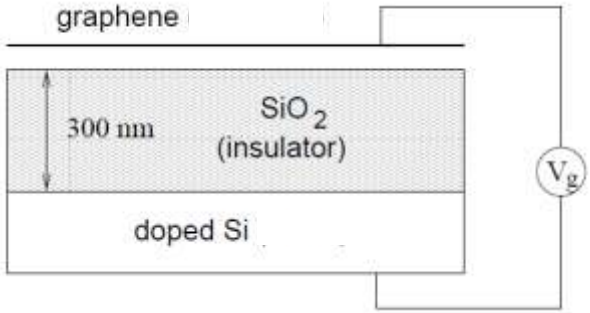

$$n = C_g V_g \frac{1}{e}$$

C_g gate capacitance per surface (F/m^2)

$$n = \alpha V_g \qquad \alpha \approx 7.2 \cdot 10^{10} \frac{cm^{-2}}{V}$$

typ. SiO2 wafer $\epsilon = 3.7$

$d = 300$ nm

field effect mobility

$$\mu_{FET} = \frac{dG}{dV_g} \cdot \frac{L}{W} \cdot \frac{1}{C_g}$$

C_g gate capacitance per surface (F/m^2)

L, W length and width of device

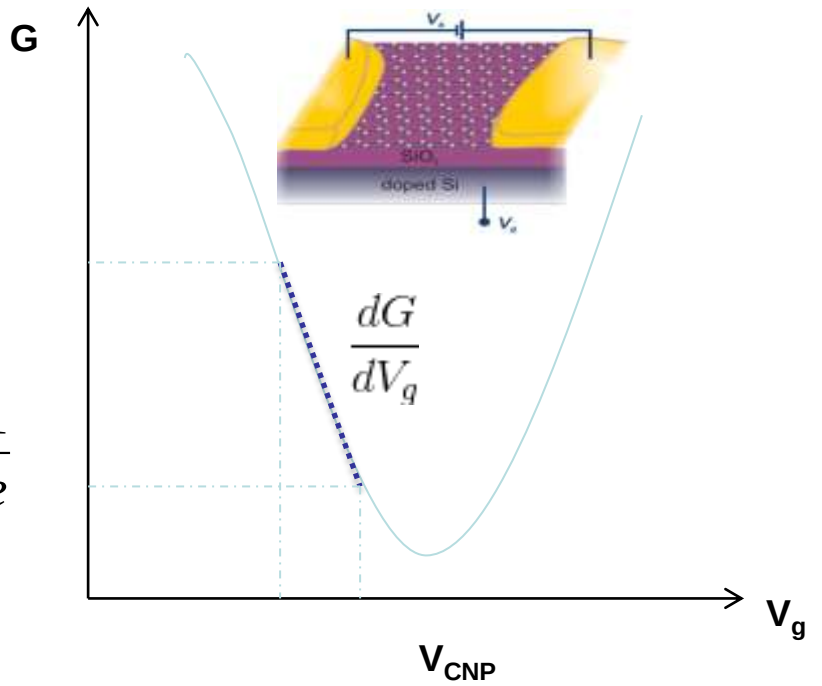

NB

(1) $V_{CNP} \neq 0$ due to residual chemical doping

$$n = C_g \left(V_g - V_{CNP}\right) \frac{1}{e}$$

(2) μ reduction due to trapped charged defects at polar insulators interface (e.g.: SiO2, HfO2, Al2O3)

Other substrates: hBN, Si3N4, *in-situ* oxidized Al

graphene-based devices

⇨ **interconnects** (high-frequency transistors & sensors)

- large current density

  see e.g. Pop et al, Nano Lett 2012 (thermal "stewardship": $j > 10^9$ A/cm^2)
- recrystallization for control

  see e.g. Johnson et al. ACS Nano, 2015
- ballistic transport in nanoribbons, *electron optics*

  see e.g. de Heer et al., Nature 2014 (on SiC, w=40nm, l>10um)

⇨ **contacts for molecular and organic electronics**

- stability (covalent crystal)
- ultimately thin contact electrode (reduced screening)
- *in-situ* junction imaging (STM, HRTEM, LEEPS)
- "soft" top electrode (organic electronics)

  see e.g. Lee et al., Adv. Mat. 2014

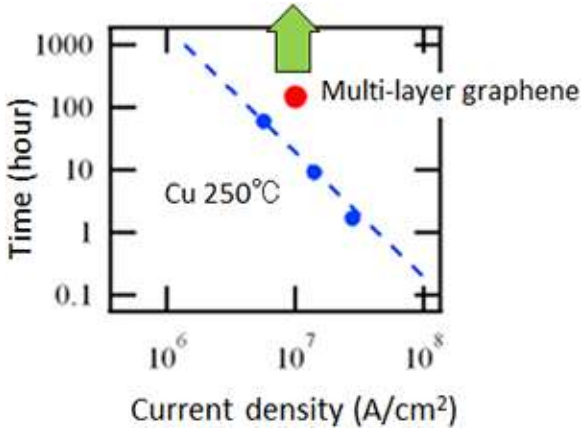

Current density tolerance at 250 ℃.
***Blue**: Cu*
***Red**: MLG, no break after 150h*

Yokoyama et al., 2013, www.aist.go.jp

graphene structure: stacking

Graphite = stacked graphene layers

stacking: distance between layers $d = 2.4a = 0.34$ nm

graphite

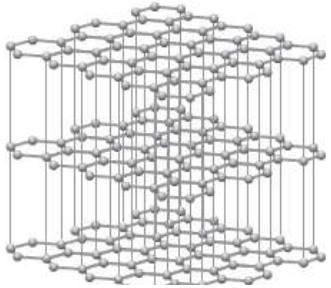

ordered graphite: two different basic stacking orders
turbostratic graphite: disorder in the stacking

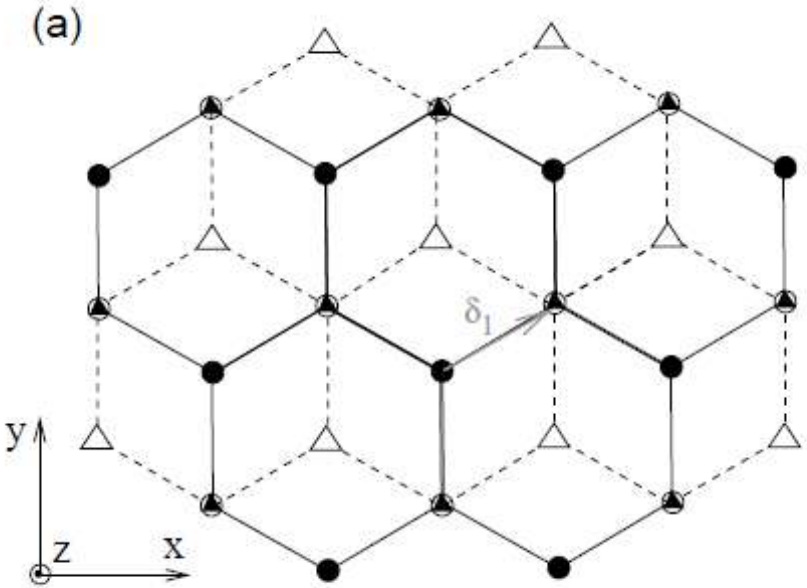

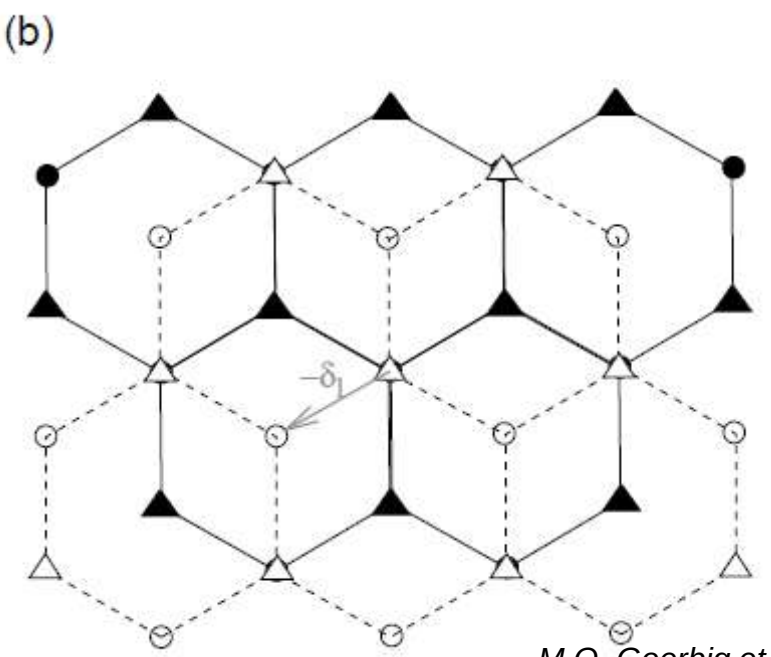

M.O. Goerbig et al.

graphene structure: Moiré

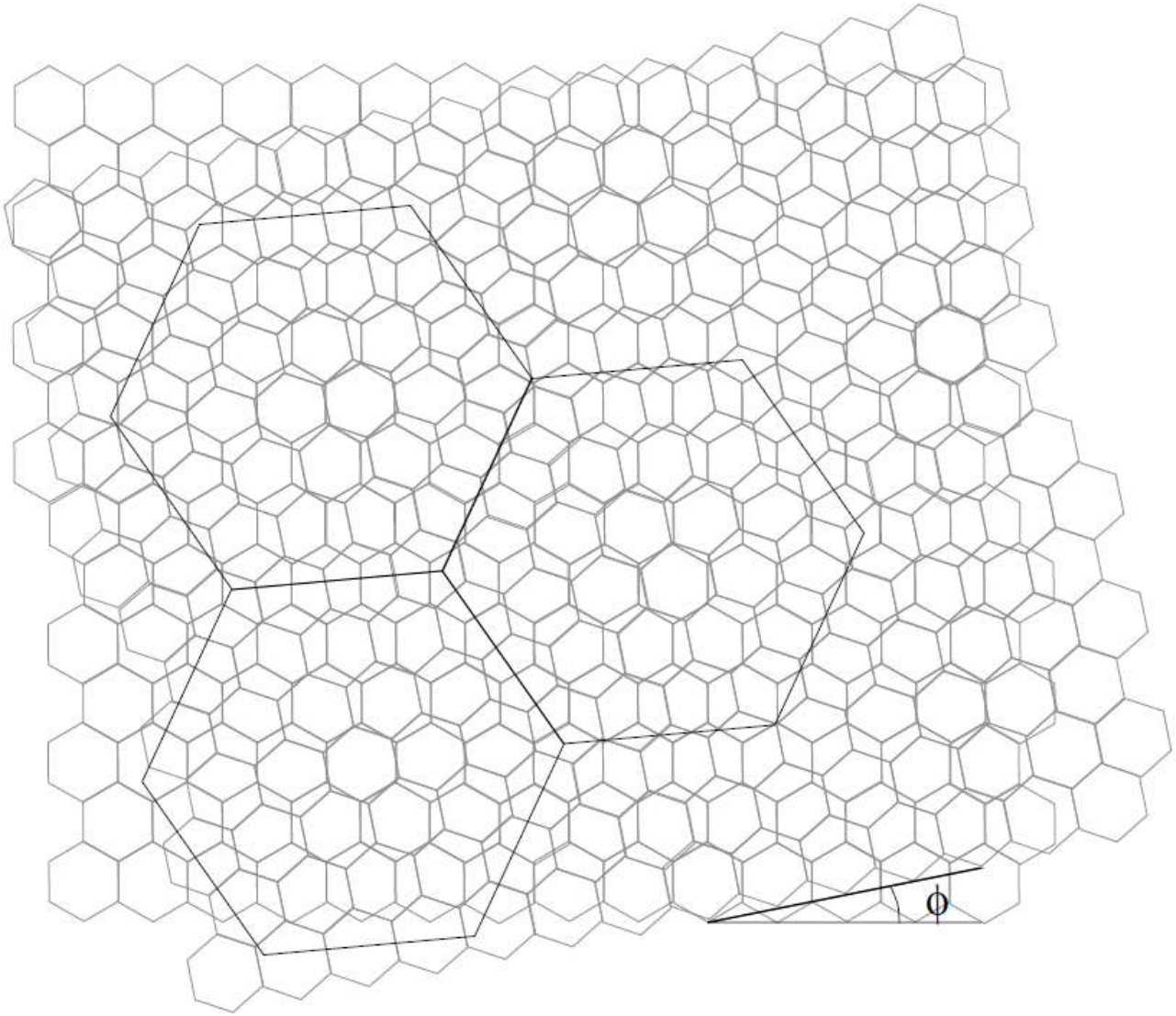

Moiré pattern obtained by stacking two honeycomb lattices (gray) with a relative (chiral) angle φ. One obtains a hexagonal superstructure indicated by the black hexagons.

M.O. Goerbig et al.

graphene structure: multilayer

bilayer graphene: two layers shifted with respect to each other, the B atoms of one are situated directly above the A atoms of the other

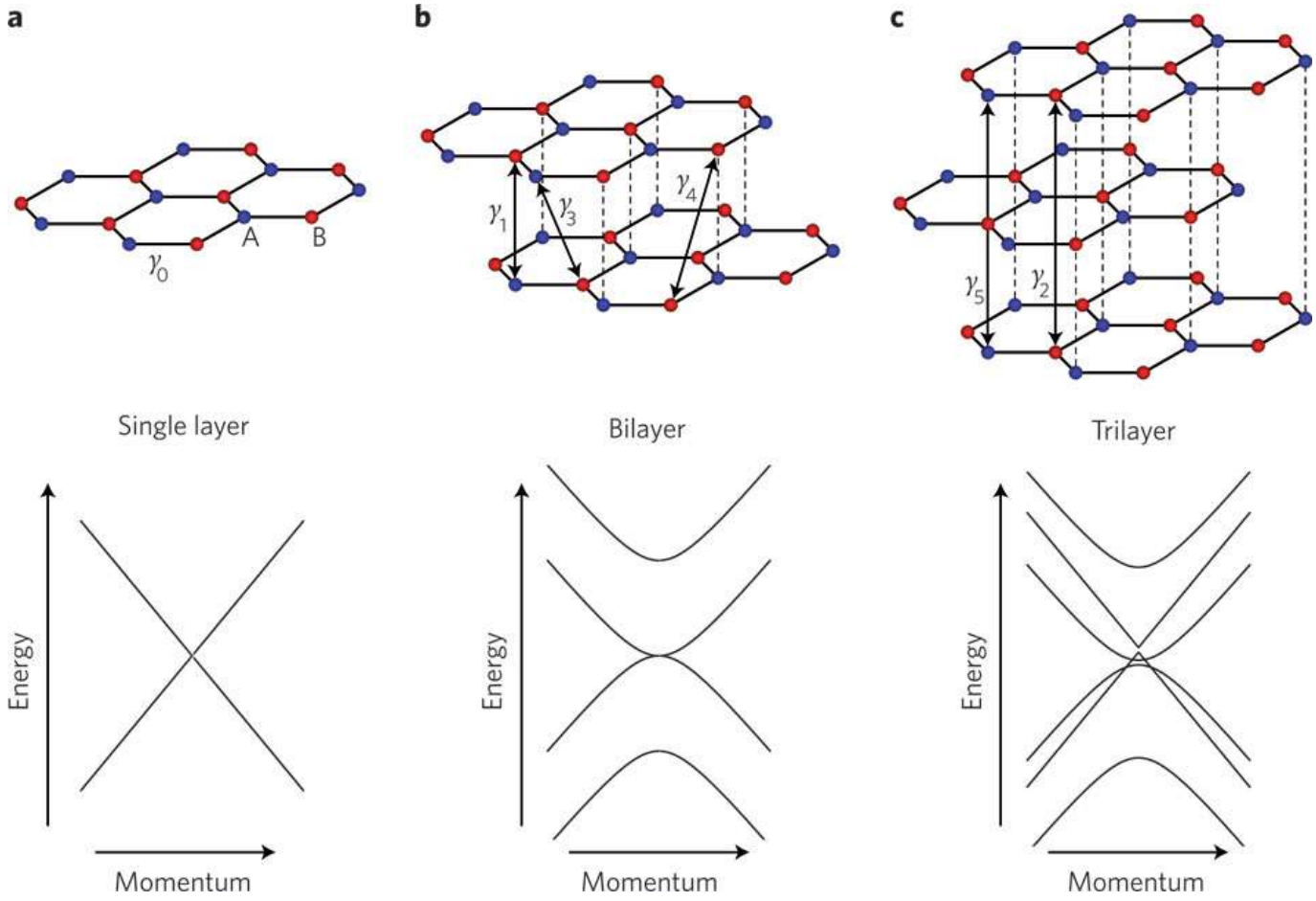

- massive chiral Fermions (no QED equivalent)
- higher energy subbands do not contribute to transport (unless high doping)

M. Freitag, Nat. Phys. 2011

- graphene structure
- fabrication and CVD growth
- characterization: Raman spectroscopy

Examples

- graphene electroburning for molecular junctions
- Quantum Hall Effect

Graphene: scotch tape

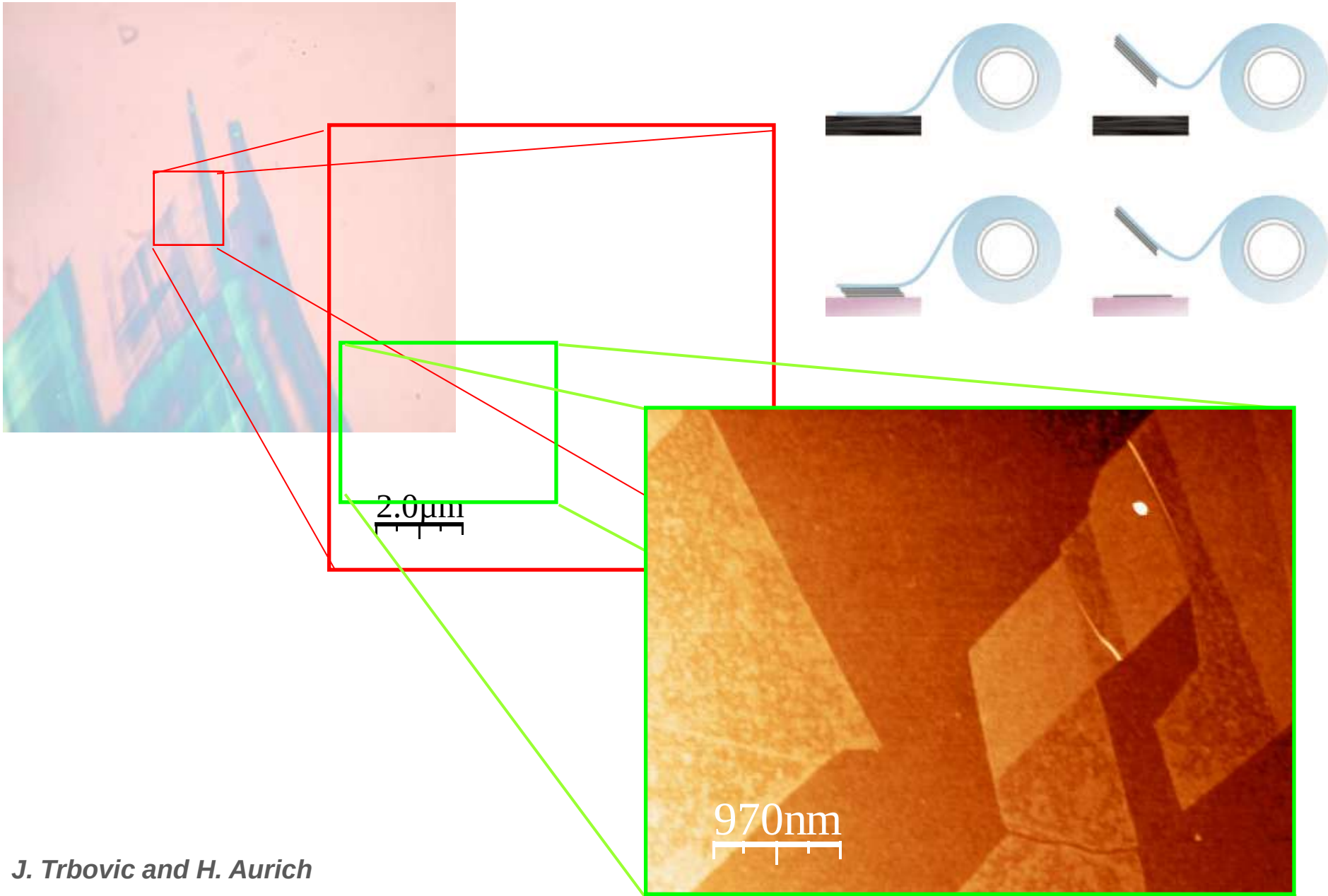

J. Trbovic and H. Aurich

Graphene: scotch tape

Q: How to isolate 2D monolayers?

A: with an atomic force microscope (AFM)

- Step 1: Prepare a layered crystal with a fresh surface.
- Step 2: Rub the layered crystal against another surface (virtually any solid surface is suitable). This produces a variety of flakes attached to the secondary surface very much as drawing by chalk on a blackboard does.
- Step 3: Use an optical microscope to identify single-layers candidates deposited on top of an oxidized *Si* wafer through the phase contrast induced by the flakes.

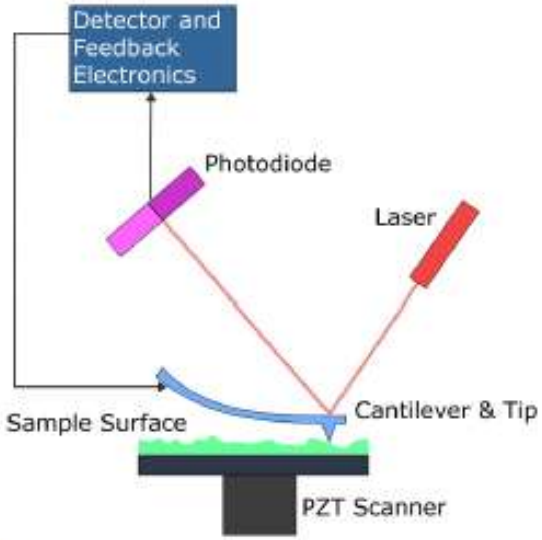

Q: Why was this simple procedure not used before?

- Monolayers are rare.
- 2D crystal have no clear signatures in transmission electron microscopy.
- Monolayers cannot be seen with an optical microscope on most substrates (glass or metals).
- AFM has very low throughput.
- It was not believed that macroscopic 2D crystals exist (by the Mermin-Wagner theorem).
- The key step was the preliminary identification with an optical microscope of 2D flakes placed on top of an oxide *Si* wafer.

C. Mudry, PSI

graphene fabrication/synthesis

Single layer	Few layers
Micromechanical cleavage of HOPG	Chemical reduction of exfoliated graphene oxide (2–6 layers)
CVD on metal surfaces	
Epitaxial growth on an insulator (SiC)	Thermal exfoliation of graphite oxide (2–7 layers)
Intercalation of graphite	Aerosol pyrolysis (2–40 layers)
Dispersion of graphite in water, NMP	
Reduction of single-layer graphene oxide	Arc discharge in presence of H_2 (2–4 layers)

from Rao et al., Ch.1 in, Graphene: Synthesis, Properties, and Phenomena Wiley (2013)
see also Avouris et al., Mat. Today (2012)

wish list…
- backgate control for electrodes and junction
- no defects, controlled edges
- scalability / parallel fabrication

good candidate: CVD

NB SiC: not self-limiting, charge density tuning a challenge

CVD process & catalyst materials

Graphene (SLG) & few-layer graphene (FLG)

- **gas precursor:** CH_4 (C_2H_2)
- **catalytic** metal surface for gas decomposition; growth kinetics depends on metal
- usually: **polycrystalline** graphene

Lattice constant of graphene: 2.46 Å

Nickel: ~ 2.49 Å
Copper: ~ 2.55 Å

} low cost, large grain size, easier to etch

other catalytic surfaces:
Co, Fe, Ir, Pd, Pt, Ru

Bocquet & Witterlin, *Surf. Sci. (2009)*

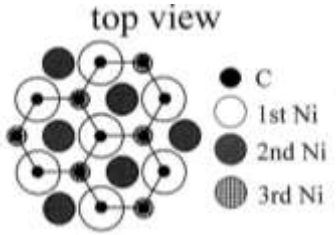

see e.g. Avouris et al., Mat. Today (2012)

CVD process & catalyst materials

Nickel

- high C solubility in Ni
  ~ 1 % atoms
- melting point: 1455˚C
- surface seggregation
- not self-limiting, monolayer control delicate

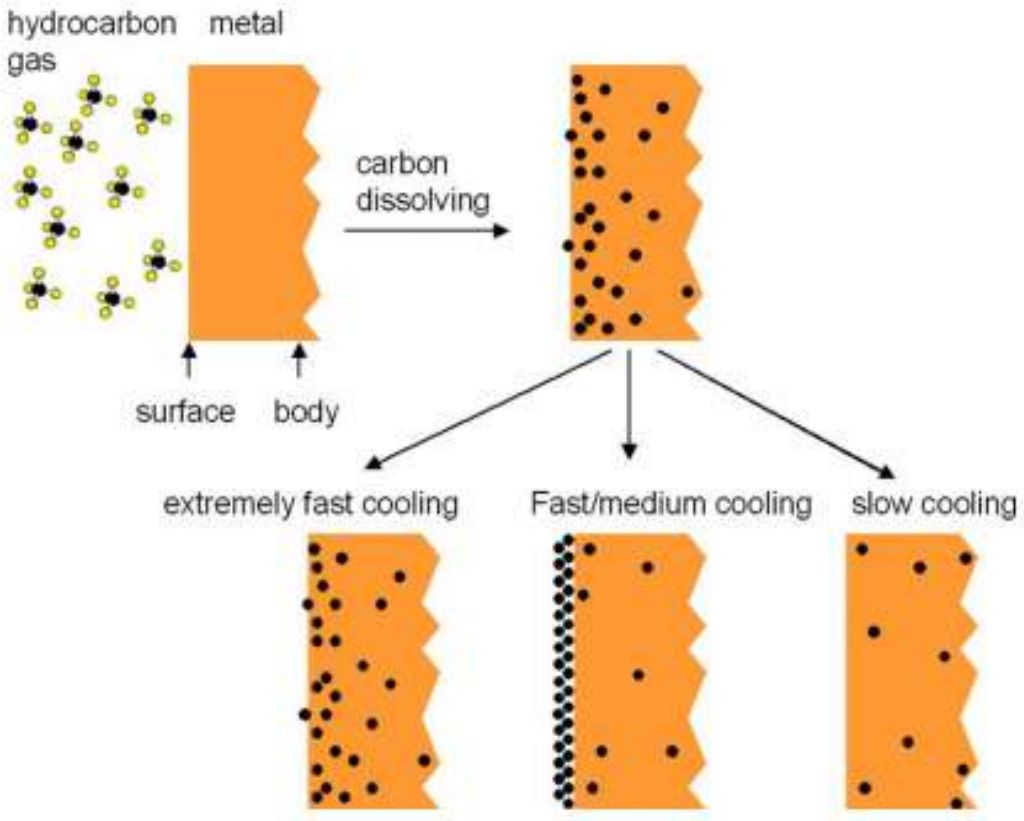

⇨ **large-scale sheets**
FLG on Ni: Dresselhaus, Kong, Nano Lett. (2009)
SLG on Ni: Choi, Hong, Kim et al., Nature (2009)

Yu et.al, APL 93, 113103 (2008)

CVD process & catalyst materials

Copper

- very low C solubility in Cu

  1000x less than in Ni
- melting point: 1084°C
- surface mediated, self-limiting

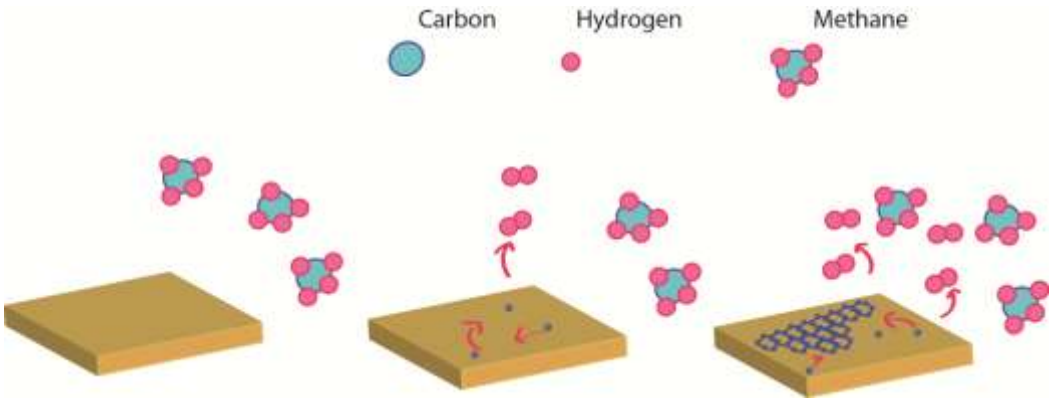

⇨**large-scale sheets**
SLG on Cu: Ruoff et al., Science (2009)

NB: **solid** C feedstock possible,
e.g: PMMA, sucrose on Cu
Tour et al., Nature (2010)

Pressure & Temperature control the boundary layer

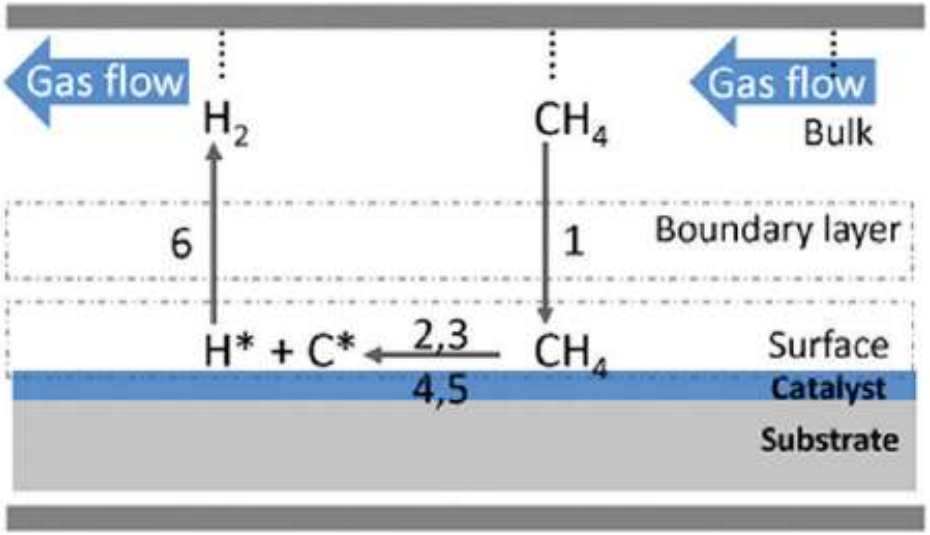

S.Bhaviripudi et.al, *Nano Lett.*, **2010**, *10* (10), pp 4128–4133

CVD process & catalyst materials

Graphene (SLG) & few-layer graphene (FLG)

- **gas feedstock:** CH_4 (C_2H_2)
- **catalytic** metal surface for gas decomposition; growth kinetics depends on metal
- usually: **polycrystalline** graphene
- **nucleation** centers/zones and **extension** of domains

*evolution of graphene growth by C isotope labeling: **inhomogeneous** distribution of ^{12}C and ^{13}C identified by Raman spectroscopy*

Lattice constant of graphene: 2.46 Å

Nickel: ~2.49 Å
Copper:~2.55 Å

low cost, large grain size, easier to etch

other catalytic surfaces:
Co, Fe, Ir, Pd, Pt, Ru

Bocquet & Witterlin, *Surf. Sci. (2009)*

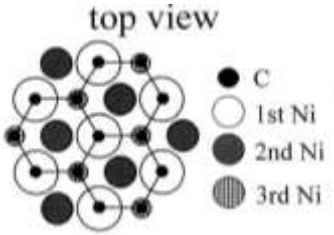

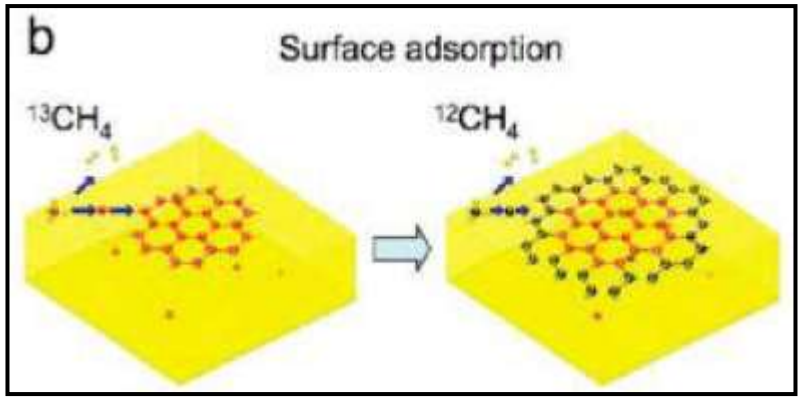

X. Li, R. S. Ruoff et al., Nano Lett. ***2009****, 9 (12), 4268-4272*

growth mechanism

Evolution of Graphene Growth on Ni and Cu by Carbon Isotope Labeling

trick: separation of the ^{12}C and ^{13}C Raman modes

Frequency of Raman modes are given by:

$$\omega = \omega_{12}\sqrt{\frac{m_{12}}{n_{12}m_{12} + n_{13}m_{13}}}$$

if the atoms are randomly mixed and the bond force constants are assumed to be equal

*X. Li, R. S. Ruoff et al., NANO LETTERS **2009**, 9 (12), 4268-4272*

CVD growth

0.05 mbar
1000°C

10 sccm H_2
25 sccm
CH_4

- Copper foil as catalyst and substrate
- Decompostion of methane at high temperatures 950 to 1050°C
- Adsorption of carbon atoms on Cu surface
- Graphene growth at different nucleation zones

*X. Li et al., Science **2009**, 324, 1312-1314*

C. Nef, W. Fu et al.

CVD growth

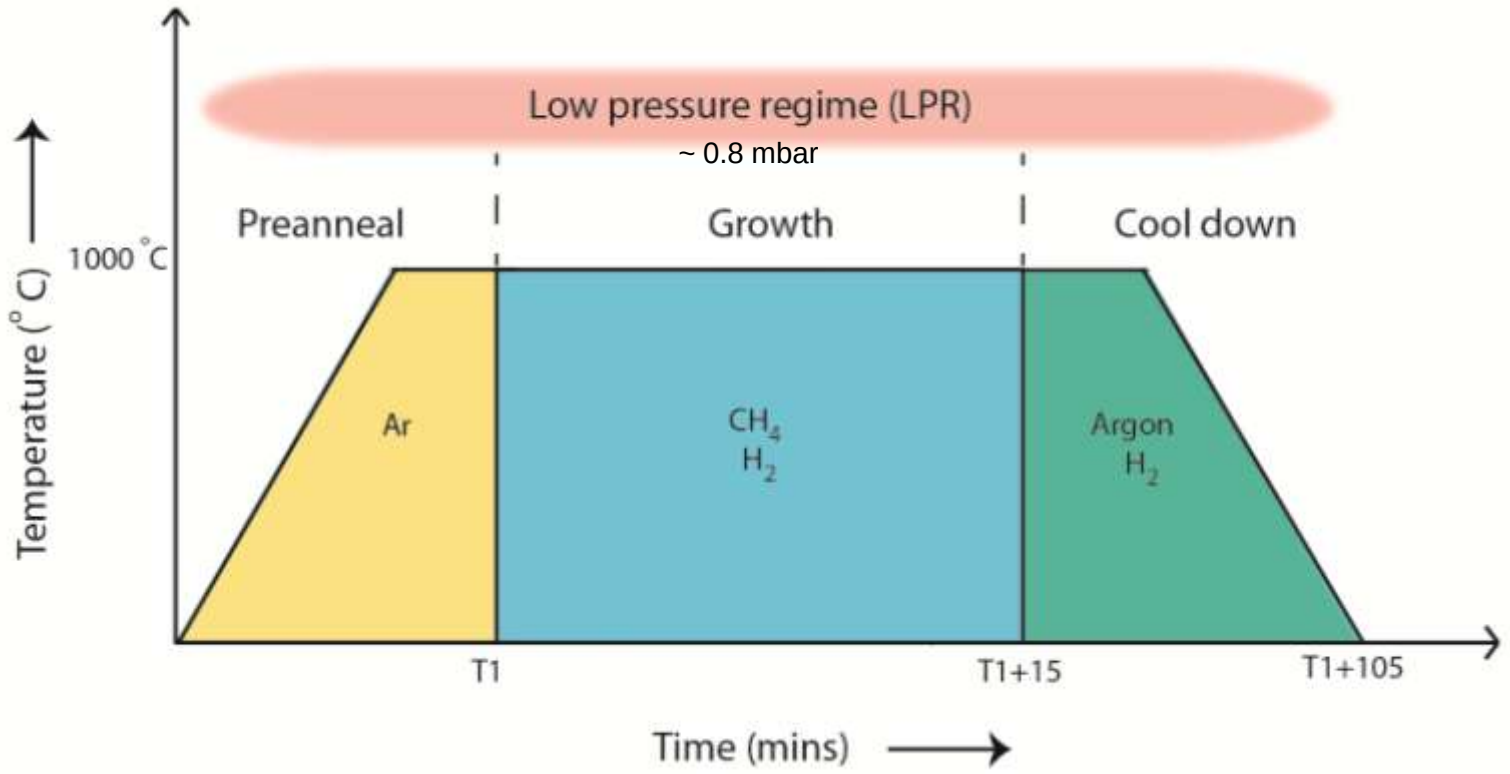

CVD Graphene growth. A Copper foil is annealed in H_2 flow for time T1 (annealing time ~ 2 hours) followed by graphene growth for 15 mins to hours and subsequent cool down to room temperature.

$$CH_4 \xrightarrow[1000\,^\circ C]{Cu} C^{\cdot} + 4\,H^{\cdot} \longrightarrow \text{graphene} + 2\,H_2.$$

*X. Li et al., Science **2009**, 324, 1312-1314*

K. Thodkar, C. Nef, W. Fu et al.

CVD growth: a few results

Growth at different boundary layer conditions: p, T, gas flow

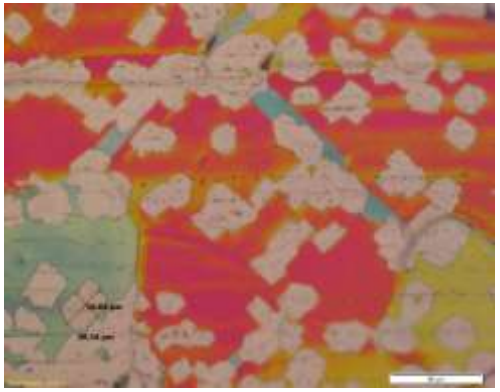

Condition 1: Low Pressure. (LP) Scale bar 50 µm

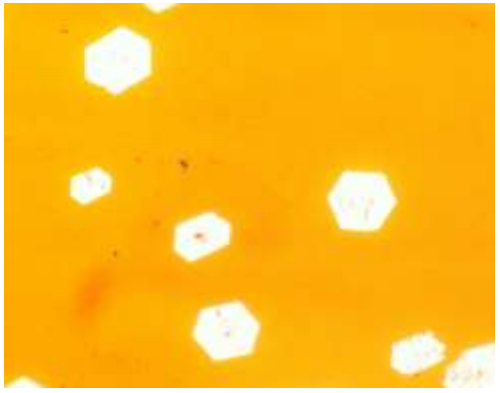

Condition 2: HP. Scale bar 20 µm.

Coalescing grains of CVD graphene

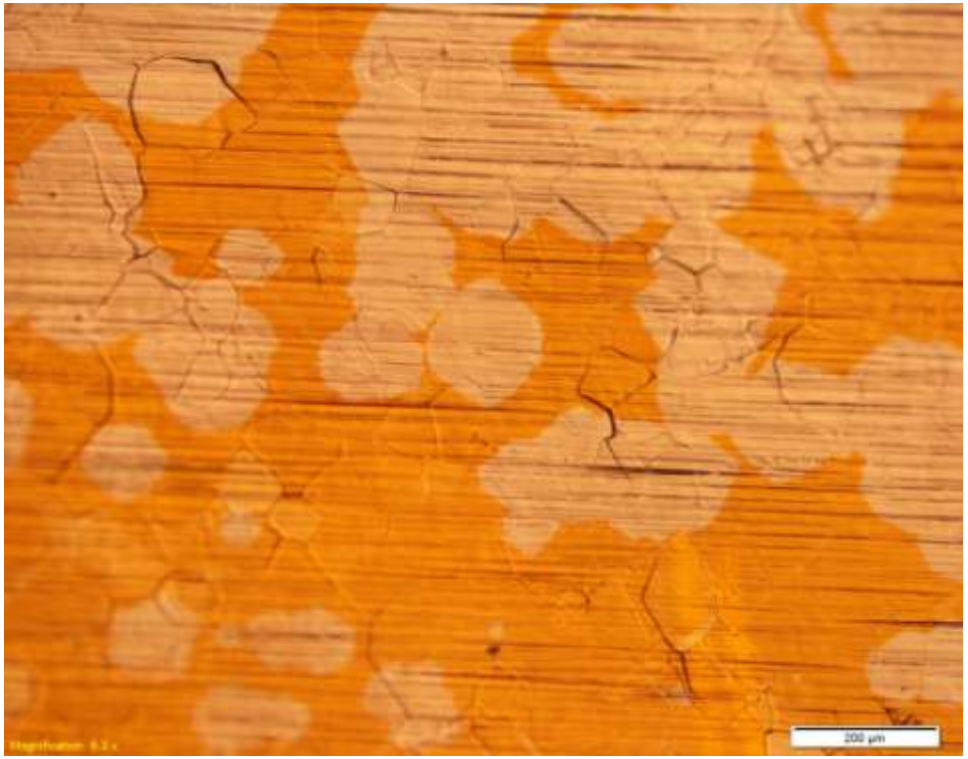

Condition 3: HP. Scale bar 200 µm.

K. Thodkar et al.

controlling growth parameters

Flow rate (sccm)	SG 11 1000 C	SG 12 1000 C	SG 16 1000 C	SG 25 1000 C	SG 30 1000 C	SG 40 1020 C	SG 55 1065 C
Ar + (200ppm)CH_4, H_2	200 100	200 100	200 20	200 5	30 10	30 5	~60 20
Pre anneal	H_2 500	H_2 500	Ar 100	Ar 100	Ar 200	Ar 200 H_2 5	Ar 200
Comments	PA: 3 GT: 6 ~20um ~ 5 mbar	PA: 3 GT: 3 ~20um ~ 100mbar	PA: 1 GT: 6 ~200um ~150 mbar	PA: 12 GT: 5 Full coverage ~200 mbar	PA: 0.5 GT: 6 ~200mbar No nucleation	PA: 0.5 GT: 4 ~0.7mbar Square shaped islands	PA: 12 GT: 2 ~1000um ~ 200 mbar

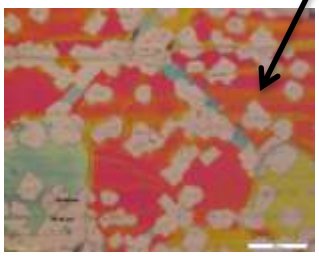

SG : Slow growth
PA : Pre Anneal
GT : Growth time in hours

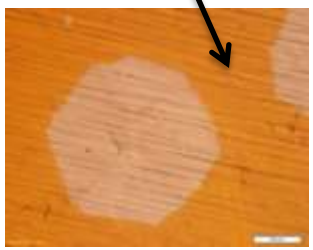

Optical images of graphene crystals on oxidized Cu substrate. Scale bar a) 50um b) 20 µm, c) 100 µm & d) 200 µm

K. Thodkar et al.

large homogeneous graphene domains

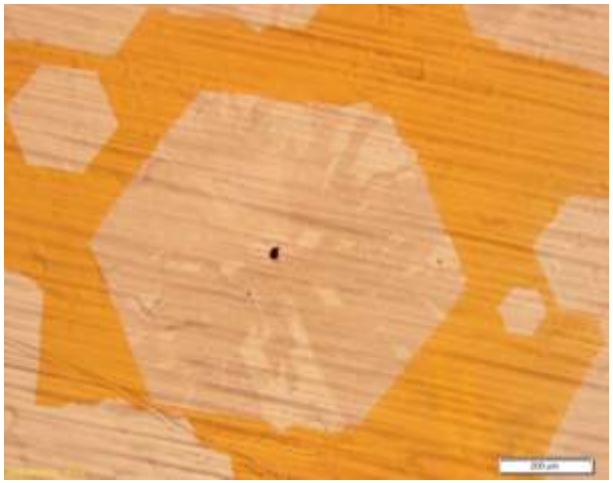

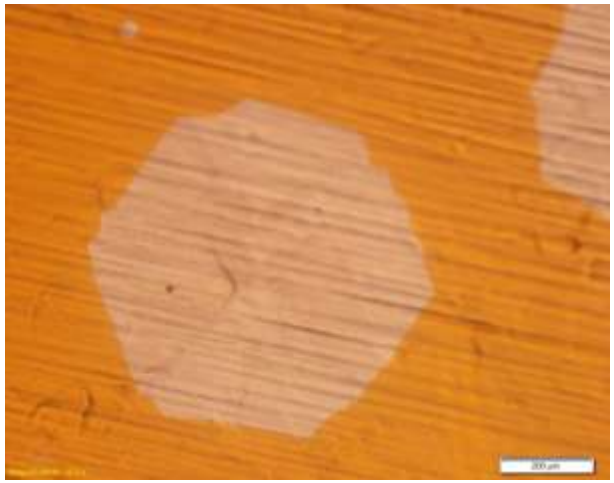

Optical images of graphene on oxidized Cu substrate.
Scale bars: 200 µm

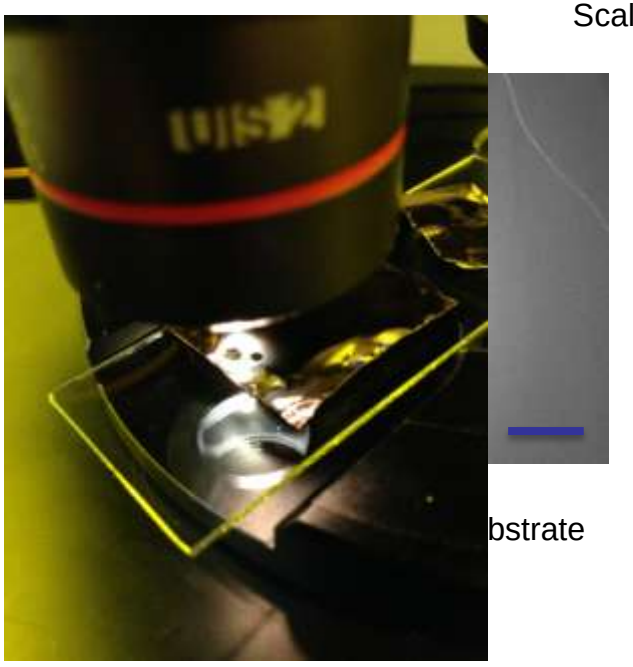

bstrate

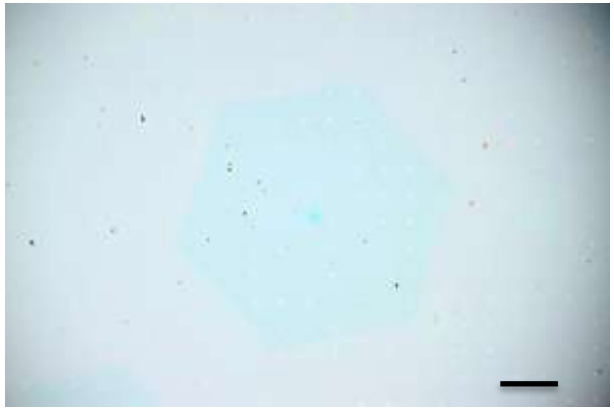

Optical Image of graphene after transfer to SiO2
Scale bar: 400 µm

K. Thodkar et al.

graphene transfer

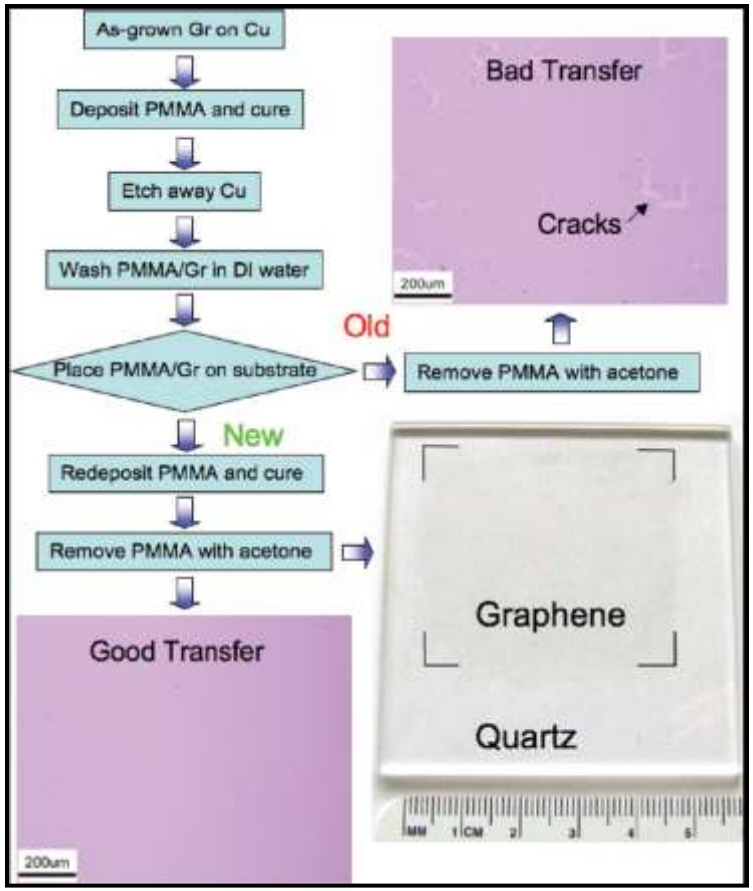

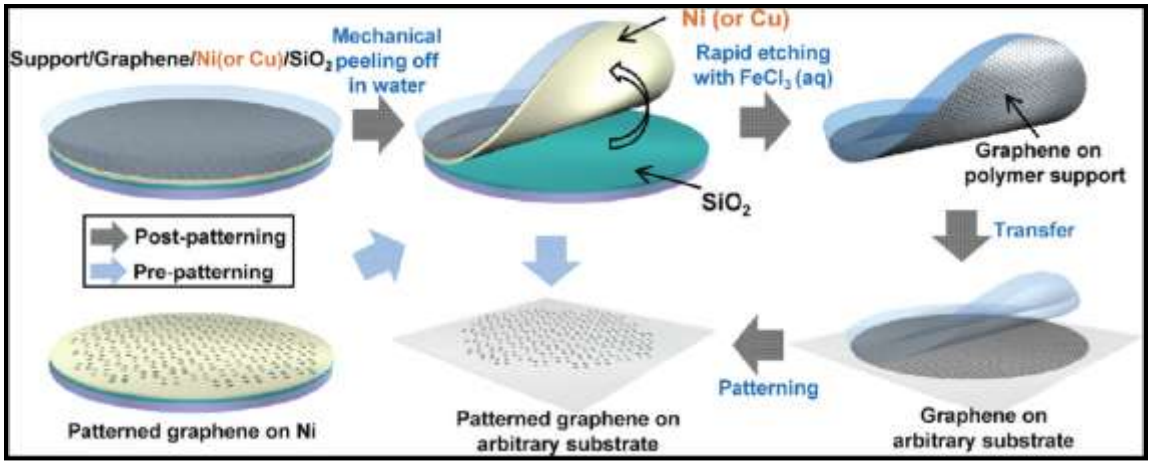

- PMMA or PDMS used as support
- Cu etched in an aqueous solution of iron nitrate or iron chloride
- Transfer to almost any substrate possible
- Transfer free processes possible, by direct prepatterning and underetching (Park, *NANO LETTERS*)

X. Li, R. S. Ruoff et al., NANO LETTERS 2009, 9(12), 4359-4363
Y. Lee, J-H. Ahn et al., NANO LETTERS 2010, 10, 490-493

graphene transfer in our lab

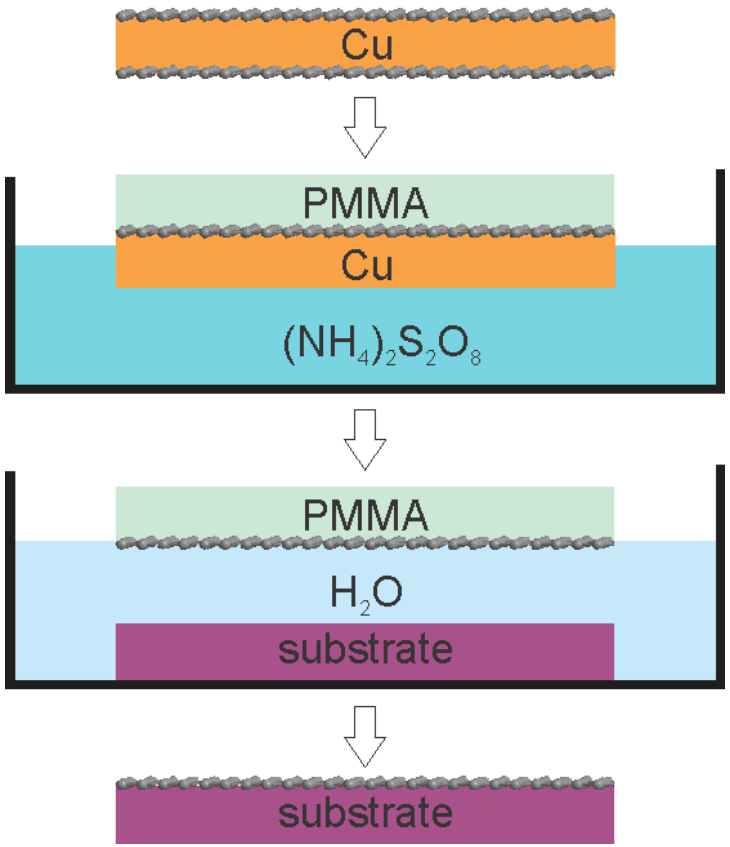

- CVD graphene on Cu foil 25 µm
- Spin coating of PMMA and cure
- Etch back side in Ar/O_2 plasma
- Etching of Cu in 0.1M $(NH_4)_2S_2O_8$ in H_2O (ca. 4 h)
- Wash PMMA/graphene in several H_2O bathes
- Substrate is cleaned in Ar/O_2 plasma
- Substrate is placed below the PMMA/graphene and the water is removed with a syringe
- Substrate/graphene/PMMA is dried over night at ambient conditions
- PMMA is dissolved in warm acetone

X. Li, R. S. Ruoff et al., *Nano Letters* **2009**, 9(12), 4359-4363
Y. Lee, J-H. Ahn et al., *Nano Letters* **2010**, 10, 490-493

C. Nef et al.

graphene imaging

Electron Microscopy on Cu

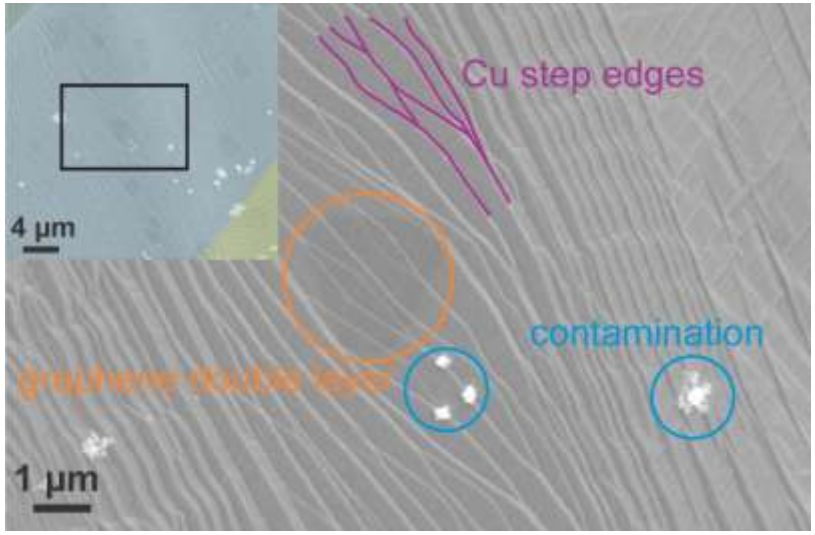

- Full coverage with graphene
- Small bi- and tri-layer flakes
- Cu grains (marked in different colors)

Optical Microscopy on SiO_2

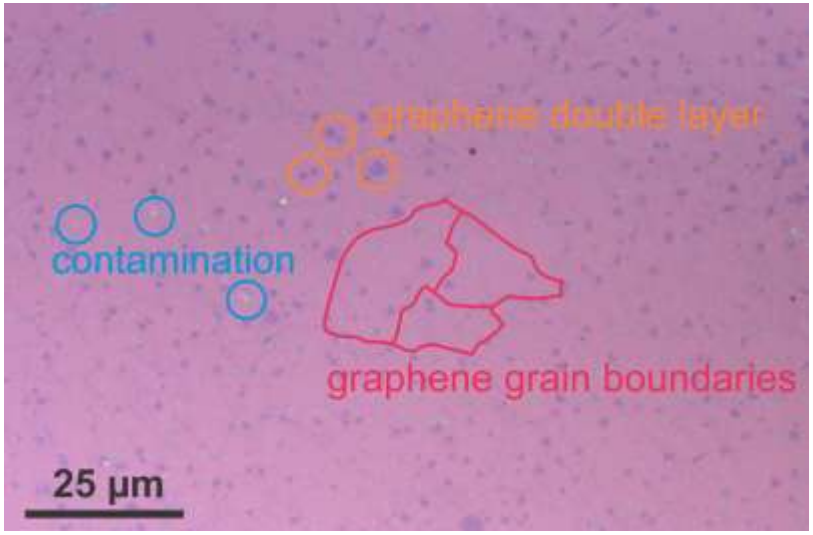

- PMMA residues from transfer
- Graphene is polycristalline

C. Nef et al.

graphene defects

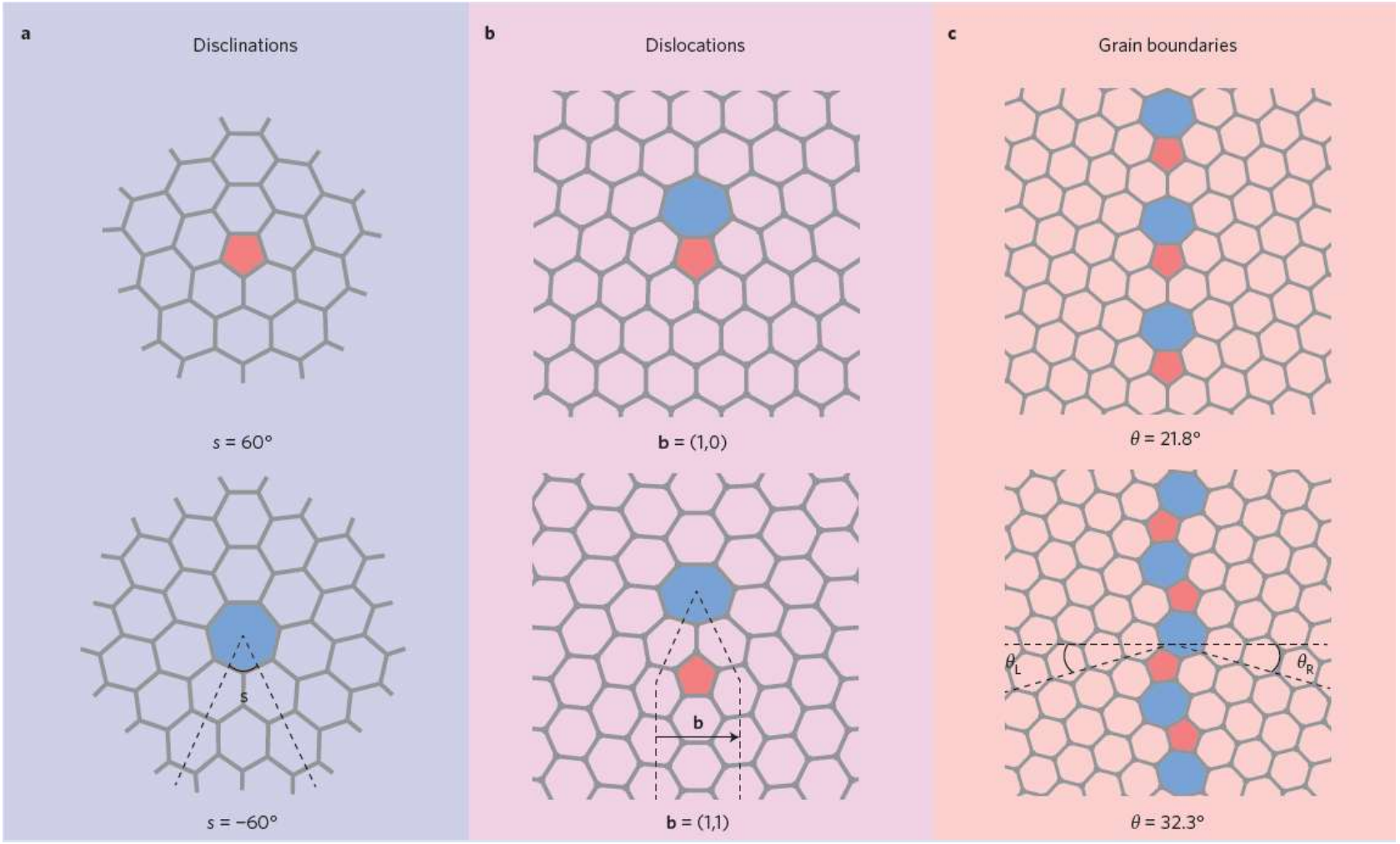

The presence of isolated disclinations in graphene is unlikely as it inevitably results in highly non-planar structures.

grain boundary (in 2D) = 1D chain of aligned dislocations

Yazyev et al., Nat. Nano (2014)

graphene defects

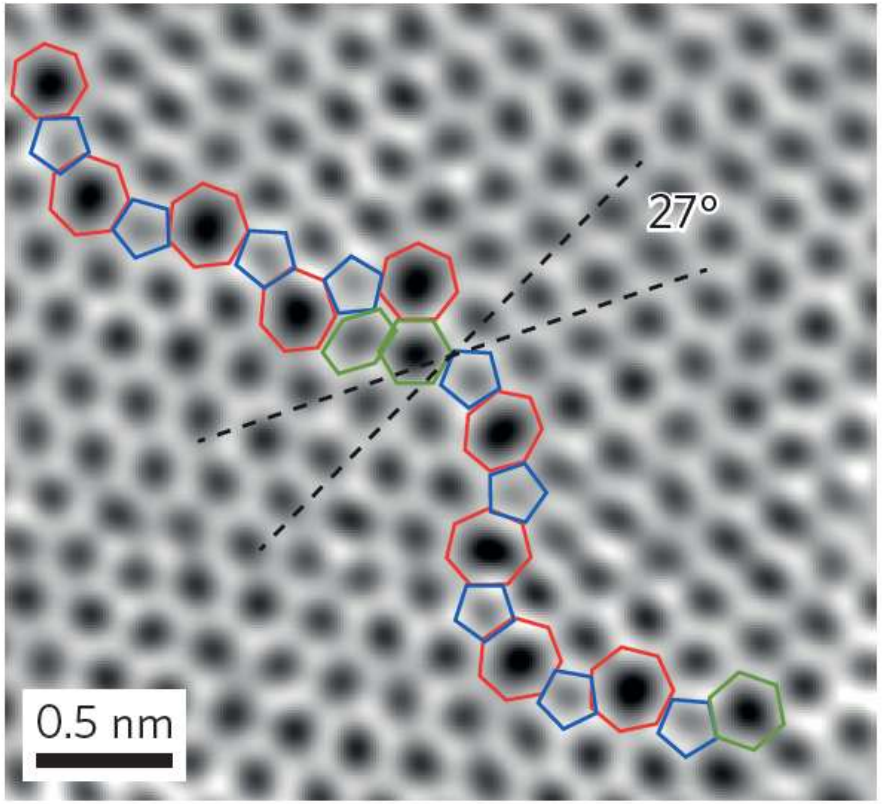

Aberration-corrected annular dark-field scanning **TEM** (ADF-STEM) image of a grain boundary stitching two graphene grains with lattice orientations rotated by ~27° with respect each other. **The dashed lines outline the lattice orientations of the two domains**. The structural model of the interface highlighting **heptagons (red), hexagons (green)** and **pentagons (blue)** is overlaid on the image.

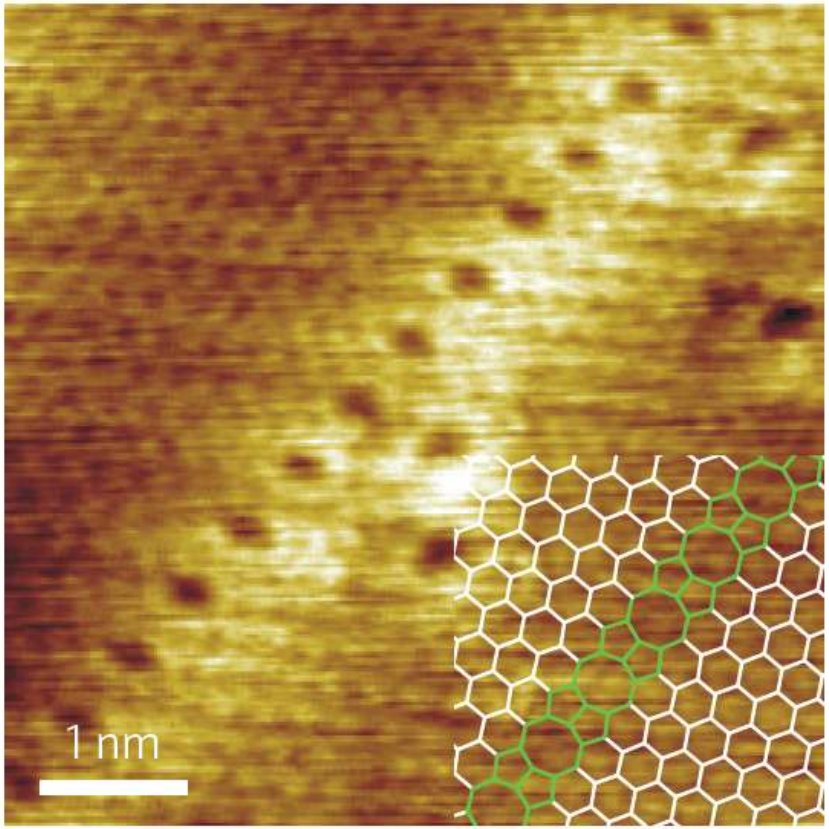

STM image of **a regular line defect in graphene** grown on Ni(111) substrate. The inset shows the structural model.

Yazyev et al., Nat. Nano (2014)

- graphene structure
- fabrication and CVD growth
- characterization: Raman spectroscopy

Examples

- graphene electroburning for molecular junctions
- Quantum Hall Effect

light matter interaction

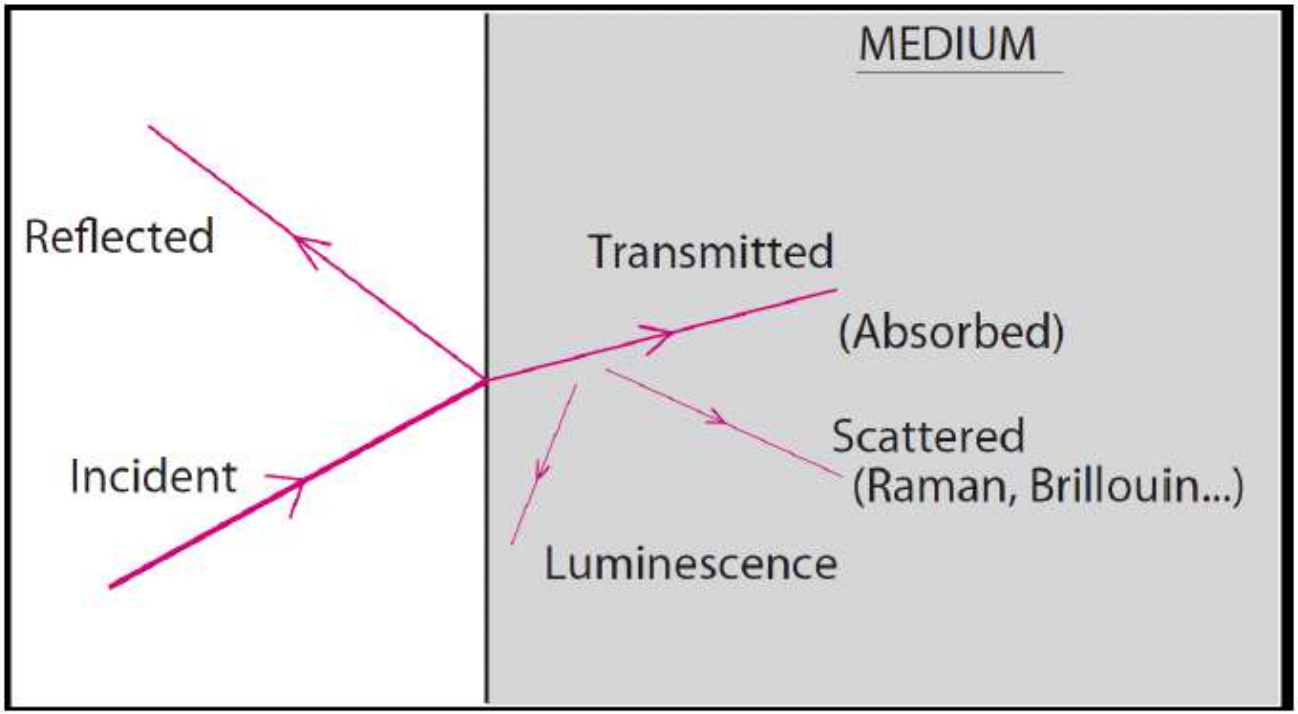

Yu & Cardona, Fundamentals of Semiconductors, Springer

optical spectroscopy

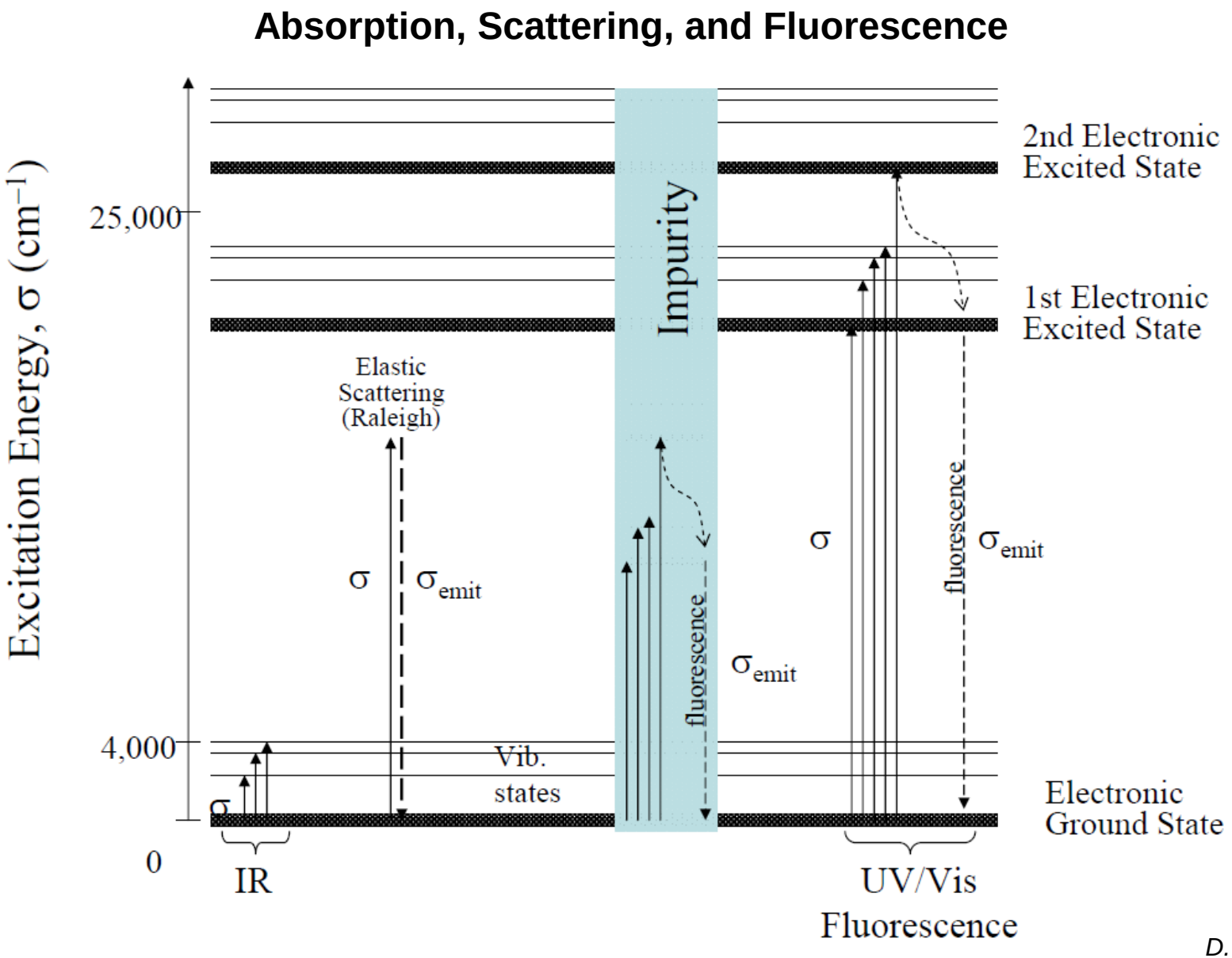

D.T. Schwartz

optical spectroscopy

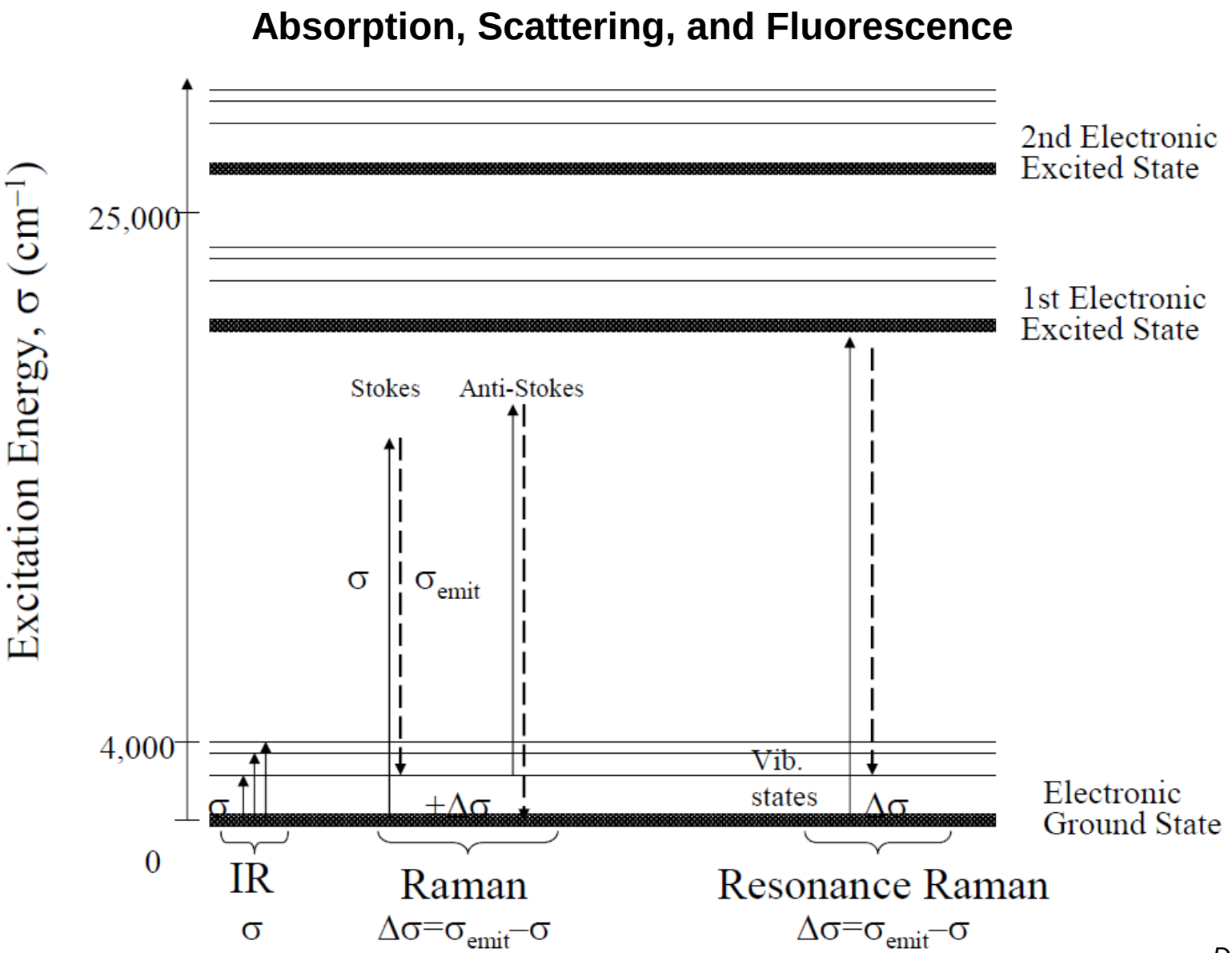

D.T. Schwartz

Raman spectroscopy

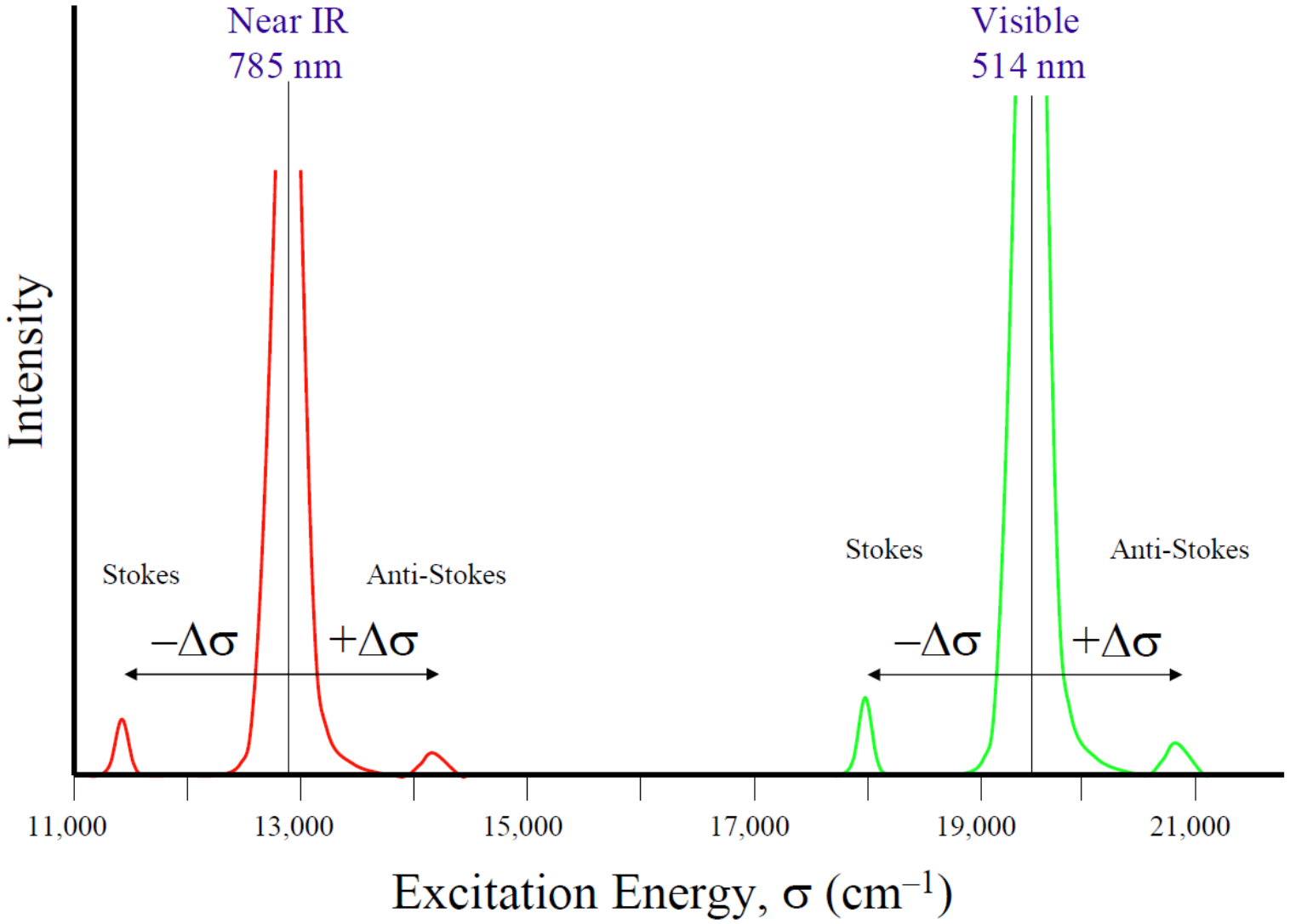

D.T. Schwartz

Raman: Effect

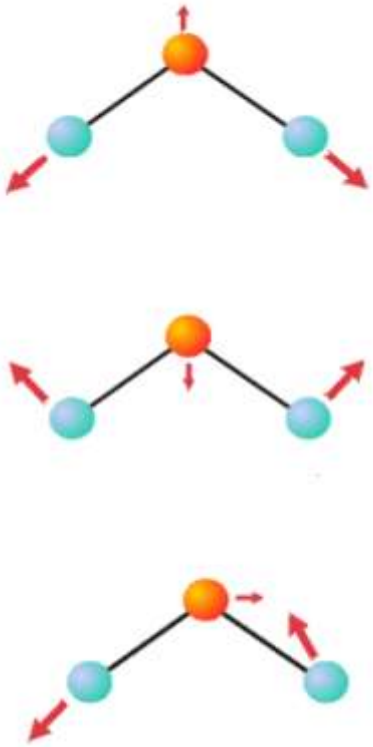

incoming light: $\vec{E} = \vec{E}_0 \sin 2\pi\nu t$

induced dipole moment (C·m): $\vec{\mu} = \alpha\vec{E} = \alpha\vec{E}_0 \sin 2\pi\nu t$

polarisability: $C \cdot m^2/V$ $\alpha = \alpha_0 + \beta \sin 2\pi\nu_v t$

hence $\vec{\mu} = (\vec{\alpha}_0 + \beta \sin 2\pi\nu_v t)\, \vec{E}_0 \sin 2\pi\nu t$

ν_v: vibrational freq. of molecule

$$\vec{\mu} = \underbrace{\alpha_0 \vec{E}_0 \sin 2\pi\nu t}_{\text{Rayleigh}} - \frac{1}{2}\beta\vec{E}_0 \left[\underbrace{\cos 2\pi(\nu + \nu_v)t}_{\text{Anti-Stokes}} - \underbrace{\cos 2\pi(\nu - \nu_v)t}_{\text{Stokes}} \right]$$

IR & Raman: selection Rules

Raman active *requires α change upon vibrational motion*

IR active *requires dipole change upon vibrational motion*

Raman inactive:

$$\beta \propto \frac{\delta\alpha}{\delta q_v} = 0$$

CO_2 molecule

		Raman	Infrared
no net dipole change	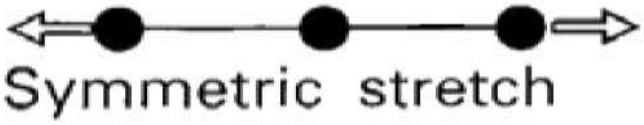	active	inactive
dipole change	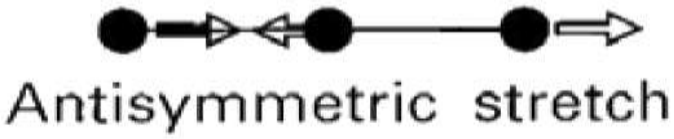	inactive	active
	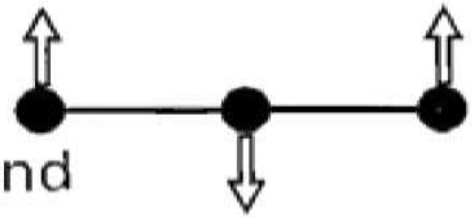	inactive	active

Raman spectroscopy

- Main drawback of Raman cross section 10^{-30} cm^2
- Compare

UV spectroscopy	10^{-18} cm^2
IR spectroscopy	10^{-20} cm^2
Fluorescence	10^{-18} cm^2
Rayleigh	10^{-26} cm^2

- Enhanced Raman: Resonant Raman
  Surface Enhanced Raman

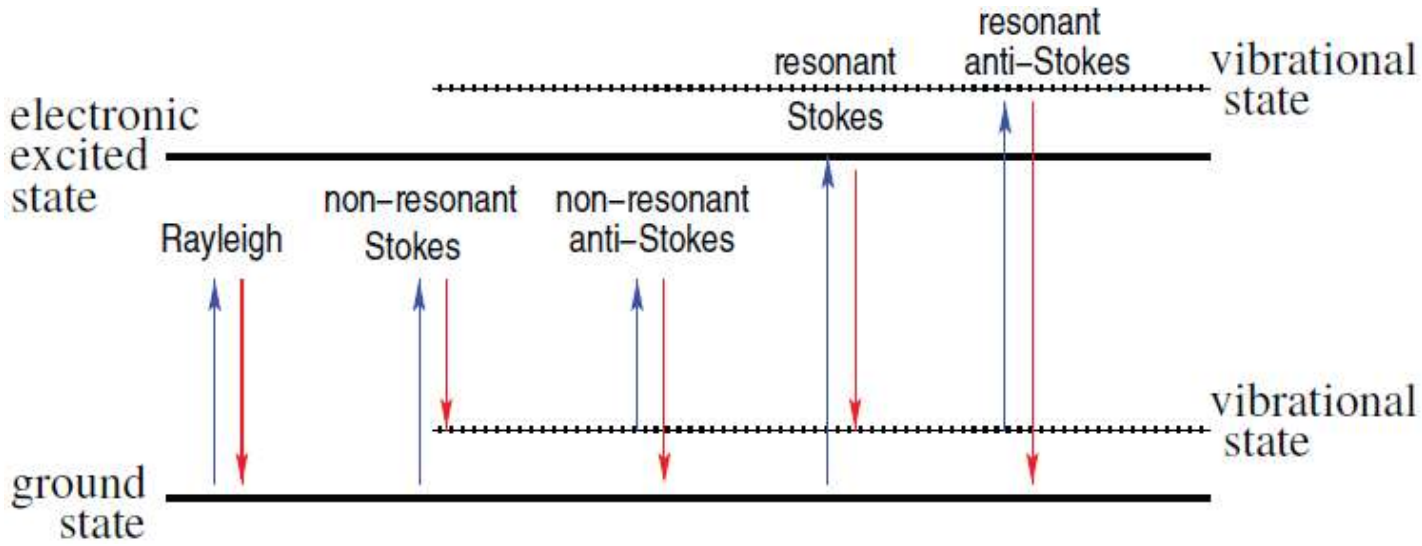

A. C. Ferrari and D. M Basko, *Nature Nanotechnology* **2013**, 8, 235 – 246

Raman example: chloroform

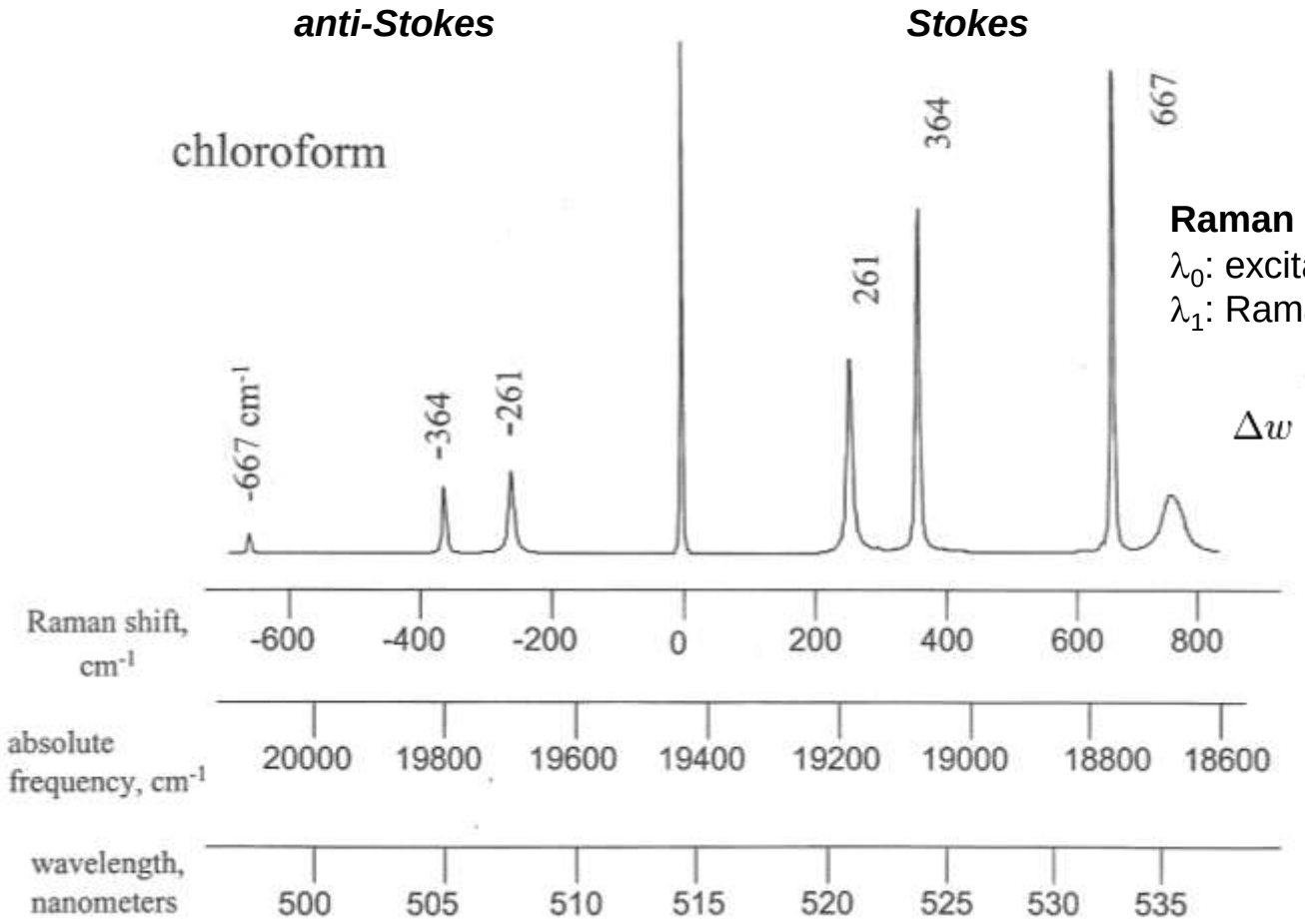

Raman shift (in wavenumer)
λ_0: excitation wavelength
λ_1: Raman line

$$\Delta w = \left(\frac{1}{\lambda_0} - \frac{1}{\lambda_1}\right) ,$$

NB: only molecules that are vibrationally excited (phonon population) prior to irradiation can give rise to the anti-Stokes line ⇨ Stokes line more intense

graphene phonon dispersion

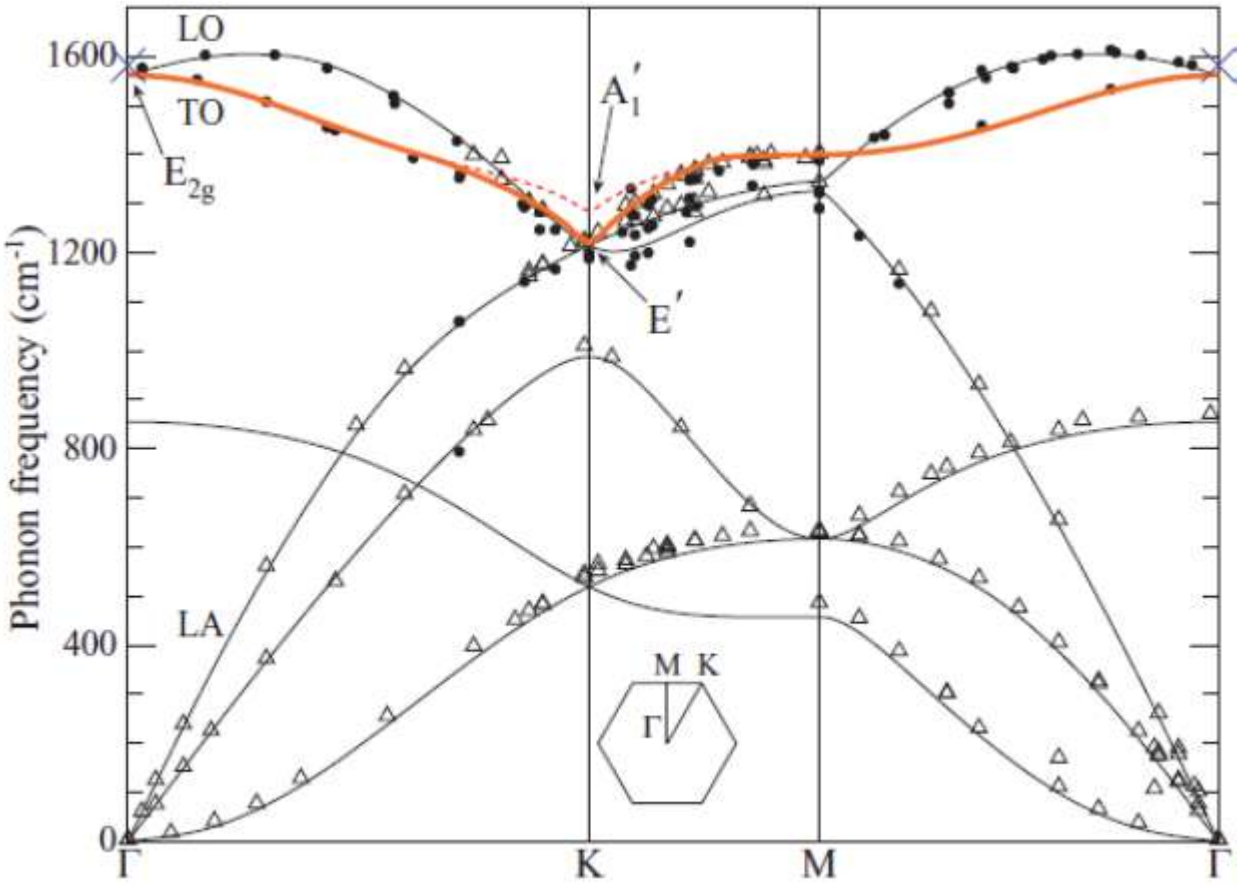

- 2 atoms per unit cell
- 6 phonon branches: 3 acoustic and 3 optical
- maximum frequency ≈1600cm^{-1}

Mauri, PRB (2011), S. Reich

Raman spectroscopy: graphene phonon dispersion

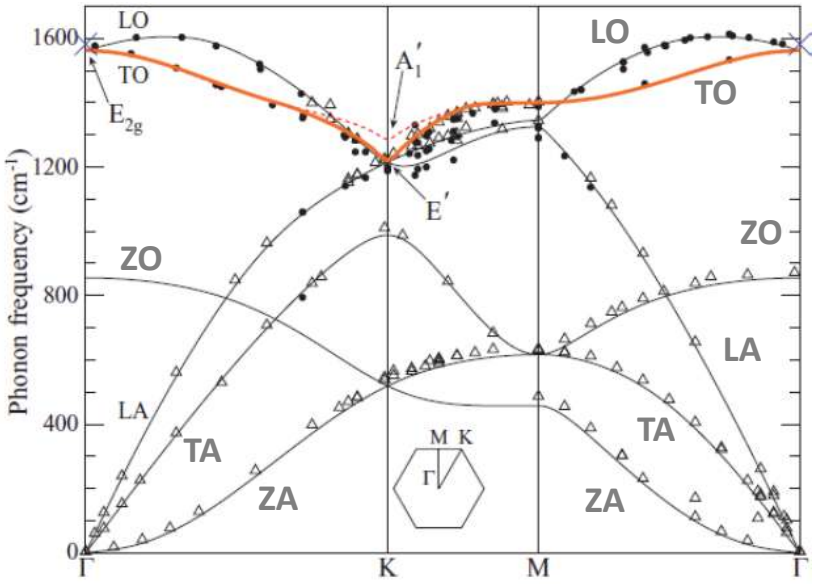

LA: Longitudinal acoustic
TA: Transverse acoustic
ZA: Out-of-plane acoustic

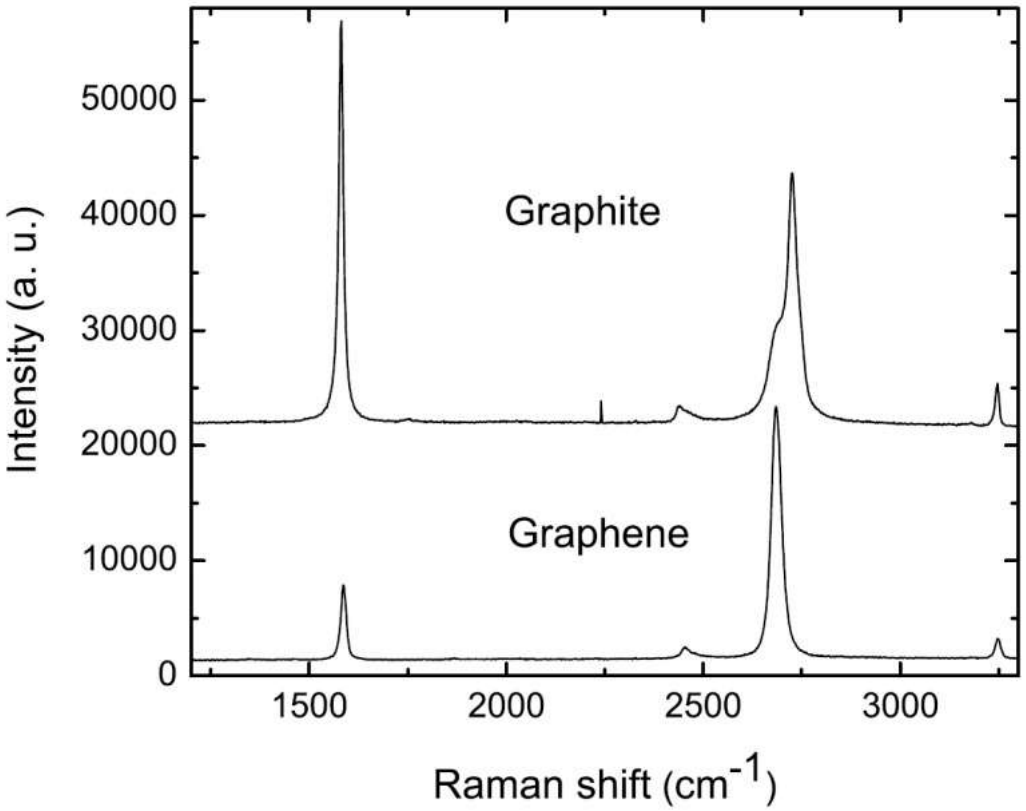

- more phonon frequencies than Raman lines
- Raman lines beyond 1600cm^{-1}
- no Raman lines below 1500cm^{-1}
  no signal from acoustic phonons

Ferrari & Basko, Nat. Nano. (2013)

graphene phonon dispersion & Raman

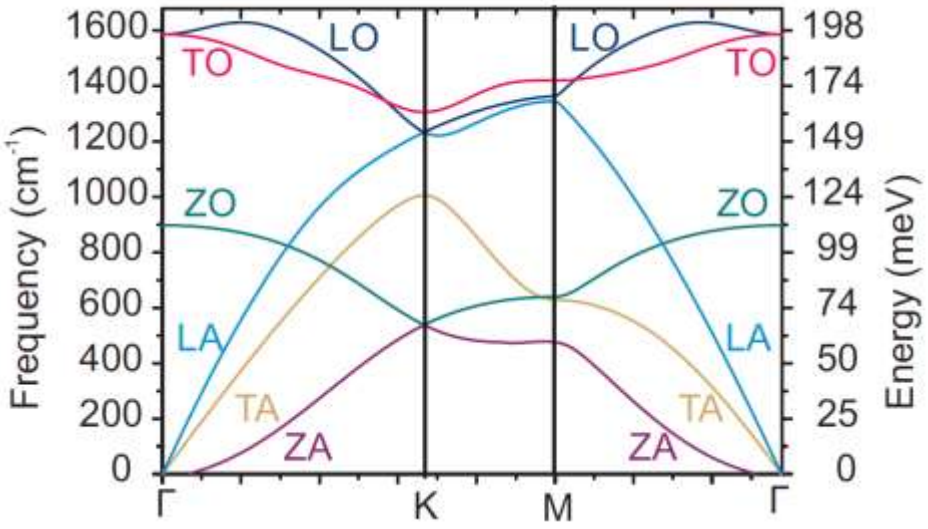

C. Nef, adapted from Yan et al., PRB (2008)

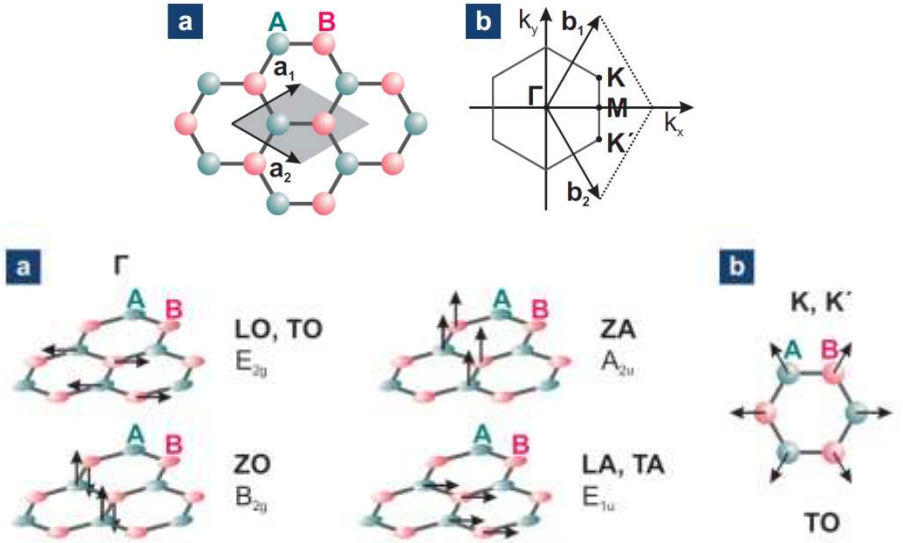

L: longitudinal; T: transverse; Z: out-of-plane

A: accoustic; O: optic

2 atoms per unit cell, 6 phonon branches

Raman spectroscopy

- inelastic light scattering
- for graphene, always resonant
  gapless linear dispersion relation
- 1st order order Raman near Γ point
  k ≈ 0, momentum conservation

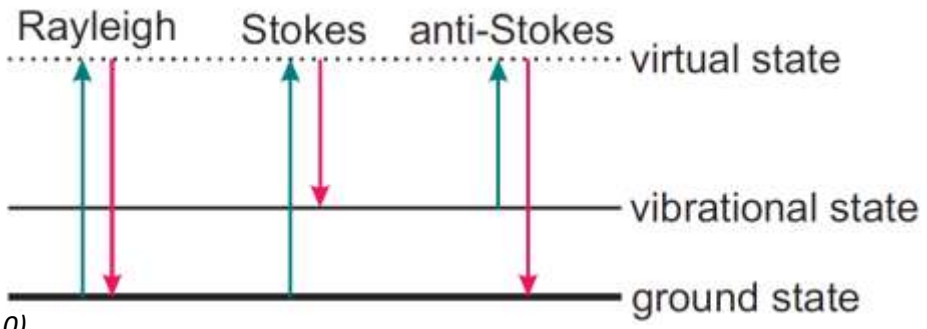

see e.g. Dresselhaus et al., Ann. Rev. Cond. Matt. Phys (2010)

graphene Raman spectroscopy

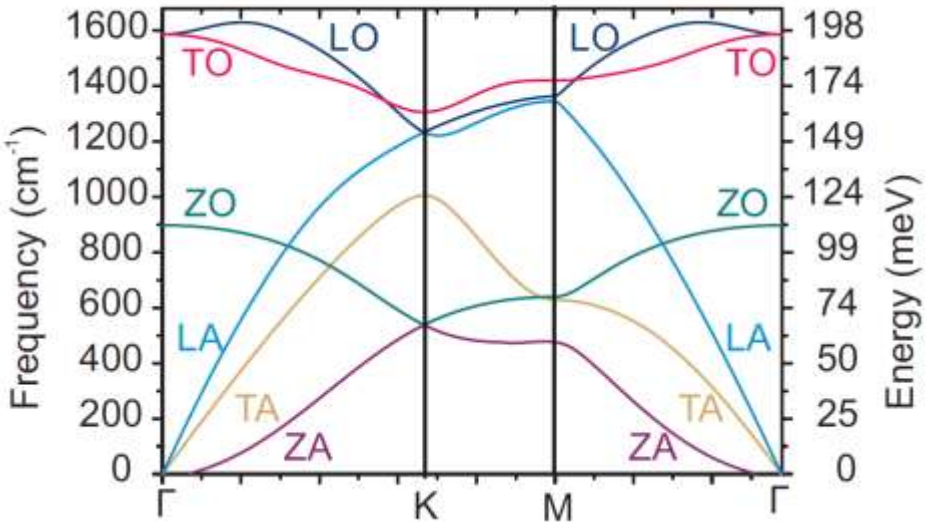

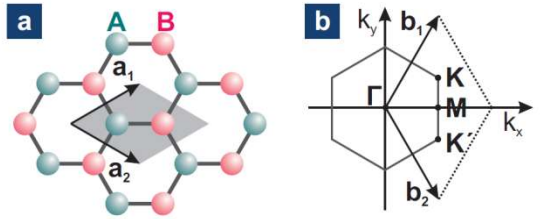

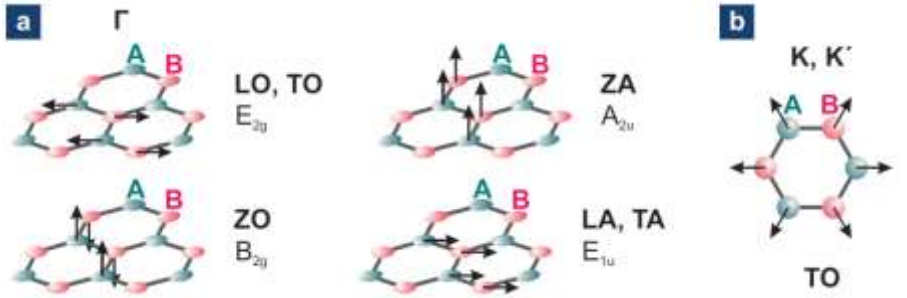

NB: amorphous C has no rings, hence no breathing mode/D band

Raman active modes in graphene

see e.g. Ferrari, Basko, Nat. Nano (2013)

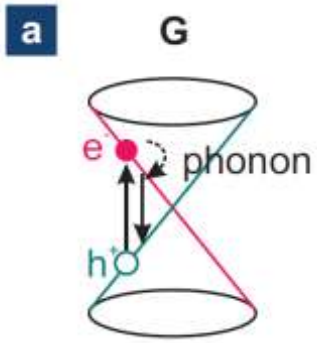

LO, TO modes
G-Band ≈ 1580cm^{-1}
stretching of C-C bond

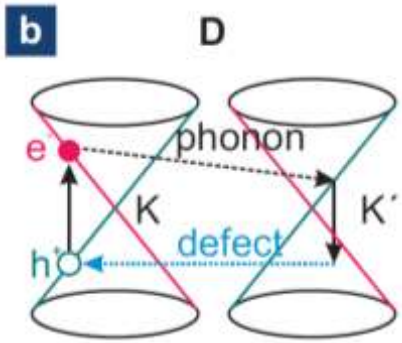

Intervalley scattering on defect

breathing mode (TO phonon at *K point)*
needs a defect/phonon activation
D-band ≈ *1350 cm^{-1}*

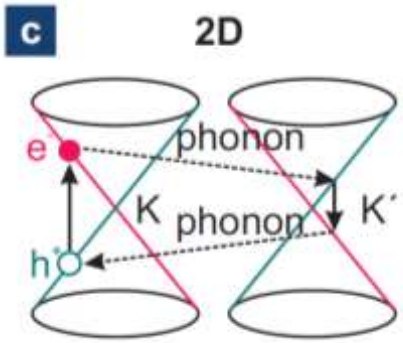

Intervalley two-phonon process

2-phonon scattering process of TO breathing mode
2D-band ≈ 2700 cm−1

graphene Raman spectroscopy

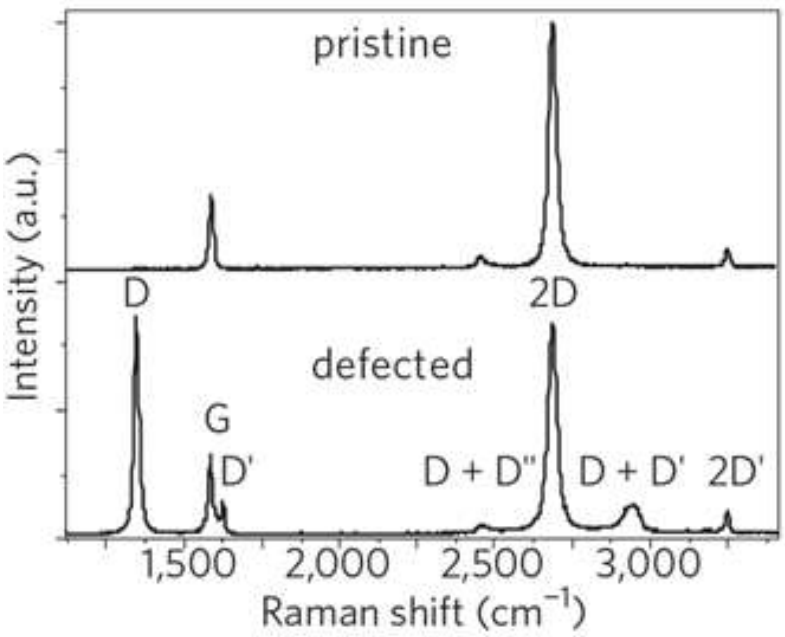

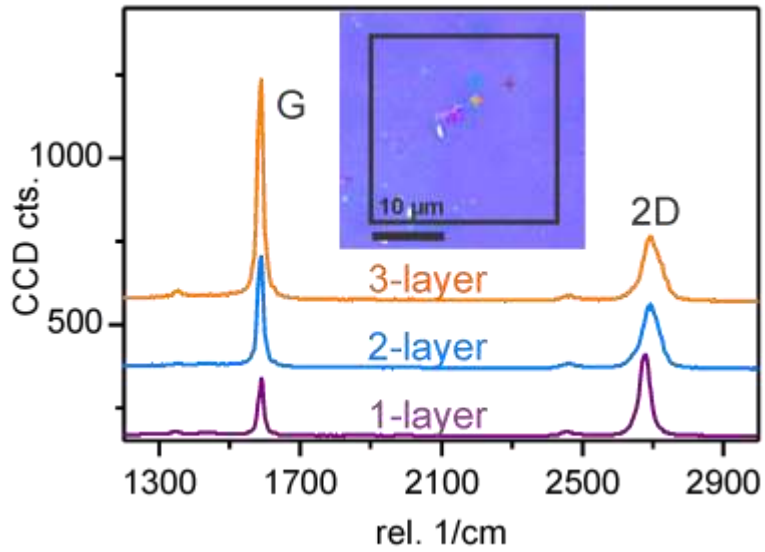

Additional contributions with lower intensity

- D'-band: ≈ *1620 cm^{-1}* LO phonons
- D"-band ≈ *1100 cm^{-1}* LA phonons
  + combination with D-band

- D, D' peak develop in presence of defects **D-band: defects**

- double-resonant overtones: 2D & 2D'
  2 phonons processes

- positions of D, 2D peaks shifts to higher wavenumber for increasing laser energy

- 2D/G band ratio gives an idea over the number of layers

C. Nef, M. El Abbassi, K. Thodkar et al.

Malard et al., Phys. Rep. (2009)
Ferrari & Basko, Nat. Nano. (2013)

graphene Raman spectroscopy

Raman spectra for different types of sp2 nanocarbons and carbon allotropes

- **G band**: C-C bond streching, common to all sp2 carbon materials
- sensitive to strain, curvature (CNTs)

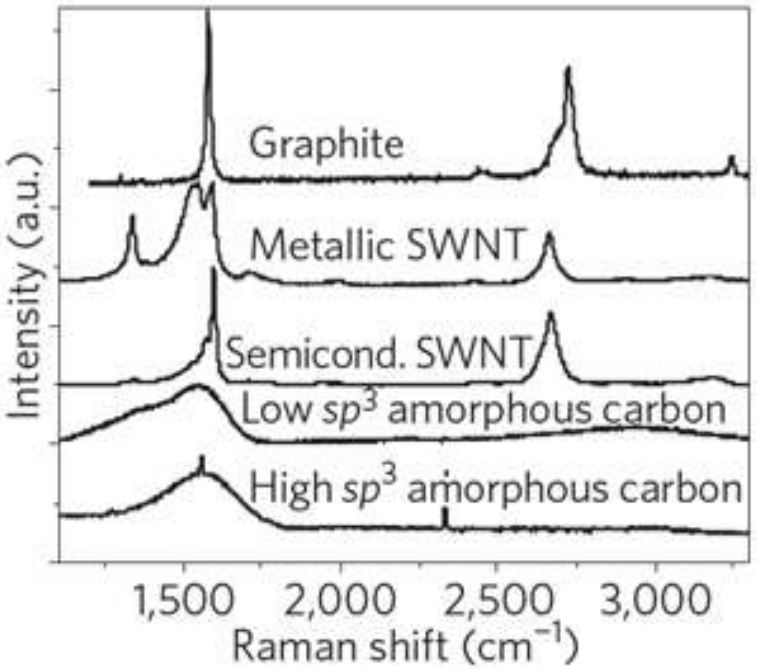

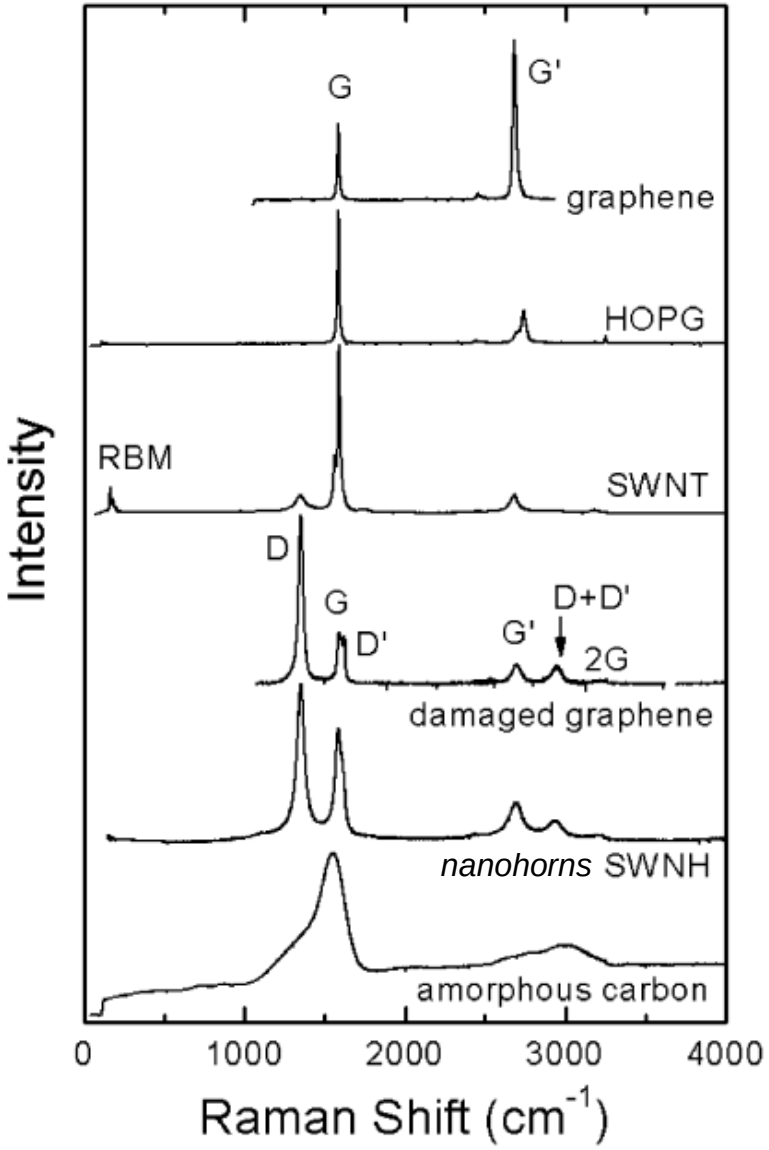

Dresselhaus et al., Nano Lett. (2010)

Raman spectra

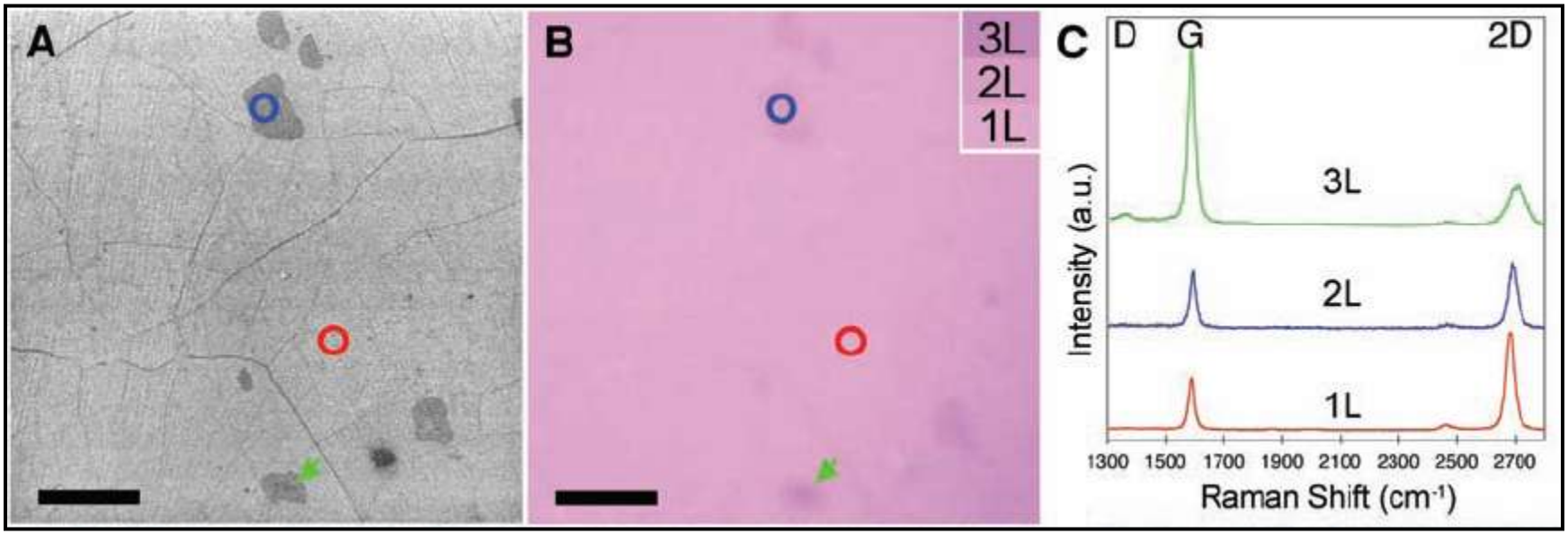

*X. Li, R. S. Ruoff et al., Science **2009**, 324, 1312-1314*

- Ratio between G and 2D bands is an (indicative) measure for the number of layers
  a change in the electronic structure (multiple layers) leads to a change in resonance condition

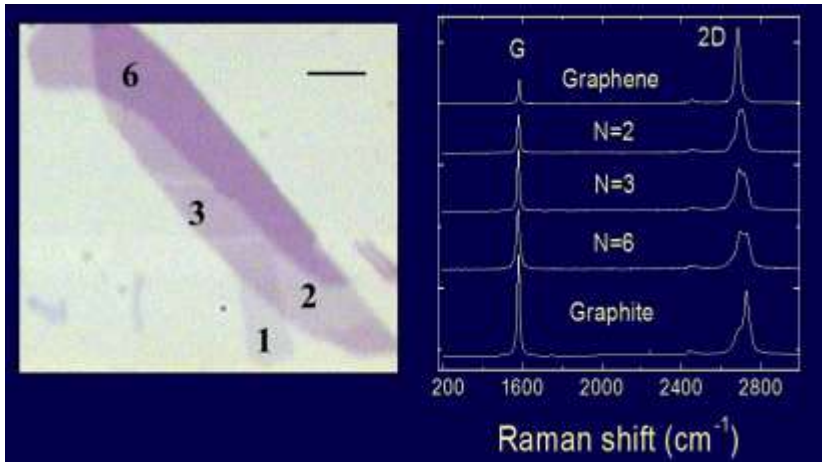

Casiraghi (2008)

Raman spectroscopy: our graphene

On Cu foil

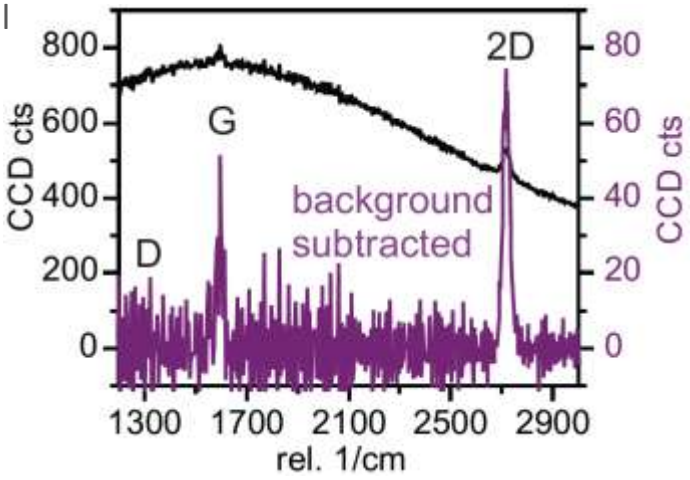

On SiO_2

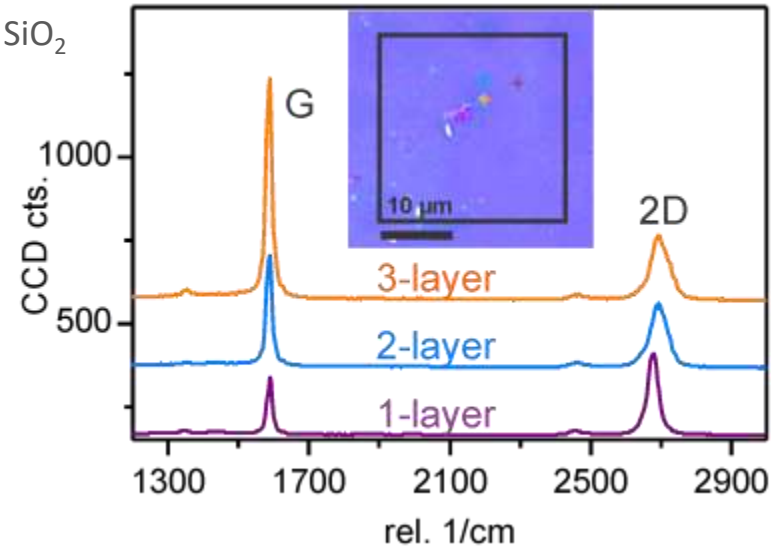

- D-band is a measure of defects and edges
- 2D/G band ratio gives an idea over the number of layers

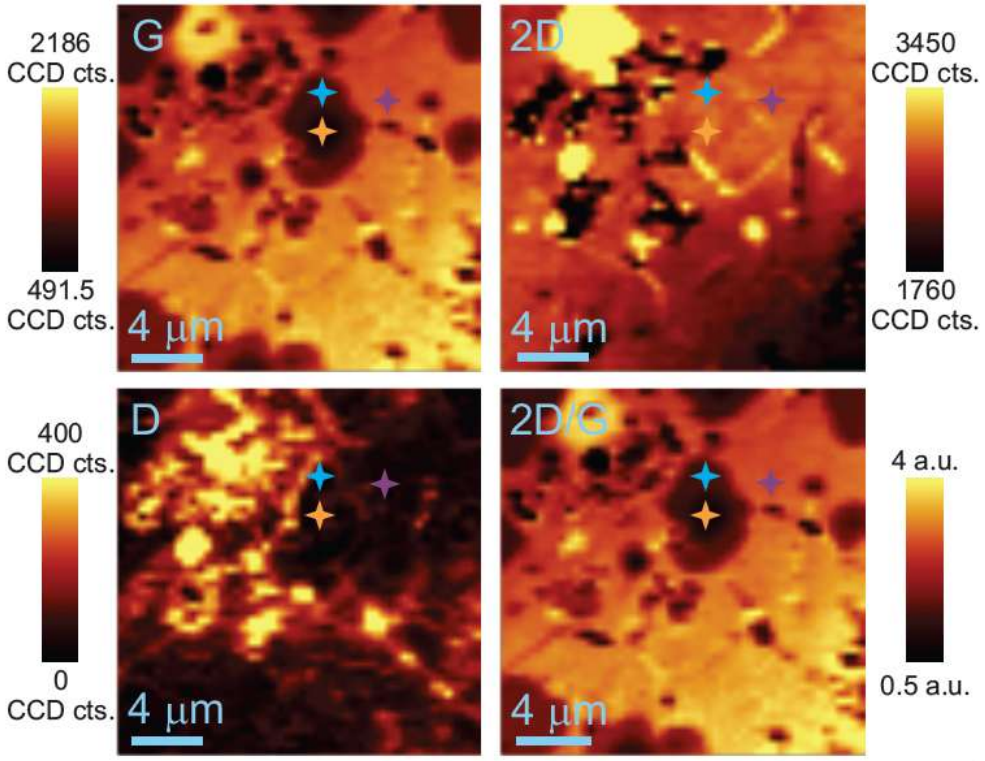

C. Nef et al.

Raman maps for large domains CVD graphene

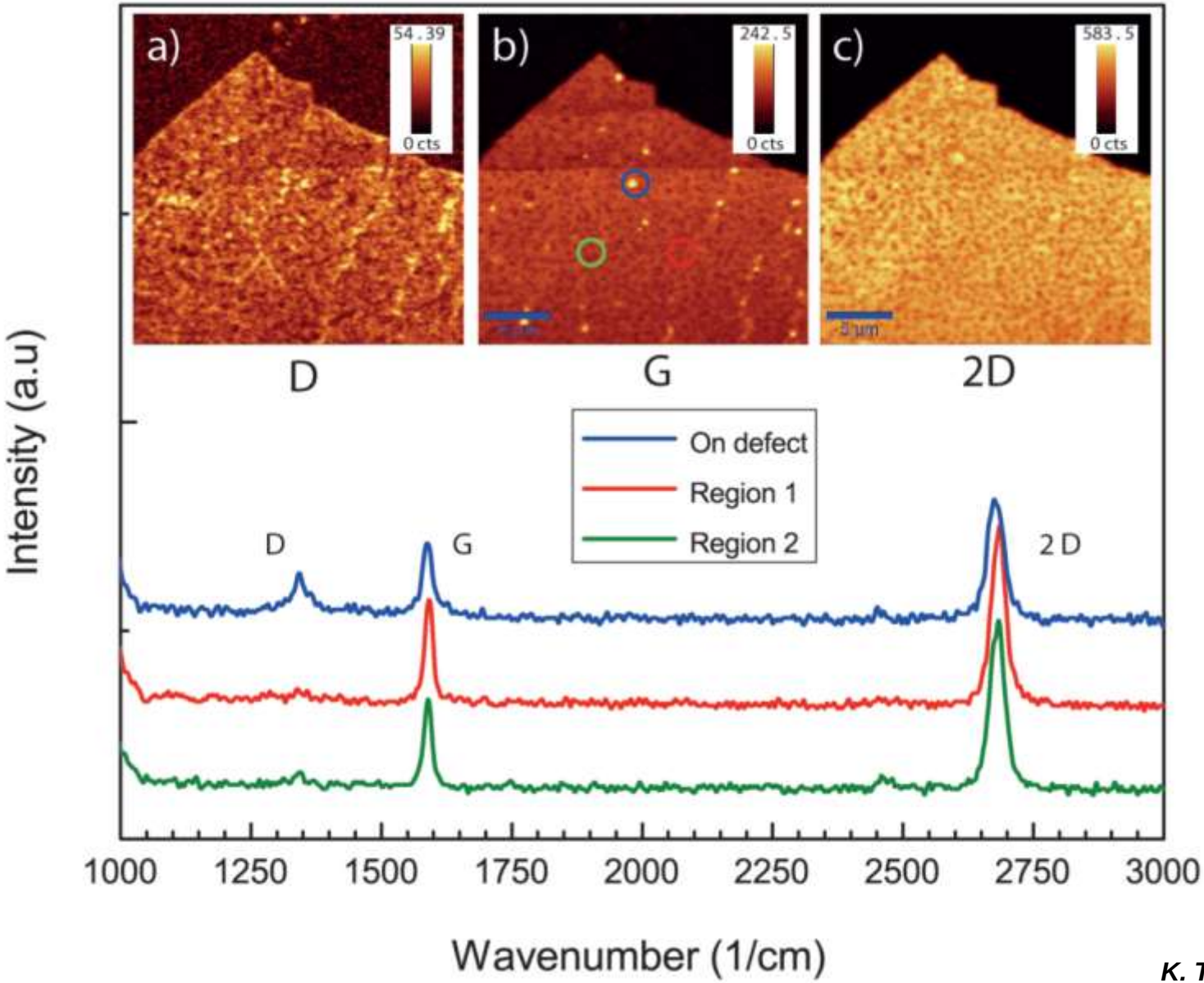

scale bar 5 μm

K. Thodkar et al.

Raman maps for small & large domains CVD graphene

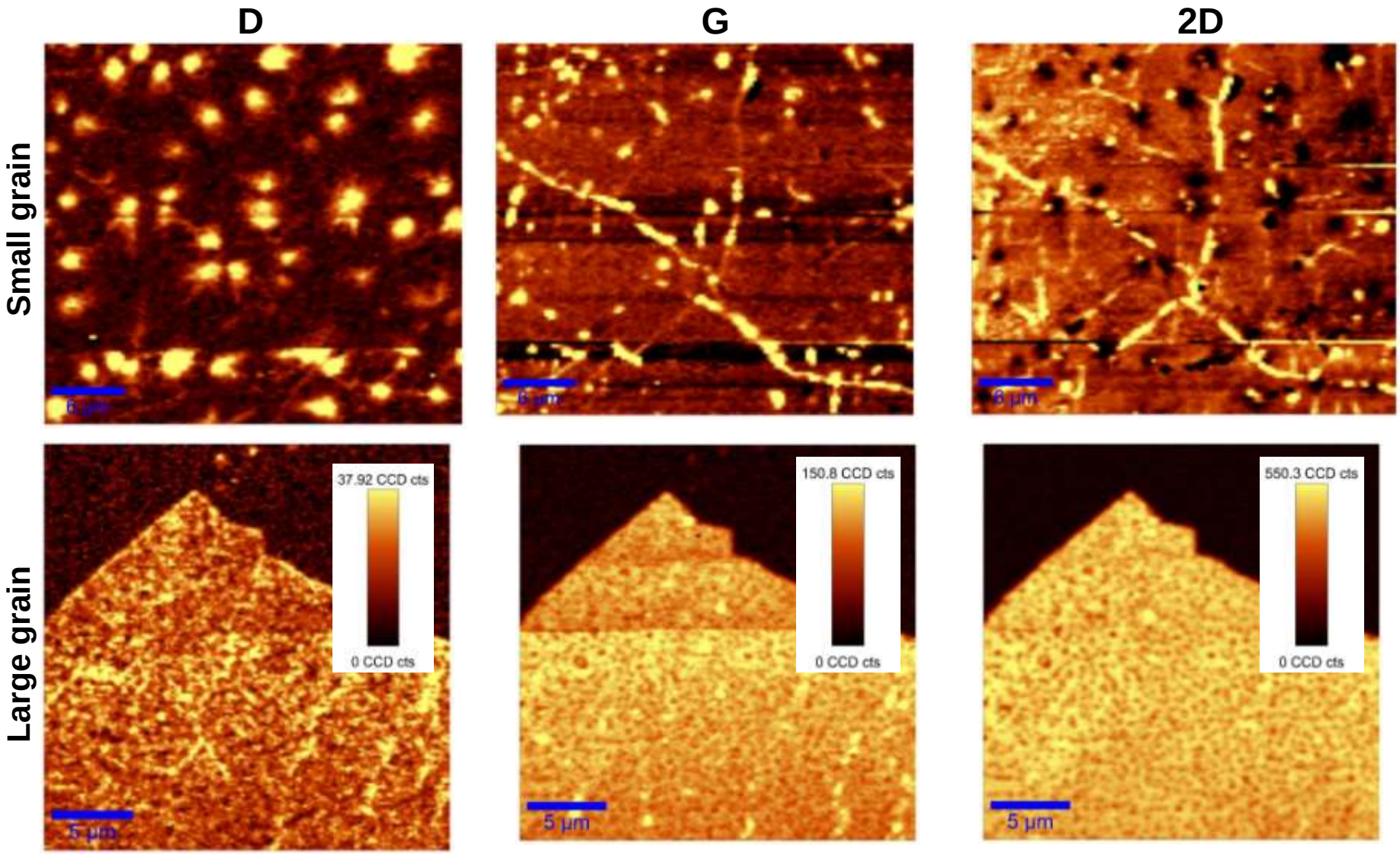

⇨ **homogeneous, low-defects large domains**

K. Thodkar et al.

- graphene structure
- fabrication and CVD growth
- characterization: Raman spectroscopy

Examples

- graphene electroburning for molecular junctions
- Quantum Hall Effect

graphene patterning

e-beam & etch *A. Vladyka et al.*

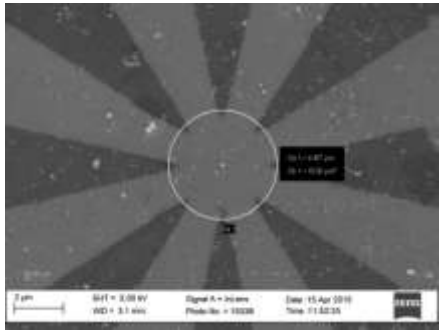

direct writing: He FIB *C. Nef et al.*

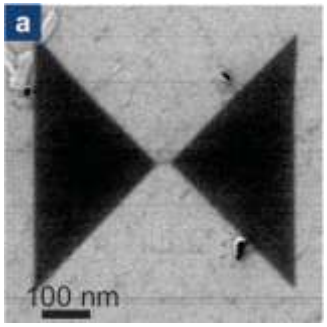

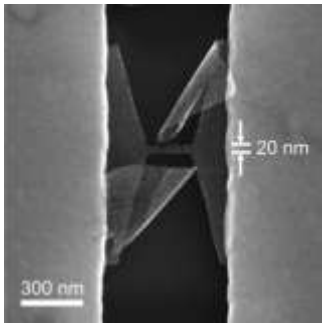

Geller et al., Sci. Rep. 2015

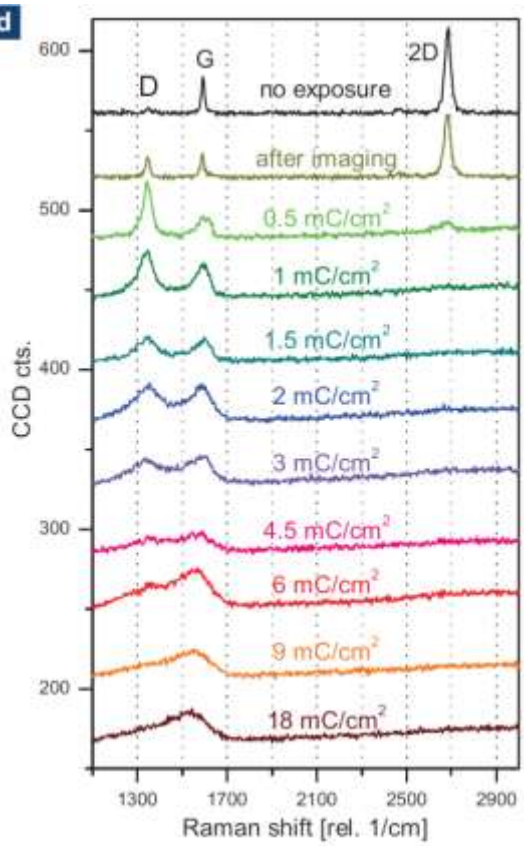

direct writing:
scanning probe (AFM, thermal AFM)
Machida et al., 2015; Stampfer, Ensslin et al.
e-beam induced etching
Geller et al., Sci. Rep. 2015
optical pulses
Lacerda et al., APL 2015

wish list

- resist-free (avoid local doping)
- no additional defects or doping (implantation) induced by patterning
- controlled edges
- upscalable
- …

Molecular and carbon-based electronic systems

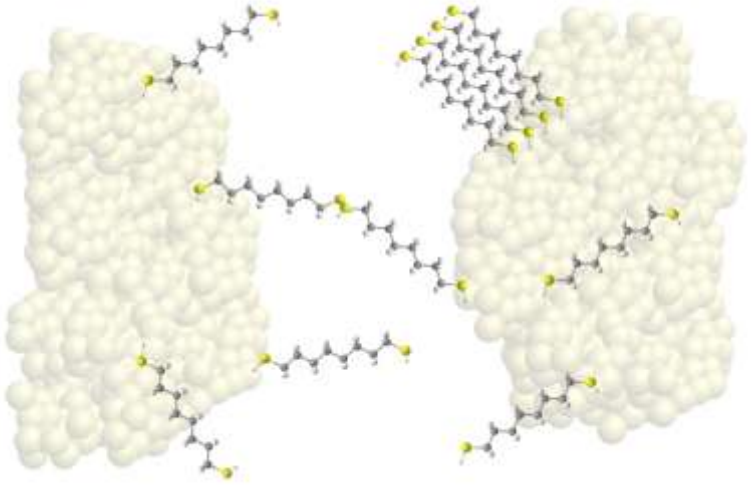

drifting molecules, stochastic anchoring, clustering ⇨ ***undefined junction geometry & conductance***

drifting surface atoms, metal protrusions ⇨ **undefined electrostatic landscape**

⇨ **variability, low-yield and lack of control in key electrical parameters**

Carbon-based contact materials as electrodes:

FLG	vd Zandt et al., Nano Lett. 2011
SWNT	Krupke et al., Nat. Nanotech. 2010
C-fiber tips	Agrait et al., Nanoscale Res. Lett. 2012

⇨ monolayer graphene ...?

paradigm shift for molecular electronics

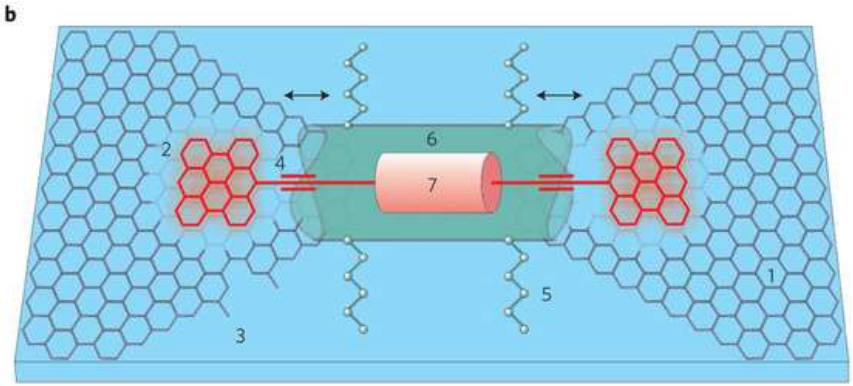

Lörtscher, Nat. Nano 2013

*FP7 ITN **MOLESCO**; see also Focus issue **Nat. Nanotech 2013***

transfer & optical characterization

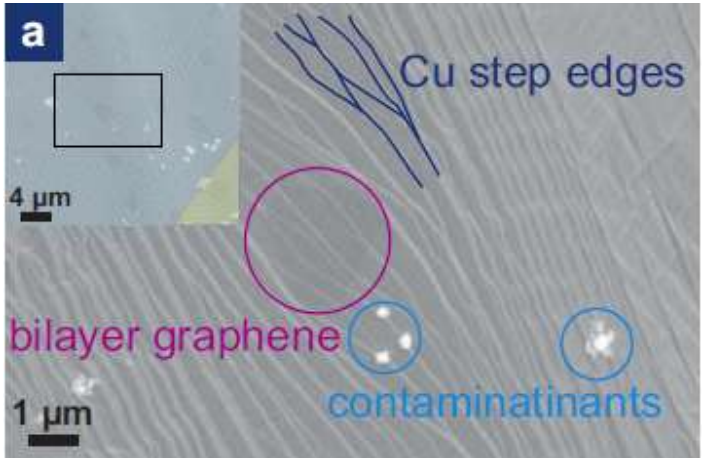

CVD growth

SEM after growth on Cu (LPCVD, CH4, ~1000˚C)

Raman spectroscopy

on Cu

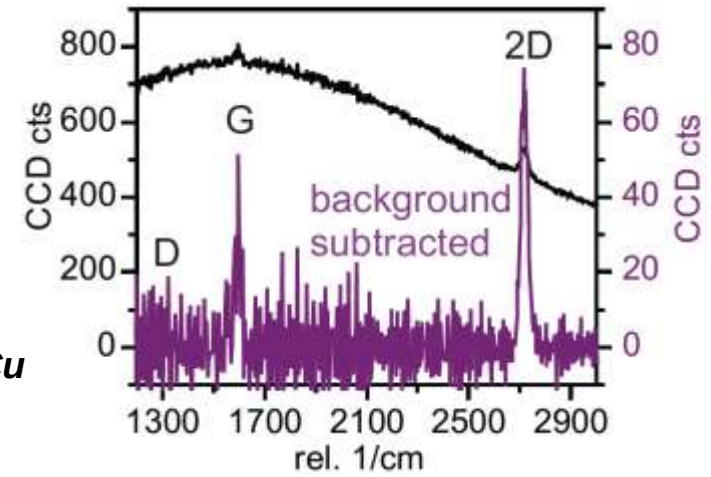

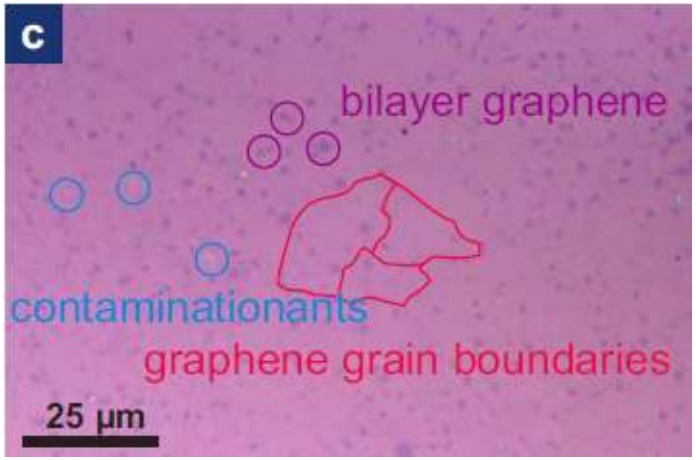

transfer

Optical image after transfer on SiO2/Si

on SiO2/Si

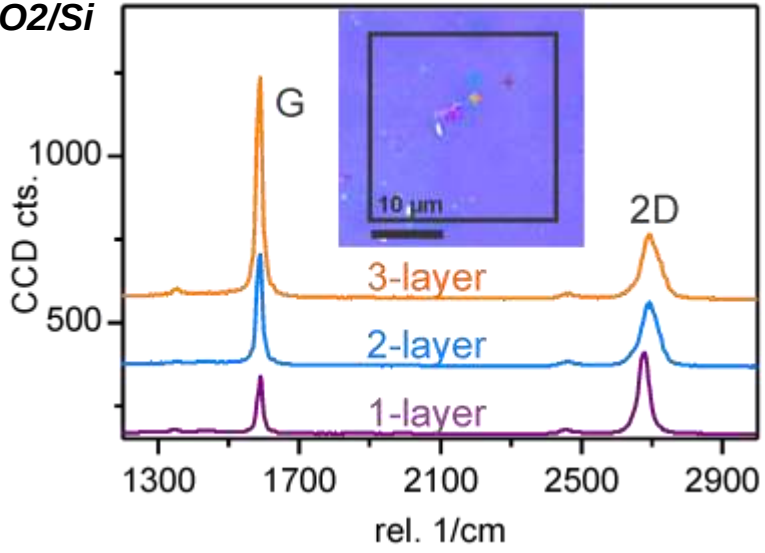

X. Li et al., *Science* **2009**, 324, 1312-1314
X. Li, R. S. Ruoff et al., *Nano Letters* **2009**, 9(12), 4359-4363

C. Nef, W. Fu et al.

Sample fabrication

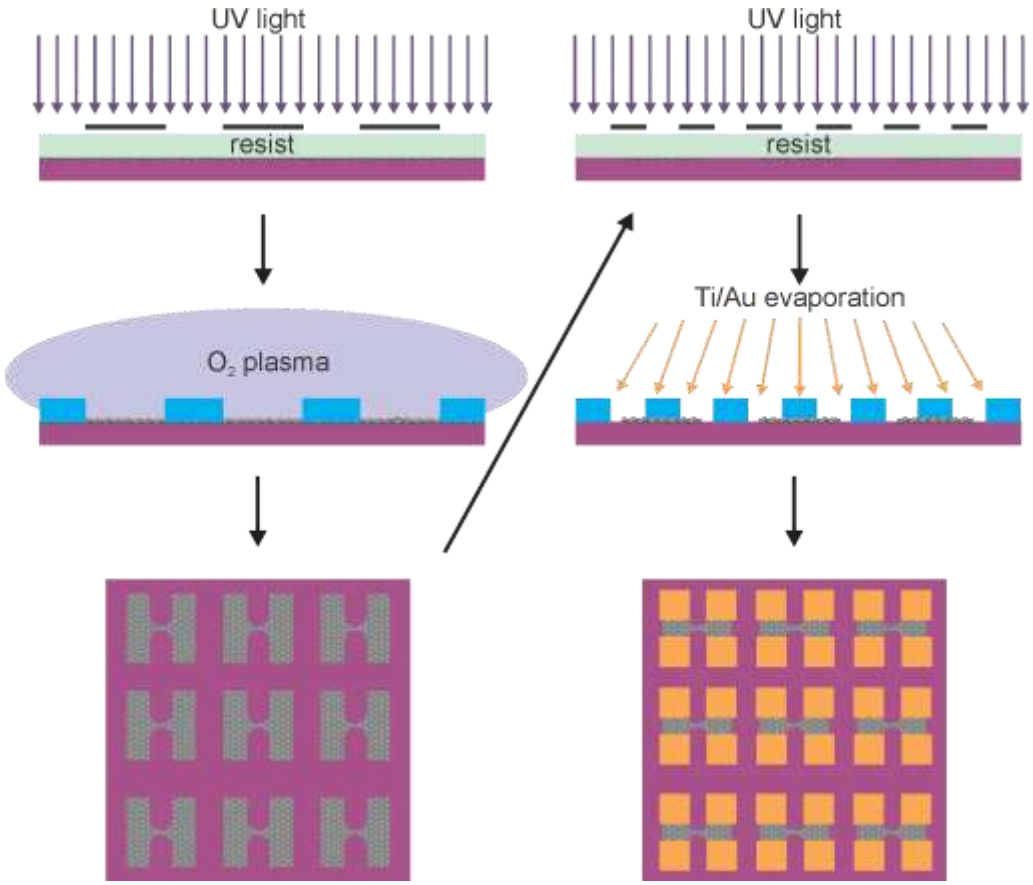

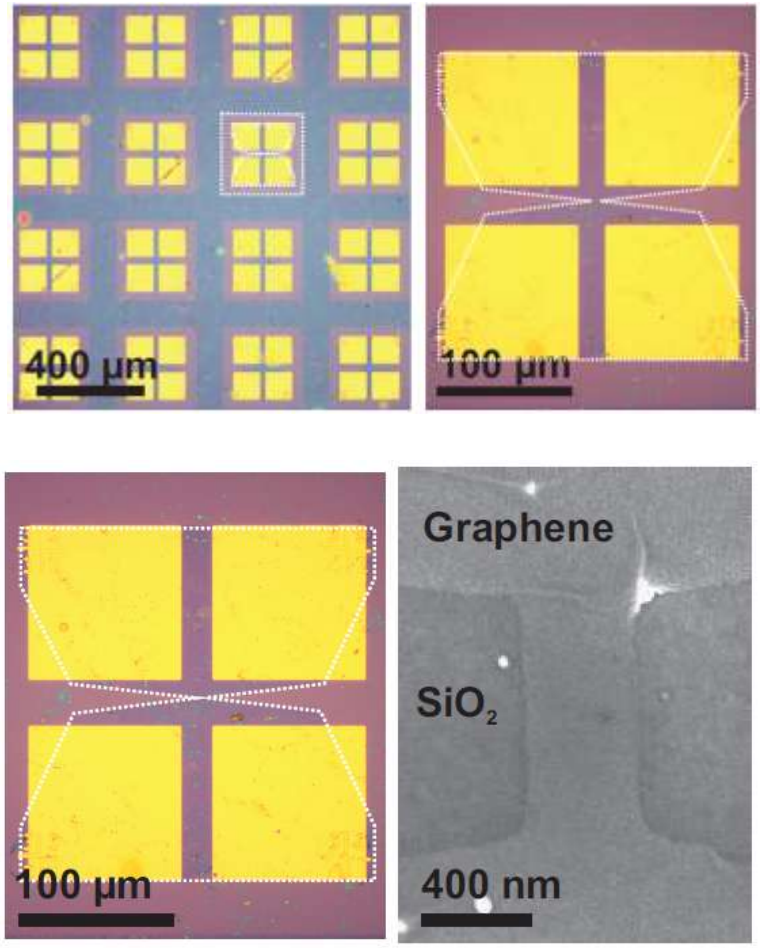

C. Nef et al.

Sample fabrication

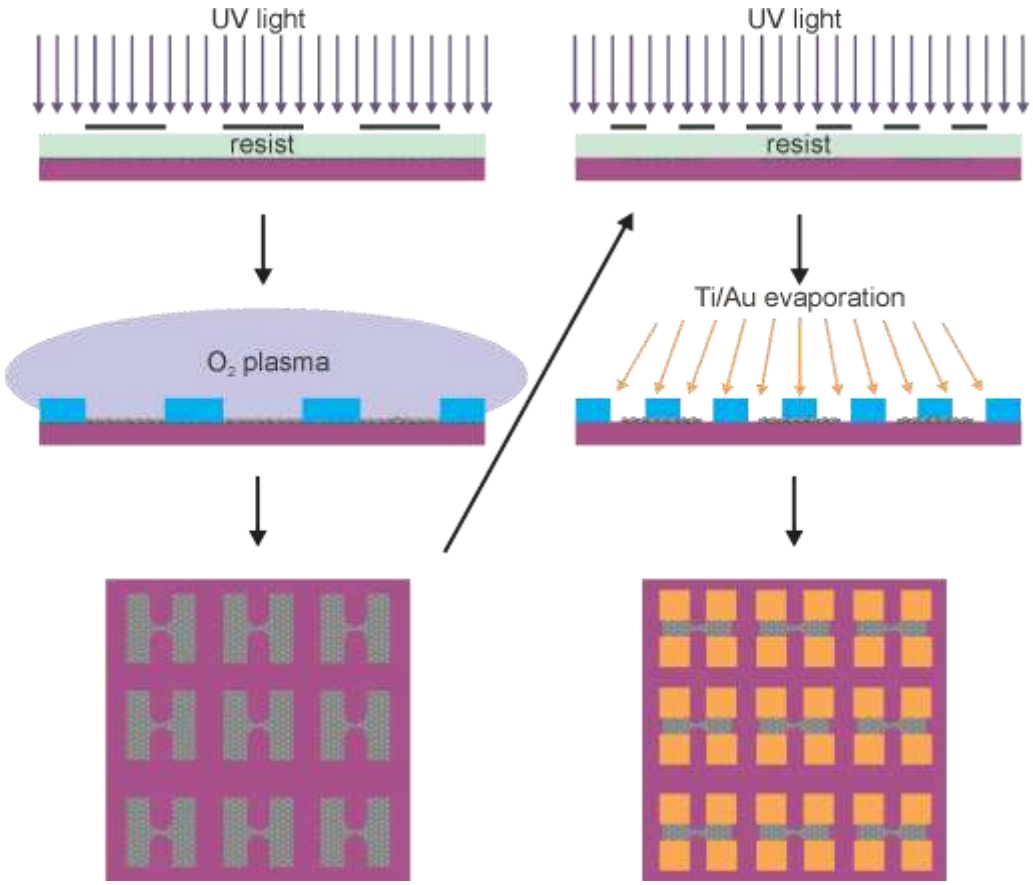

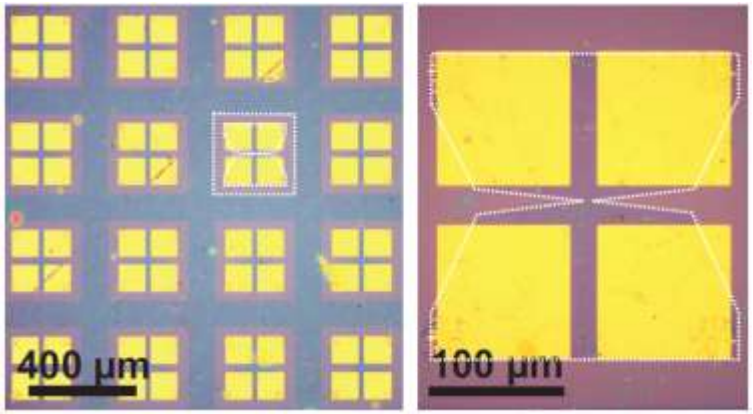

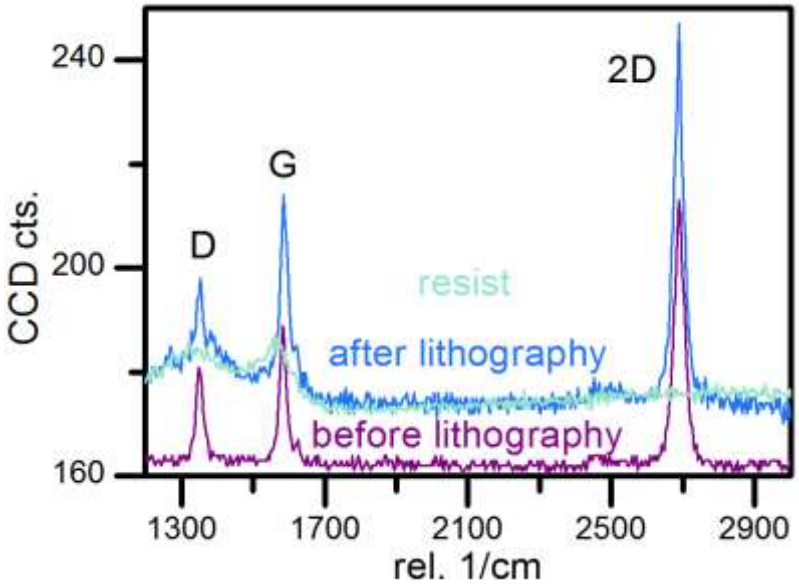

C. Nef et al.

electroburning process

Applied voltage

*similar approach as **electromigration** in metal contacts*

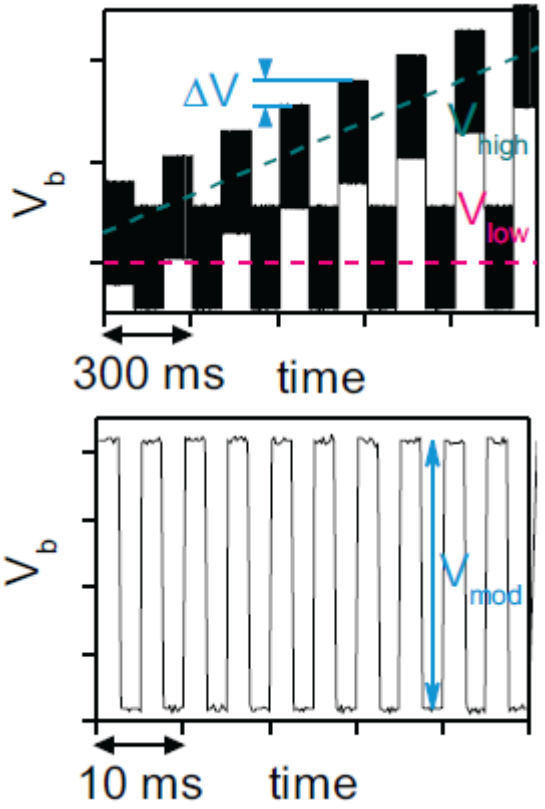

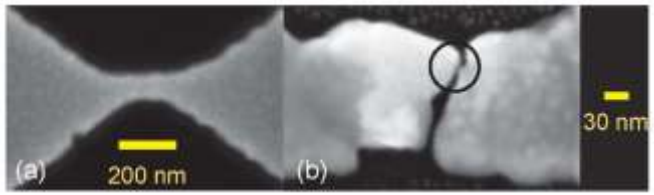

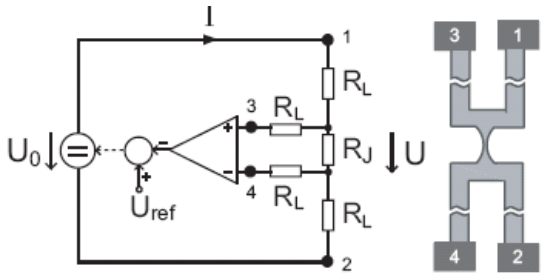

Z.-M. Wu et al., APL (2007); PRB (2008)

graphene

FLG: Prins et al., *Nano Lett. 2011*

MLG: **Nef, Posa et al**., *Nanoscale 2014*

Lau et al., *PCCP 2014*

electroburning process

Applied voltage

similar approach as electromigration in metal contacts

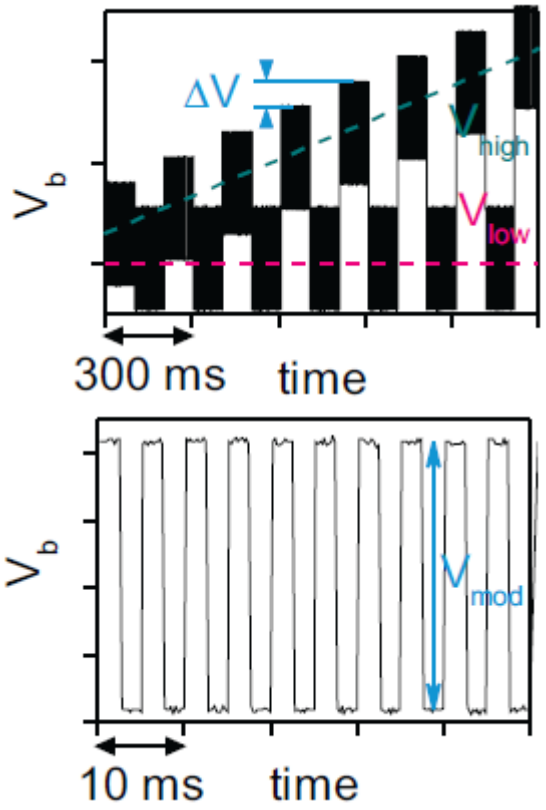

Differential resistance

$R=\Delta I/V_{mod,}$ at high and low bias vs time

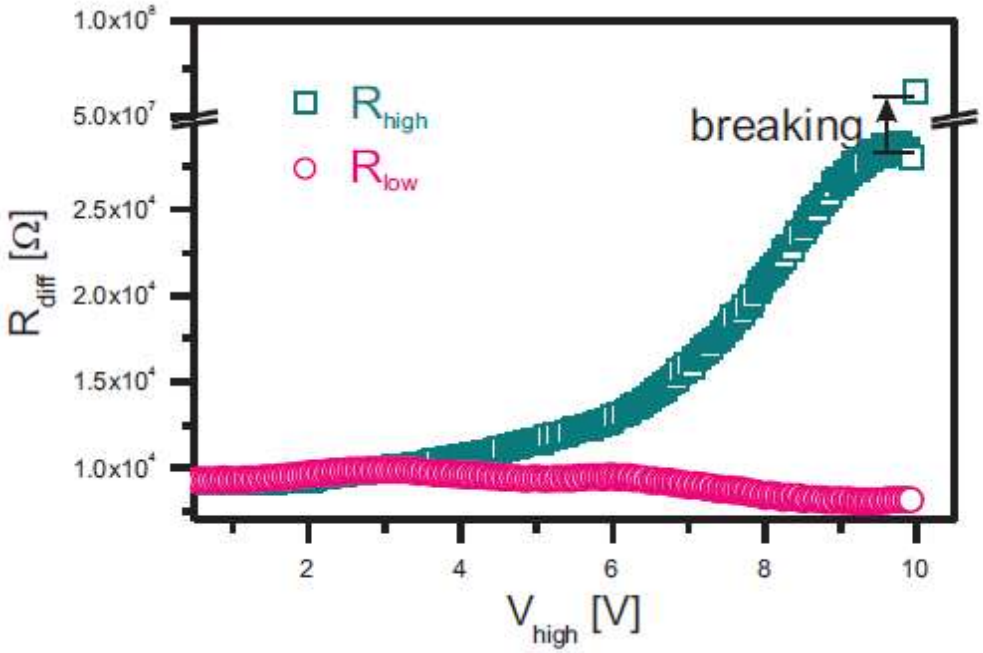

- Joule heating seen as a difference between R_{high} and R_{low}
  - Junction breaks after a certain V_b is reached

NB: EB performed on annealed devices

C. Nef, et al., Nanoscale 2014

nanoscale gaps in graphene

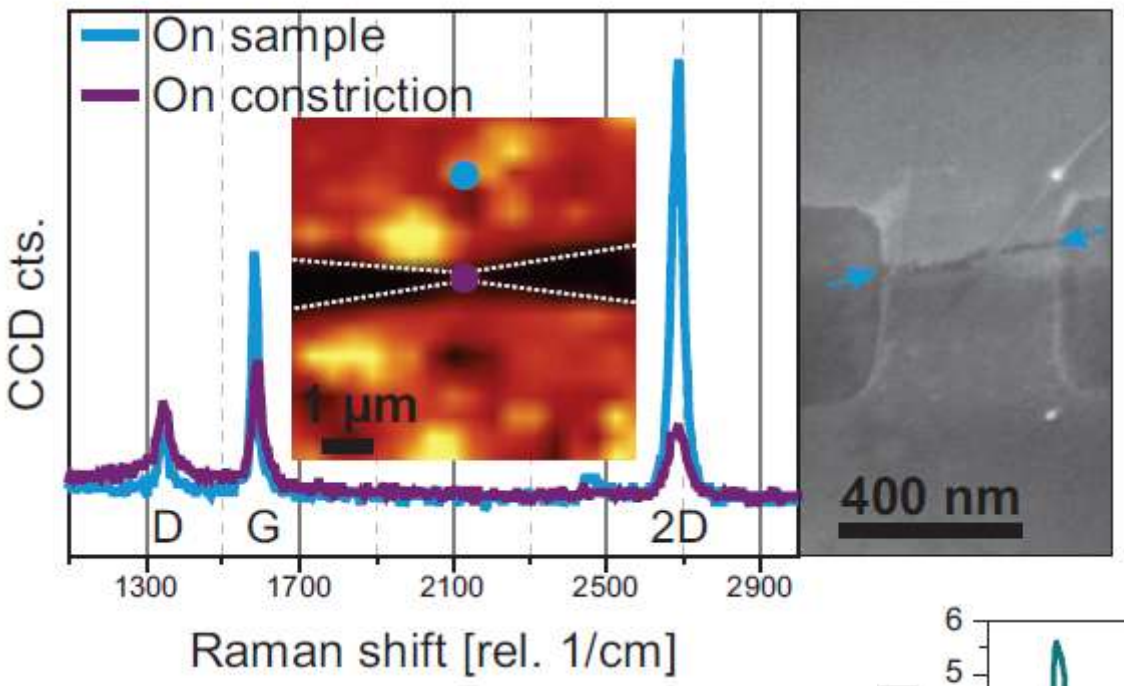

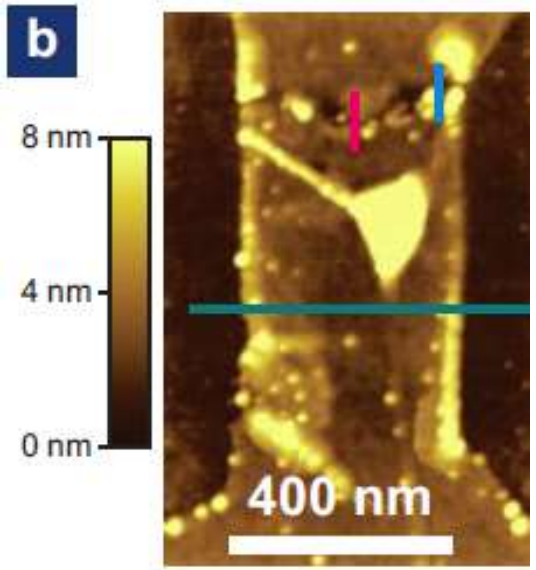

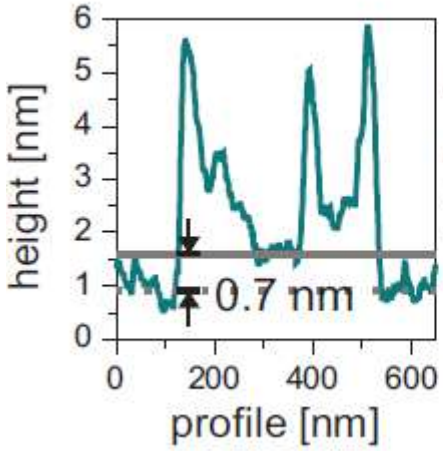

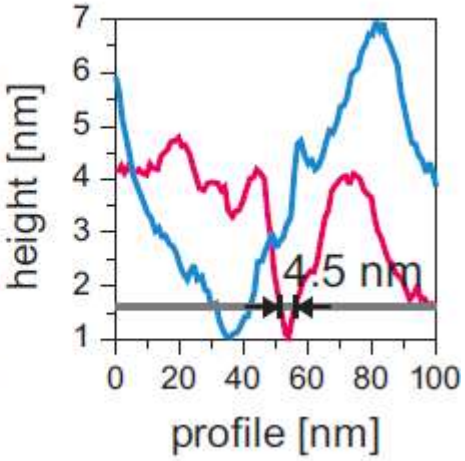

⇨ **amorphous C in gap**
enhanced bck, G/2D change

⇨ **gap/slit creation** (yield >95%)
typ. a few nm wide

C. Nef, et al., Nanoscale 2014

nanoscale gaps in graphene: tunnneling behavior

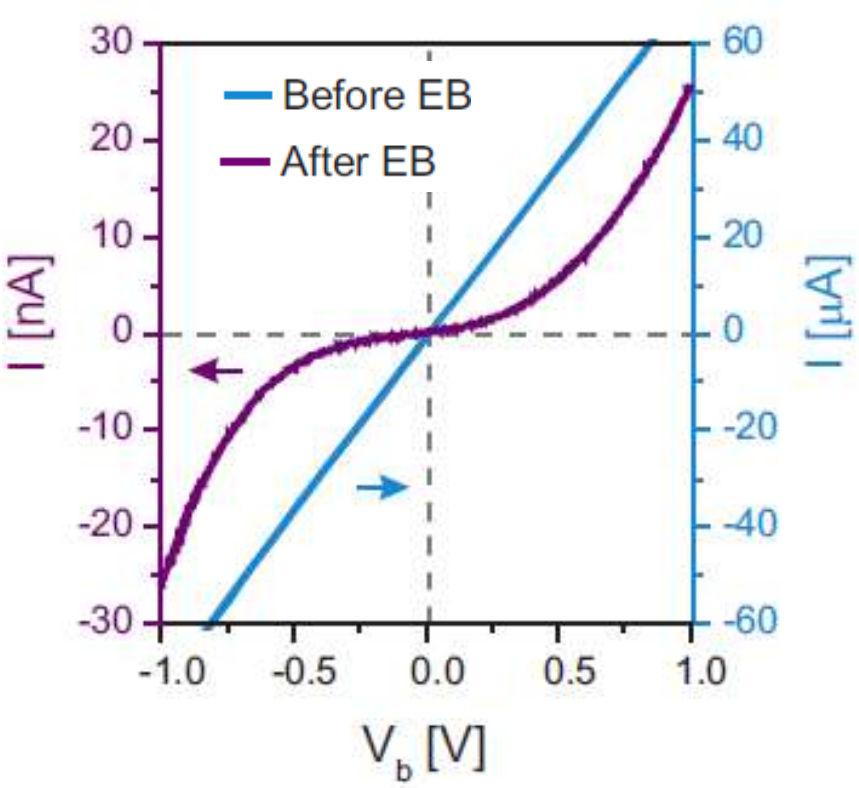

- A and Φ are not robust, but d changes by max 50%

- fitting of junctions with lower R leads not to a shorter d, but a lower Φ

Gap width estimates (Simmons fitting)

⇨ **0.3nm ≤ d ≤ 2.2nm**

$$I = Ac_1\left(\frac{\Phi - eV}{2}e^{-c_2\sqrt{\frac{\Phi-eV}{2}}} - \frac{\Phi + eV}{2}e^{-c_2\sqrt{\frac{\Phi+eV}{2}}}\right)$$

$$c_1 = \frac{e}{2\pi h d^2}; \qquad c_2 = \frac{4\pi d}{h}\sqrt{2m}$$

A : Junction area
d : Gap width
Φ : Barrier height

breakdown mechanism
burning ? *(p=10^{-5}mbar)*

NB: carbon sublimation
A.Barreiro et al., NL 2012
F. Börrnert et al., NL 2012

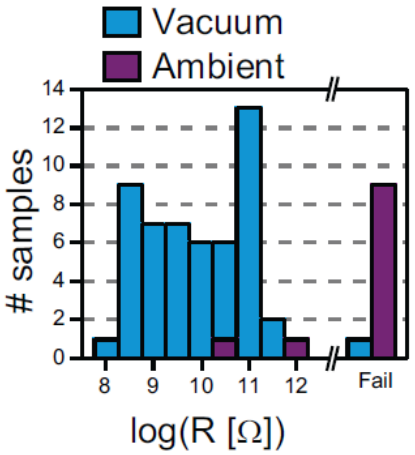

C. Nef, et al., Nanoscale 2014

phonons in graphene

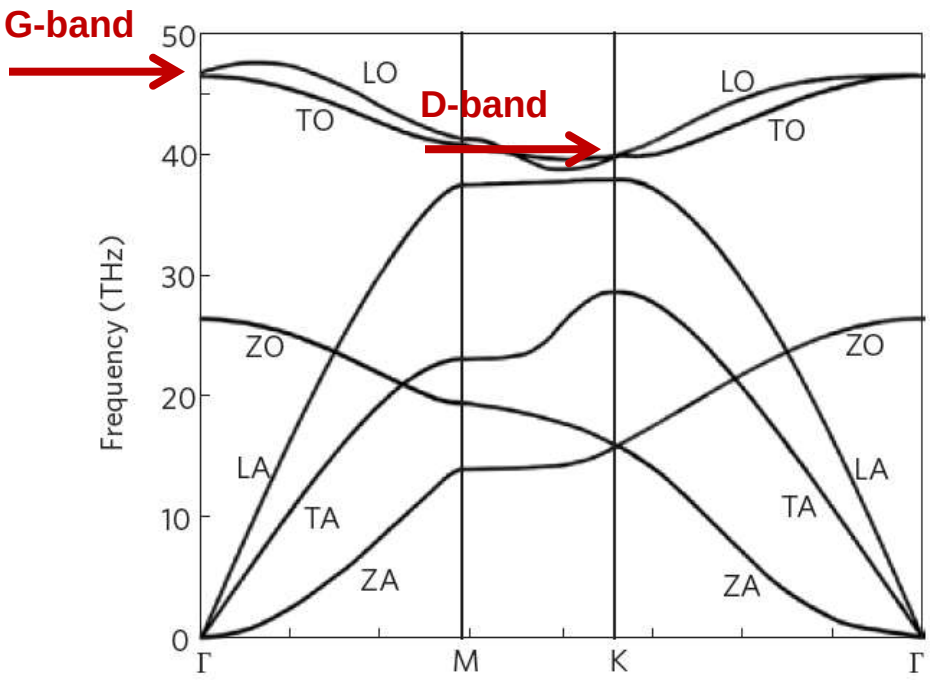

At room temperature:

$$\omega \sim \frac{k_B T}{\hbar} \sim 6 \text{ THz}$$

Phonon branches carrying heat:

- Longitudinal acoustic (LA)
- Transverse acoustic (TA)
- Out-of-plane acoustic (ZA)

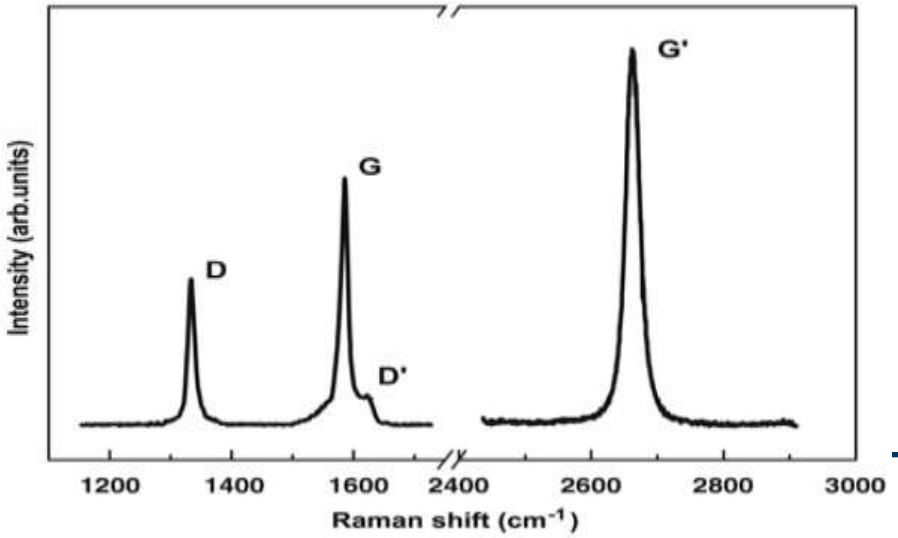

A. A. Balandin et al., *Nature materials* **2011**, 10, 569

temperature calibration

Raman peak shift as thermometer

- increasing T leads to softening of phonon modes
NB: 2D peak (Intervalley 2-phonon process) shift more marked, see e.g. Balandin et al., APL 2007

shifts for Si (520 cm^{-1}), D & 2D peaks

NB: G peak and FWHM peaks depend on carrier concentration n and n=n(T)

⇨ **2D peak shift -0.051 cm^{-1}K^{-1}**

Si: inelatic phonon scattering model

$$Pos(Si) = \omega_0 + \gamma\left(1 + \frac{2}{e^x - 1}\right)$$
$$x = \hbar\omega_0 / k_B T$$

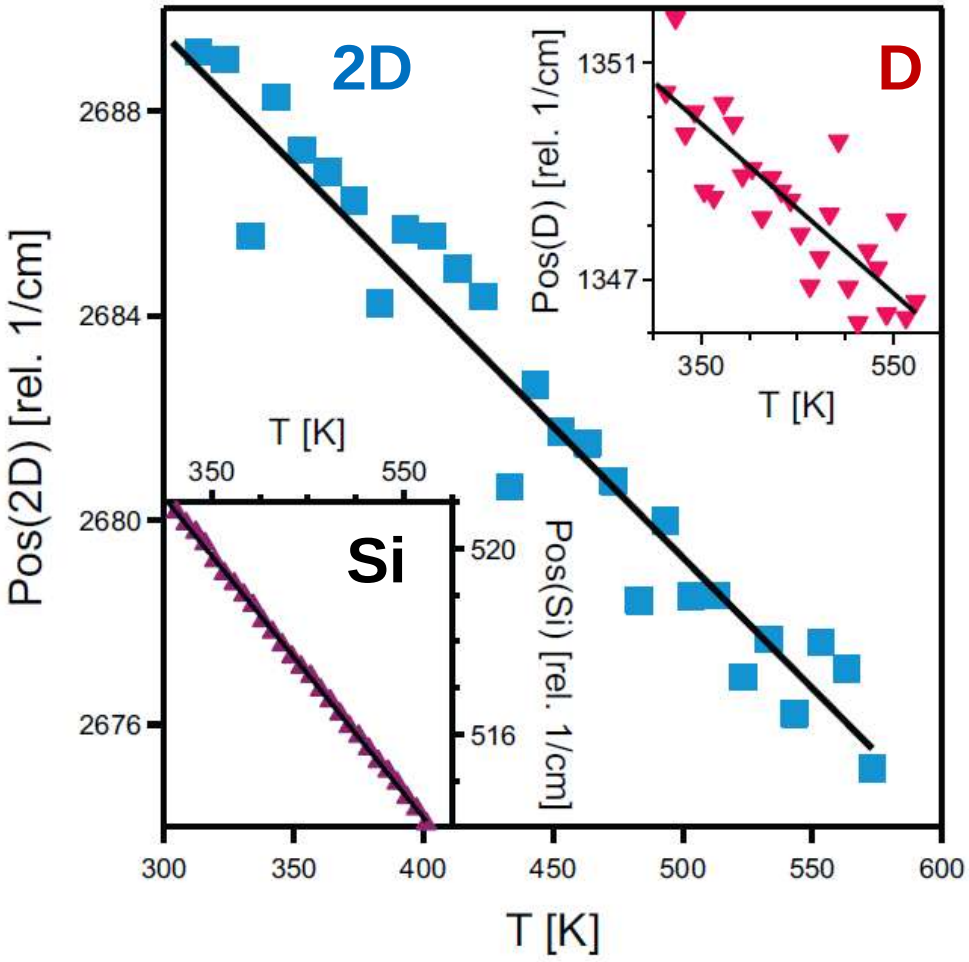

⇨ **calibration of Raman peaks shift** (heating stage)

C. Nef, et al., Nanoscale 2014

temperature during electroburning

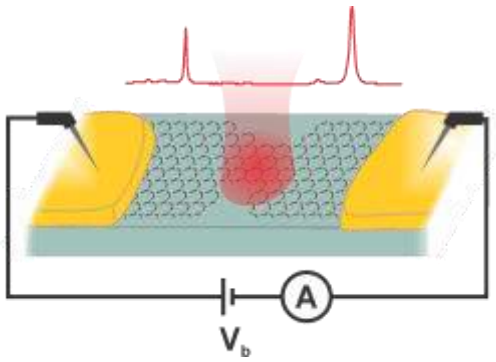

Raman spectroscopy at constriction during EB
⇨ **2D peak shift**

using T dep. observed -0.051 $cm^{-1}K^{-1}$

~600K
at breakdown

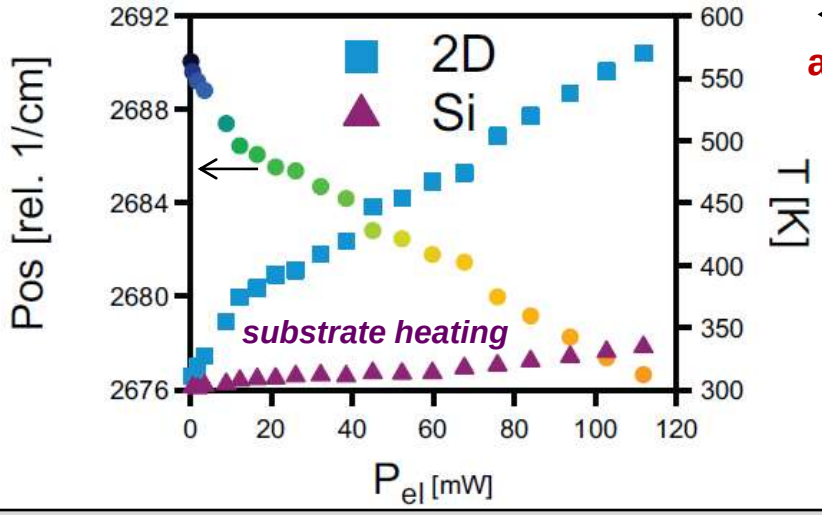

NB: T averaged over laser spot size (≈400nm)

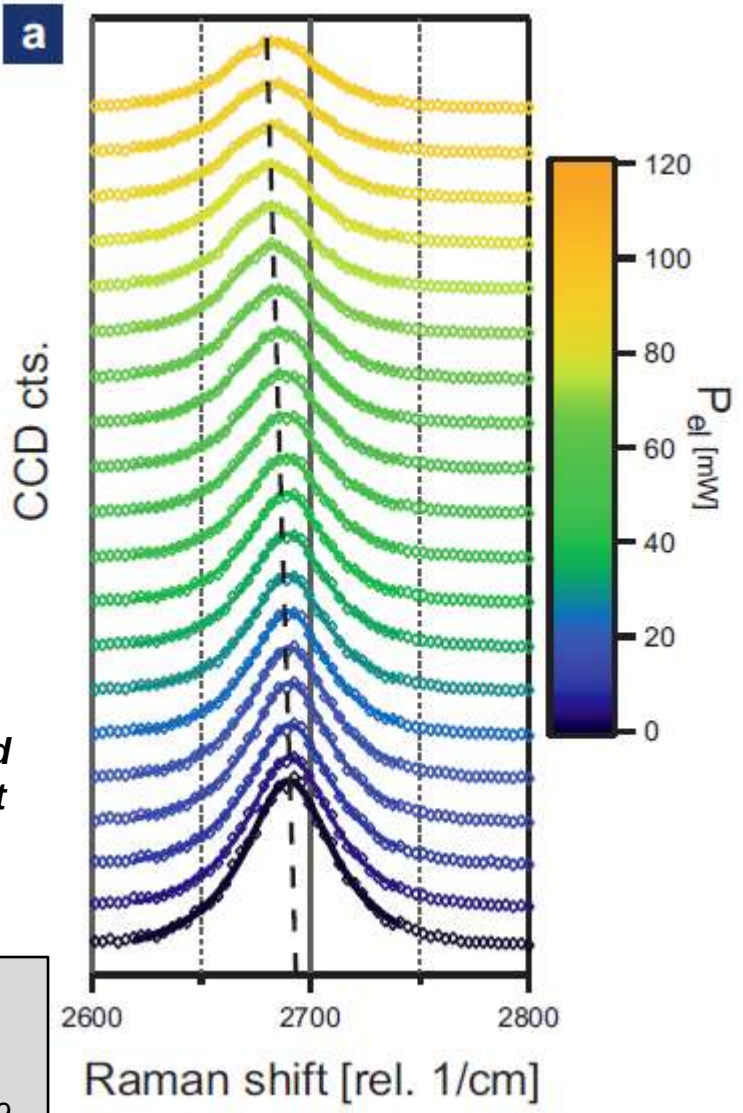

470K	graphene oxidation	*Liu et al., Nano Lett. 2008*
720K	spontaneous etch pits	
1'000K	breakdown, supported	*Freitag et al., Nano Lett. 2009*
2'000K	breakdown, suspended	*Dorgan et al., Nano Lett. 2013*

C. Nef, et al., Nanoscale 2014

temperature dependence of the resistance

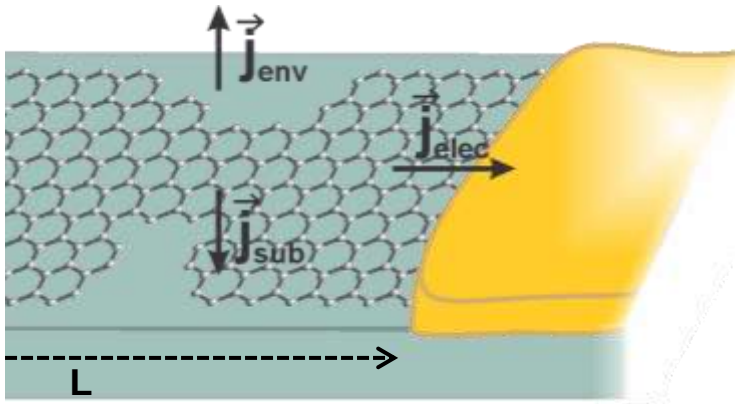

heat dissipation

- **diffusive** at RT

mfp: $\lambda_{ph} \approx 100nm$, $\lambda_e \approx 20nm$; $L = 20\mu m \gg \lambda_e, \lambda_{ph}$ *(supported graphene)*

- $\mathbf{J_{sub}} \gg \mathbf{J_{env}}, \mathbf{J_{elec}}$

vacuum, remote electrodes

Joule heating: e-ph scattering

$$\rho(T) = \rho_0 + \underbrace{\alpha T}_{\rho_A} + \underbrace{\beta \left(\frac{1}{e^{E_0/k_B T} - 1} \right)}_{\rho_B}$$

acoustic ph ***optical ph & remote interface ph*** *(SiO_2-graph.)*

$\rho_A \ll \rho_B$ $\alpha \sim 0.15\ \Omega/K$ (linear fit: 3.9 Ω/K)

Fit $\boldsymbol{E_0 = 141}$ **meV**

SiO_2 surface phonons at 59 meV and 155 meV

Graphene optical phonons ~ 149 meV

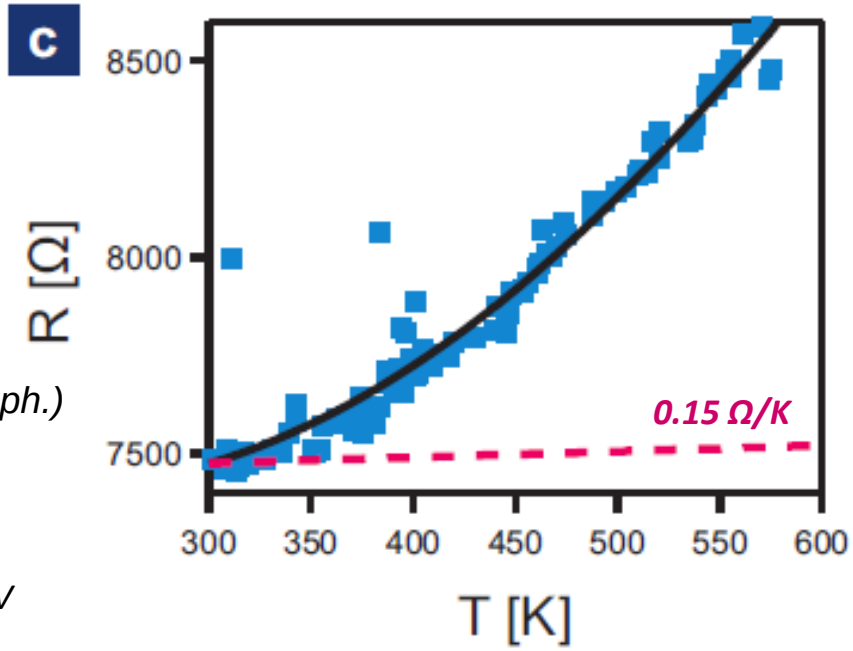

E. Pop et al., *Nat. Comm. 2013*

NB: valid at saturating charge carrier density, far from CNP

C. Nef, et al., Nanoscale 2014

preliminary hints of molecular conductance

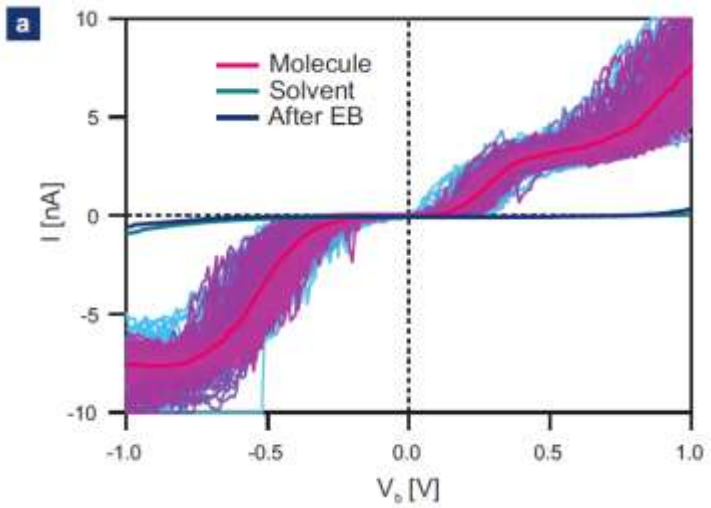

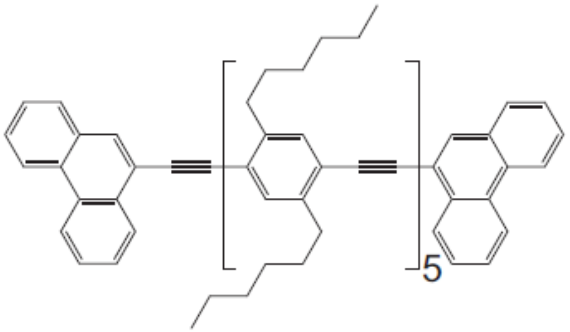

molecule: M. Mayor et al.

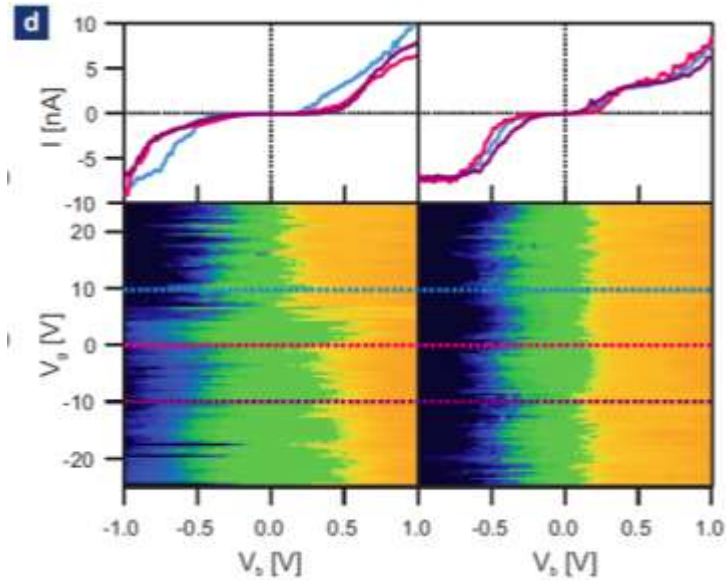

gating: solvent only

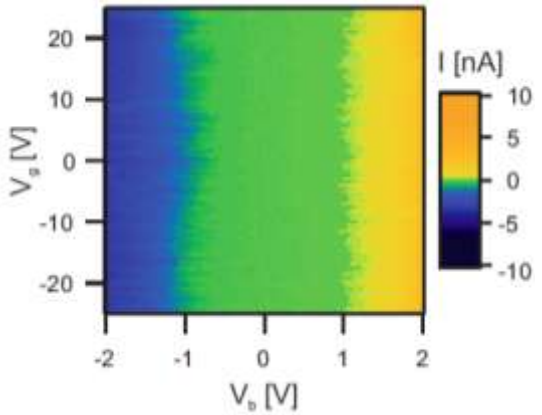

C. Nef, et al.

simple one-level model

Analytical expression for the current

$$I(E,V) = \frac{2e}{h} \int_{}^{\infty} T(E,V)[f(E-\mu_2) - f(E-\mu_1)]dE$$

At low T , Fermi functions ≈ Heaviside step functions, and

$$I(V) = \frac{2e}{h} \int_{\frac{-eV}{2}}^{\frac{eV}{2}} T(E,V)dE$$

Using the expressions

$$T(E,V) = \frac{4\Gamma_1\Gamma_2}{\left(E - E_0(V)\right)^2 + \left(\Gamma_1 + \Gamma_2\right)^2}$$

$$E_F(V) = \frac{eV}{2} \cdot \frac{\Gamma_1 - \Gamma_2}{\Gamma_1 + \Gamma_2}$$

we can write

$$I(V) = \frac{8e}{h} \cdot \frac{\Gamma_L\Gamma_R}{\Gamma_L + \Gamma_R} \left[\arctan\left(\frac{2E_0 + eV\left(\frac{\Gamma_L - \Gamma_R}{\Gamma_L + \Gamma_R} + 1\right)}{2\left(\Gamma_L + \Gamma_R\right)} \right) - \arctan\left(\frac{2E_0 + eV\left(\frac{\Gamma_L - \Gamma_R}{\Gamma_L + \Gamma_R} - 1\right)}{2\left(\Gamma_L + \Gamma_R\right)} \right) \right]$$

3 fit parameters Γ_1, Γ_2, $E_0 = E_0(V)$

preliminary hints of molecular conductance

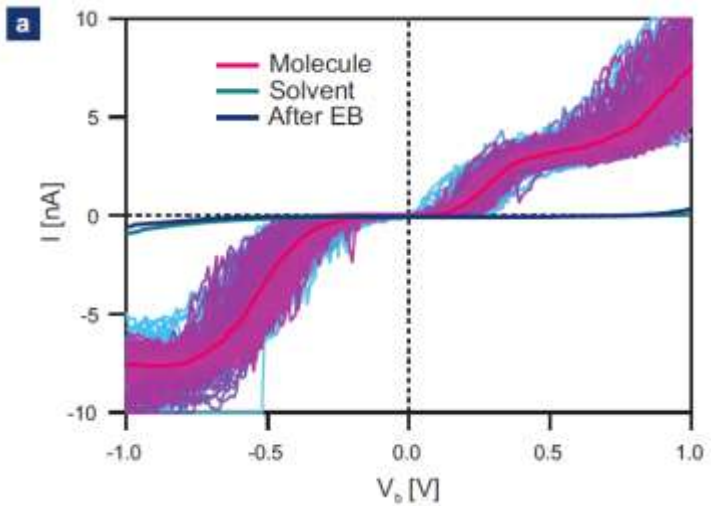

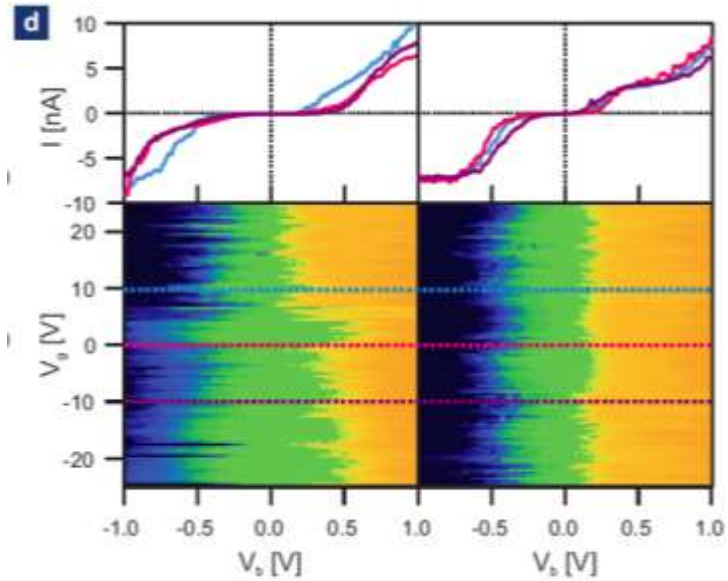

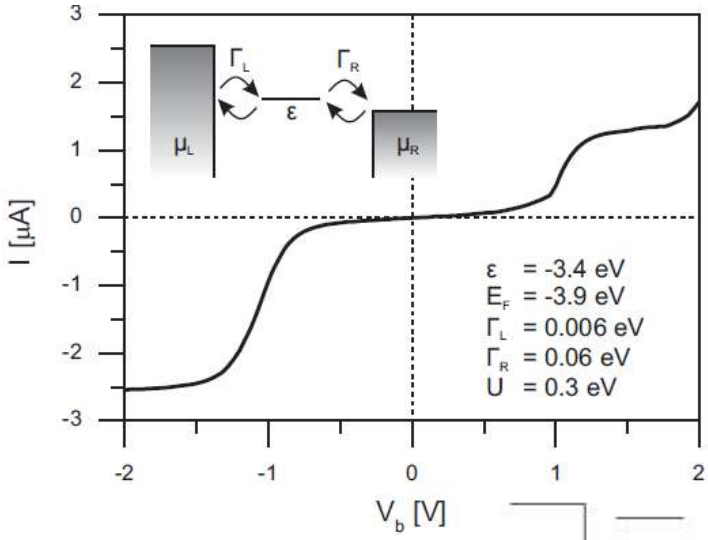

***qualitative* behavior using simple 1 level model**

including CB and level broadening

(Datta et al. Nanotech. 2004)

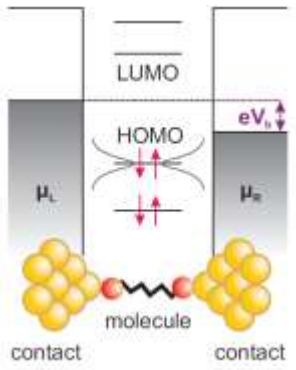

$$I = \frac{2e}{\hbar}\int_{-\infty}^{\infty} D(E)\frac{\Gamma_L\Gamma_R}{\Gamma_L+\Gamma_R}[f_L(E,\mu_L) - f_R(E,\mu_R)]dE$$

$$D(E) = \frac{1}{2\pi}\frac{\Gamma_L+\Gamma_R}{(E-\varepsilon)^2 + ((\Gamma_L+\Gamma_R)/2)^2}$$

C. Nef, et al.

- graphene structure
- fabrication and CVD growth
- characterization: Raman spectroscopy

Examples

- graphene electroburning for molecular junctions
- Quantum Hall Effect

classical Hall effect

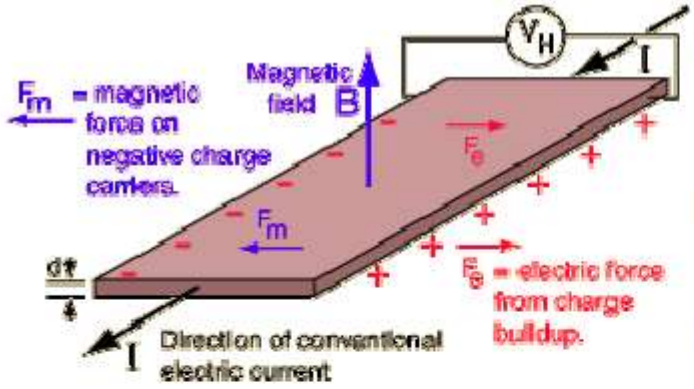

Force: $\vec{F} = \vec{F}_e + \vec{F}_m = q(\vec{E} + \vec{v} \times \vec{B})$

Electric Field (F_y=0): $E_y = v_x B_z$

Current density: $J_x = nqv_x$

q = charge of carrier

n = carrier density

Hall Conductivity $\rho_{xy} = \frac{E_y}{J_x} = \frac{B}{nq}$

The Hall conductivity measures

- The density of the mobile charge carriers
- The sign of the charge carriers (e<0!)

Kane, Princeton

Hall effect

klassisch

E. H. Hall:
„On the New Action of Magnetism on a Permanent Electric Current“,
PhD-thesis,
The Johns Hopkins University, 1880

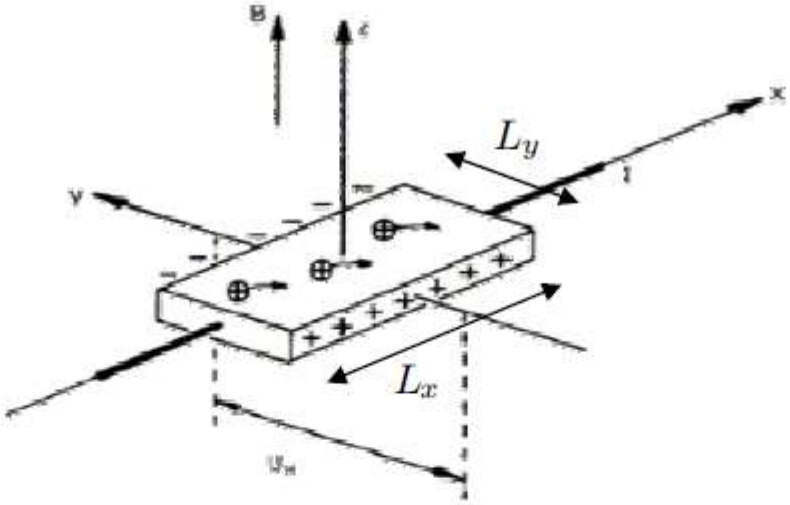

$$R_x = \frac{1}{en\mu}\frac{L_x}{L_y}$$

$$R_H = \frac{U_H}{I_x} = \frac{B}{en} \qquad (1)$$

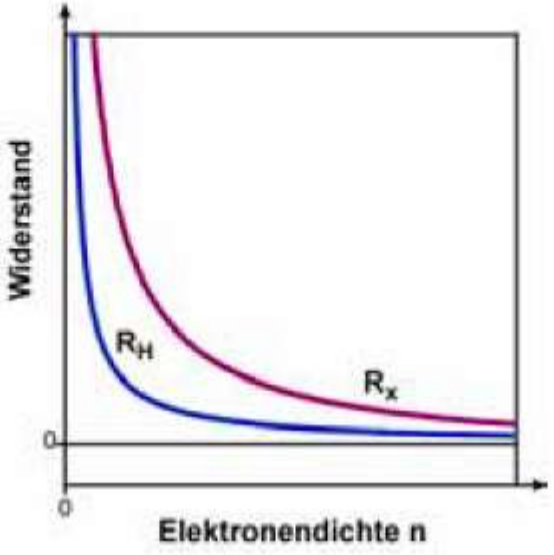

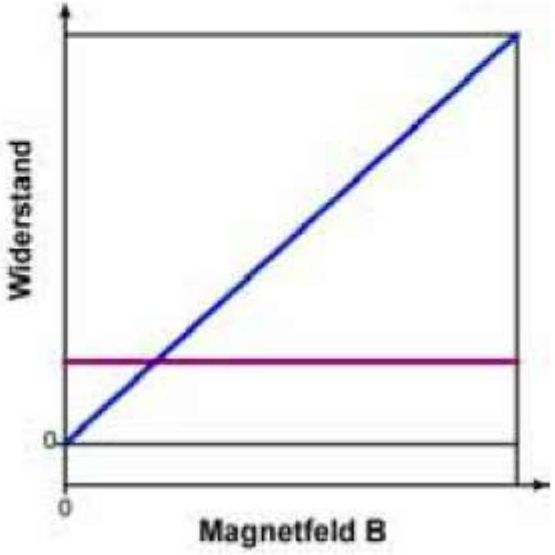

quantum Hall effect

Quantum Hall effect in 2D MOSFET

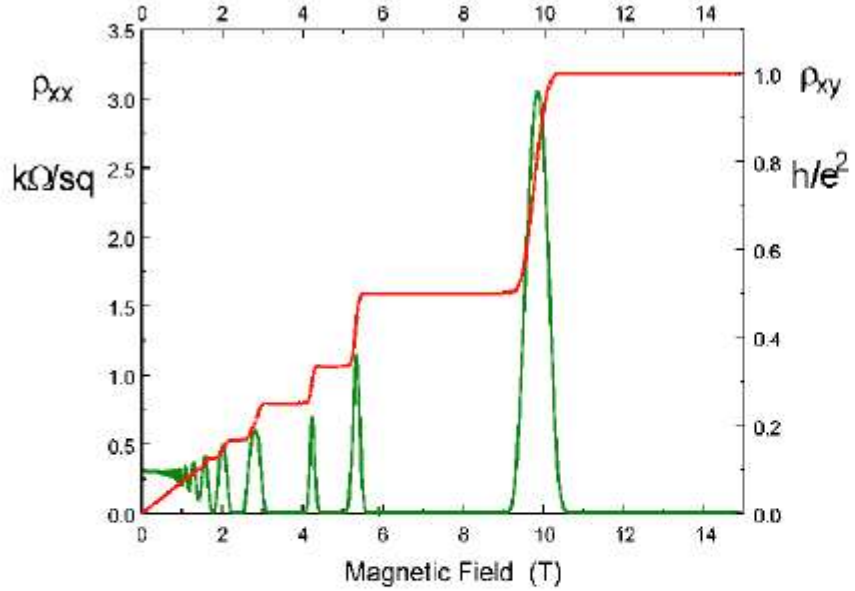

Von Klitzing,1981 (Nobel 1985)

- Quantization: $\rho_{xy} = R_Q / n$ n = integer accurate to 10^{-9} !
- Quantum Resistance: $R_Q = h / e^2 = 25.812\ 807\ \text{k}\Omega$
- Explained by quantum mechanics of electrons in a magnetic field

Kane, Princeton

quantum Hall effect

Quanten-H.E.

Phänomenologisch:

- *Plateaus im Hall-Widerstand*

$$R_H = \frac{1}{\nu}\frac{h}{e^2}, \quad \nu = 1, 2, 3 \ldots$$

- *Longitudinaler Widerstand wird Null:*

$$R_x = 0 \quad \text{für} \quad \nu = 1, 2, 3 \ldots$$

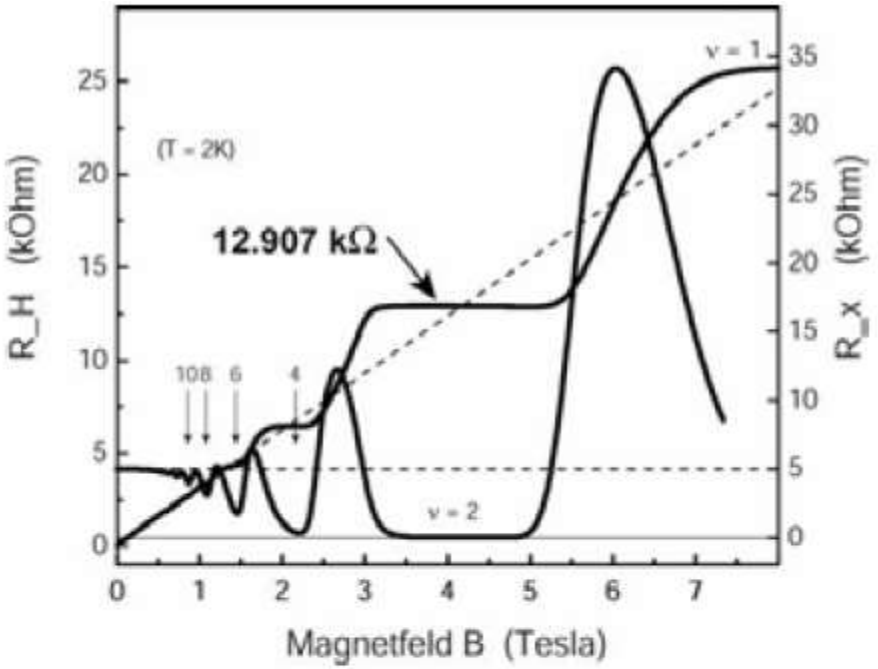

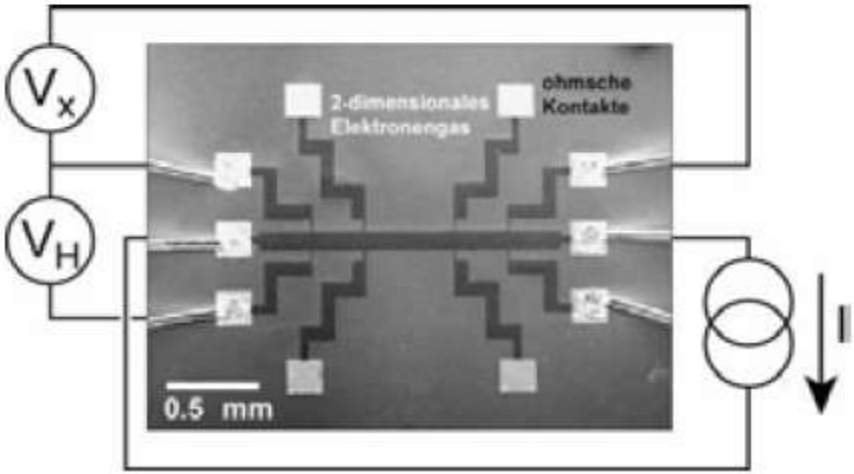

S. Oberholzer

quantum Hall effect

Klassisch:

Zyklotron-Bahnen mit Kreisfrequenz $\omega_C = \frac{eB}{m}$

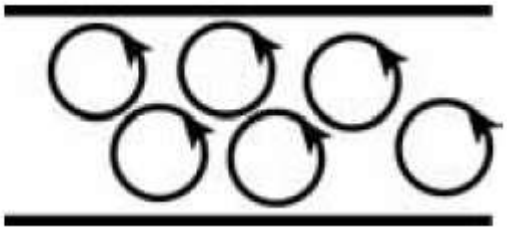

Bohr-Sommerfeld-Quantisierung:

$$2\pi r_C = n\lambda_B = n\left(\frac{h}{mv}\right)$$

$$r_C^2 = \frac{\hbar}{m\omega_C}$$

$$\epsilon_n = \frac{mv^2}{2} = \frac{m\omega_C^2 r_C^2}{2} = n\frac{\hbar\omega_C}{2}$$

Landau-Niveaus (levels) (LL):
(magnetische Sub-bänder)

$$\epsilon_n = \hbar\omega_C(n+1/2)$$ ***n: integer***

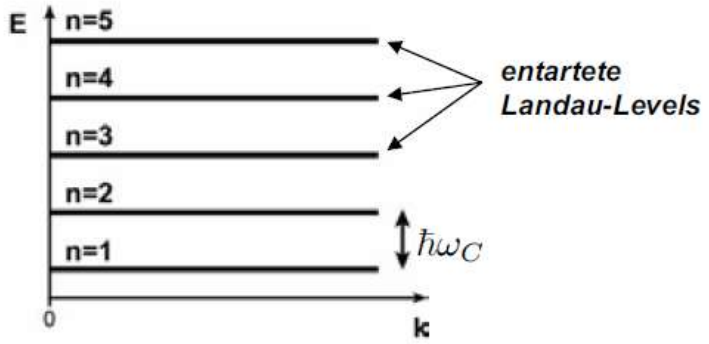

effect becomes relevant once $\omega_C\tau > 1$
i.e.: once electrons perform at least one complete circular motion without collision

critical field $B_c \simeq m_b/e\tau = \mu^{-1}$

for B>Bc, ρ_{xx} *starts to oscillate; high mobilty ⇔ low Bc*
Shubnikov-de Haas

quantum Hall effect

Landau-Quantisierung

Die 2-dimensionale Zustandsdichte geht von einer Stufenform im Nullfeld in eine Sequenz von Peaks über bei genügend starkem Magnetfeld:

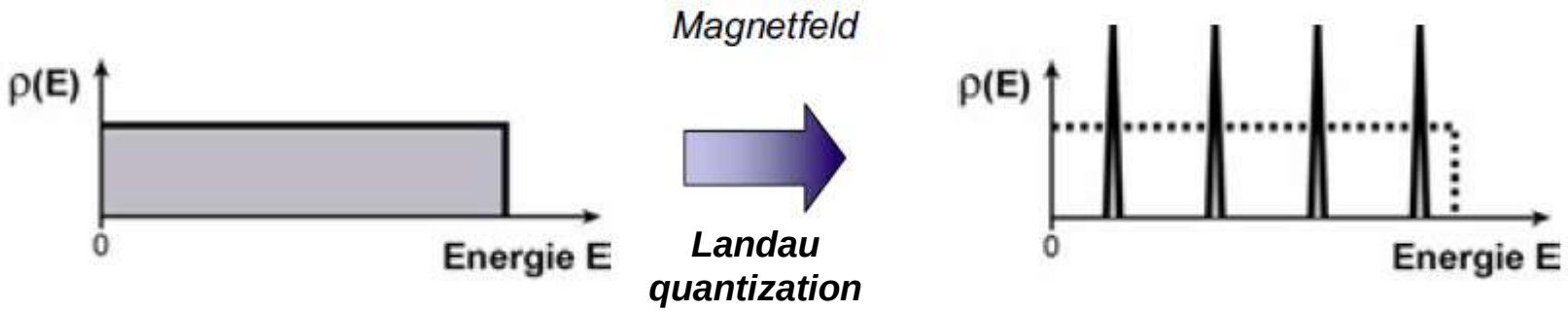

Boltzmann transport eq. ⇨ Einstein relation
conductivity as diffusion eq.

$$\sigma_L = e^2 D \rho(E_F)$$

density of states (DOS) at E_F

$$\rho(E_F)$$

Landau quantisation

DOS:sequence of delta peaks

$$\rho(\epsilon) = \sum_n g_n \delta(\epsilon - \epsilon_n)$$

g_n*: degenracy of level n*

$$\epsilon_n = \hbar\omega_C(n + 1/2)$$

S. Oberholzer

quantum Hall effect

Landau levels for classical particles

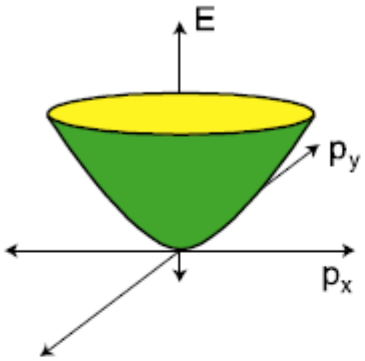

$$E_n = (n + \frac{1}{2})\frac{\hbar eB}{m}$$

for n=0, 1, 2, ...

Landau levels for relativistic particles

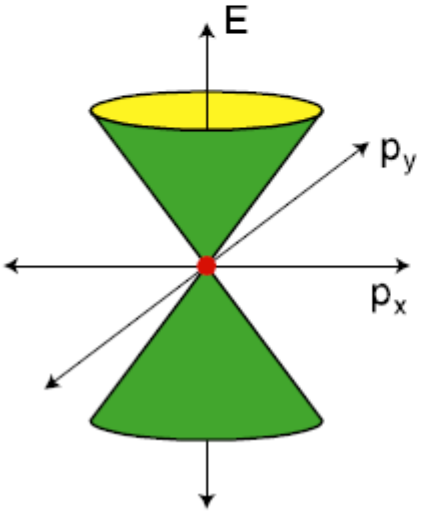

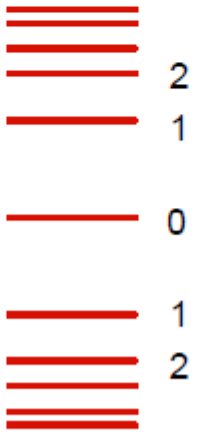

$$E_n = \pm\sqrt{e\hbar v_F^2 Bn}$$

for n=0, 1, 2, ...

Existence of landau level at 0 is deeply related to spin in Dirac Eq.

Kane, Princeton

quantum Hall effect

non-relativistic case

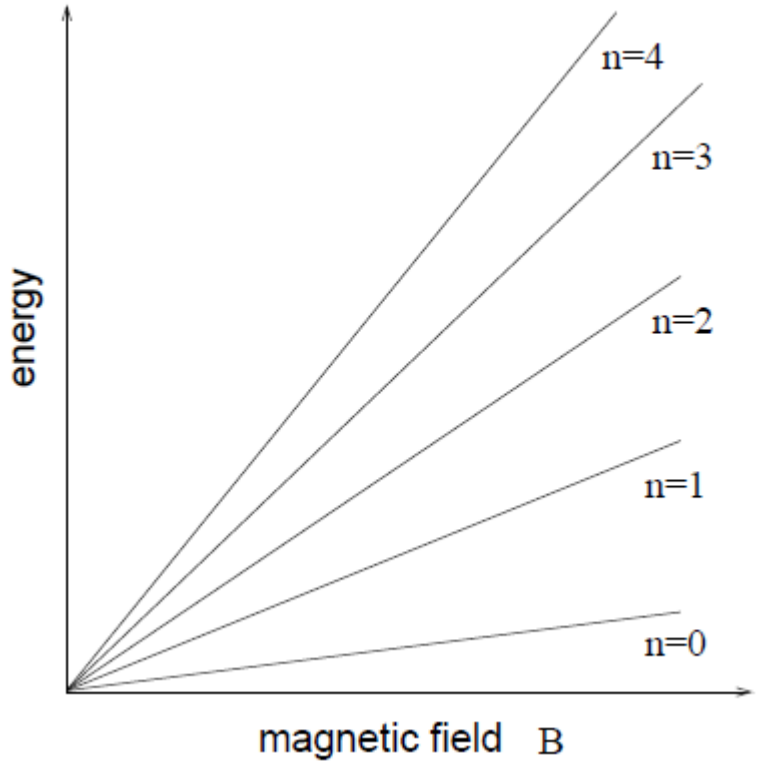

$$\epsilon_n = \hbar\omega_C(n+1/2) \propto B(n+1/2)$$

relativistic case

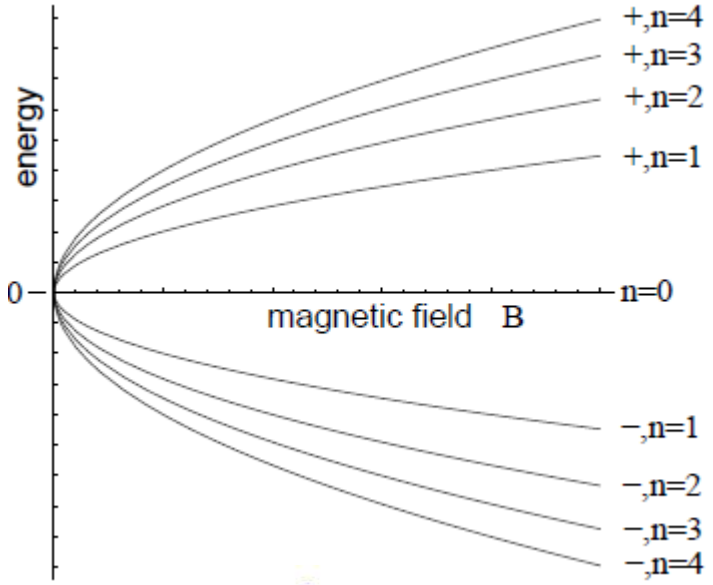

$$\epsilon_{\lambda,n} = \lambda\frac{\hbar v_F}{l_B}\sqrt{2n}$$

$$\hbar v_F/l_B \simeq 36\ \text{meV}\sqrt{B[\text{T}]}$$

magnetic length

$$l_B = \sqrt{\hbar/eB} \simeq 26\ \text{nm}/\sqrt{B[\text{T}]}$$

λ: band index, + (CB) or – (VB)

Goerbig, Cargèse,(2014)

quantum Hall effect in graphene

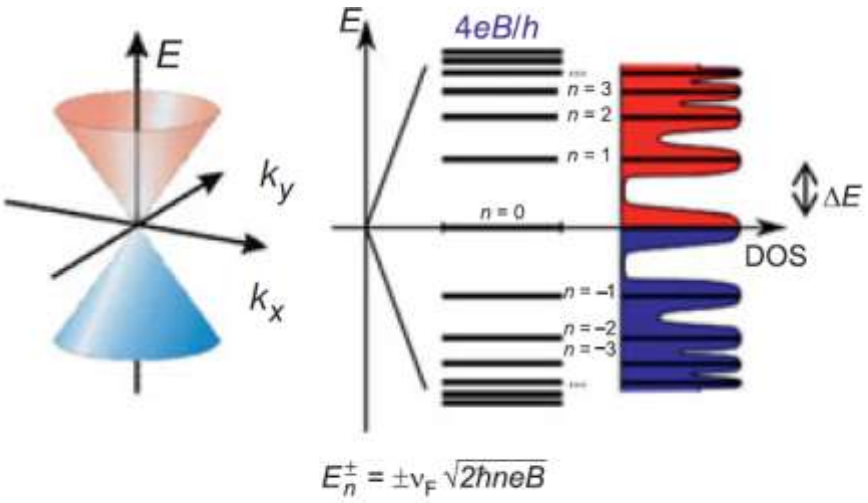

Sequence of Landau levels (LLs), indexed by the integer n, with energies $E^{\pm}_n$ and energy gaps ΔE, formed at high magnetic field

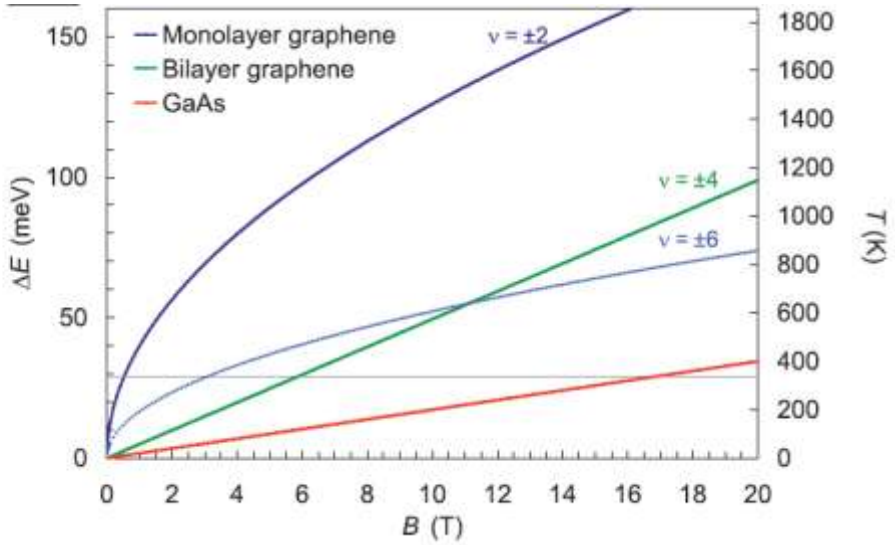

Magnetic-field dependence of the energy gaps (ΔE, left scale) and equivalent temperatures (T, right scale)

NB: The value of the energy gap in monolayer graphene at v = 2 is much larger than that in GaAs at low magnetic field.

Poirier et al., MRS Bulletin, 2012

QHE graphene

2D semiconductor

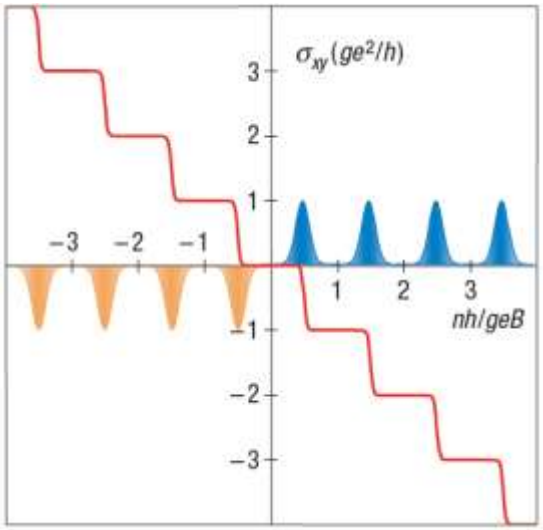

Schematic illustration of the conventional integer QHE found in 2D semiconductor systems

Landau levels as a function of carrier concentrations n are shown in blue and orange for electrons and holes, respectively

Graphene

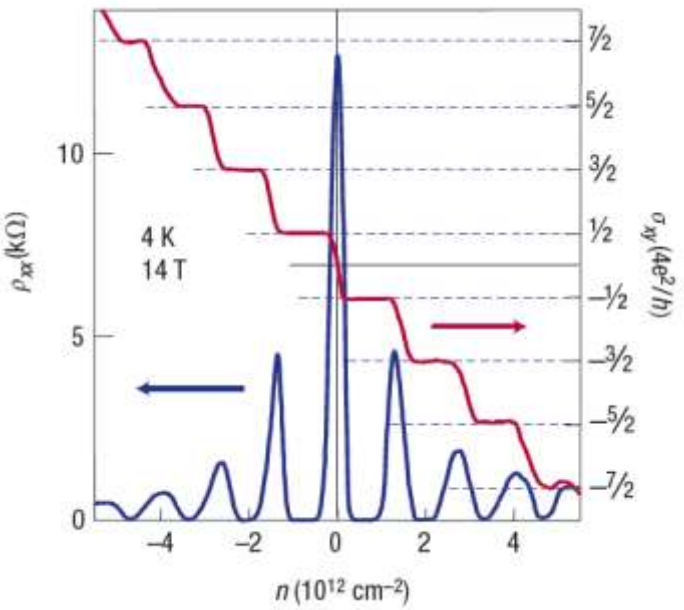

Hallmark of massless Dirac fermions:
QHE plateaux in σ_{xy} at half integers of $4e^2/h$

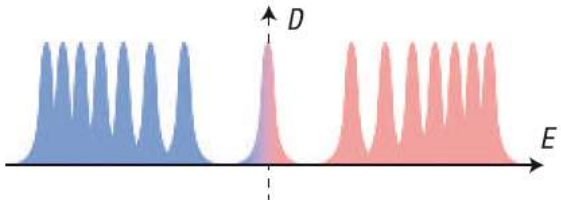

Landau quantization in graphene. The sequence of Landau levels in the density of states *D is described by* $E_N \propto \sqrt{N}$ for massless Dirac fermions in single-layer graphene

Geim, Novoselov, Nat. Phys 2006; Nat. Mat. 2007

QHE graphene

2D semiconductor

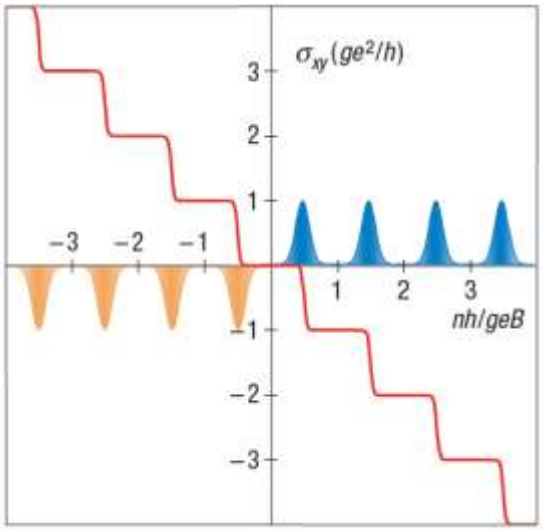

Schematic illustration of the conventional integer QHE found in 2D semiconductor systems

Landau levels as a function of carrier concentrations n are shown in blue and orange for electrons and holes, respectively

Graphene

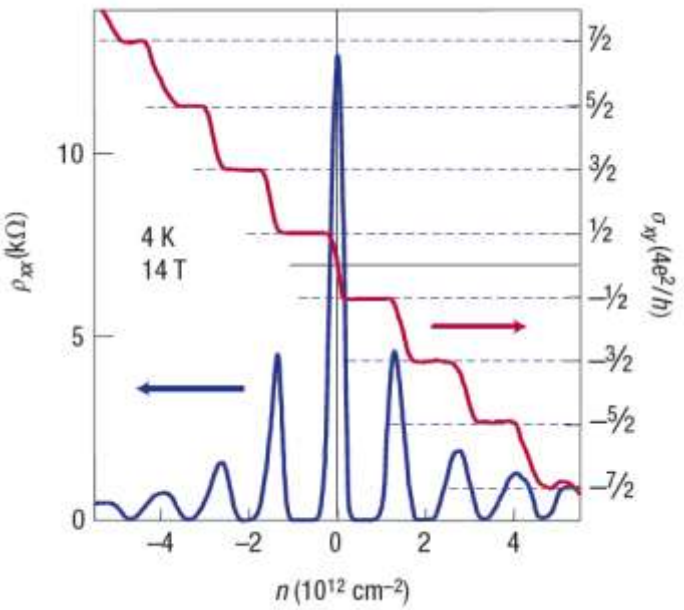

Hallmark of massless Dirac fermions:
QHE plateaux in σ_{xy} at half integers of $4e^2/h$

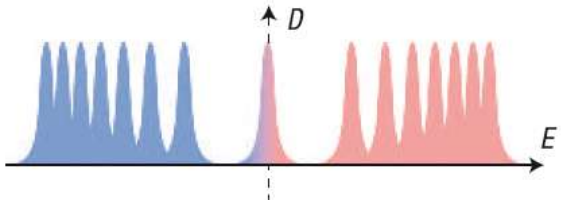

Landau quantization in graphene. The sequence of Landau levels in the density of states *D is described by* $E_N \propto \sqrt{N}$ for massless Dirac fermions in single-layer graphene

Geim, Novoselov, Nat. Phys 2006; Nat. Mat. 2007

QHE graphene

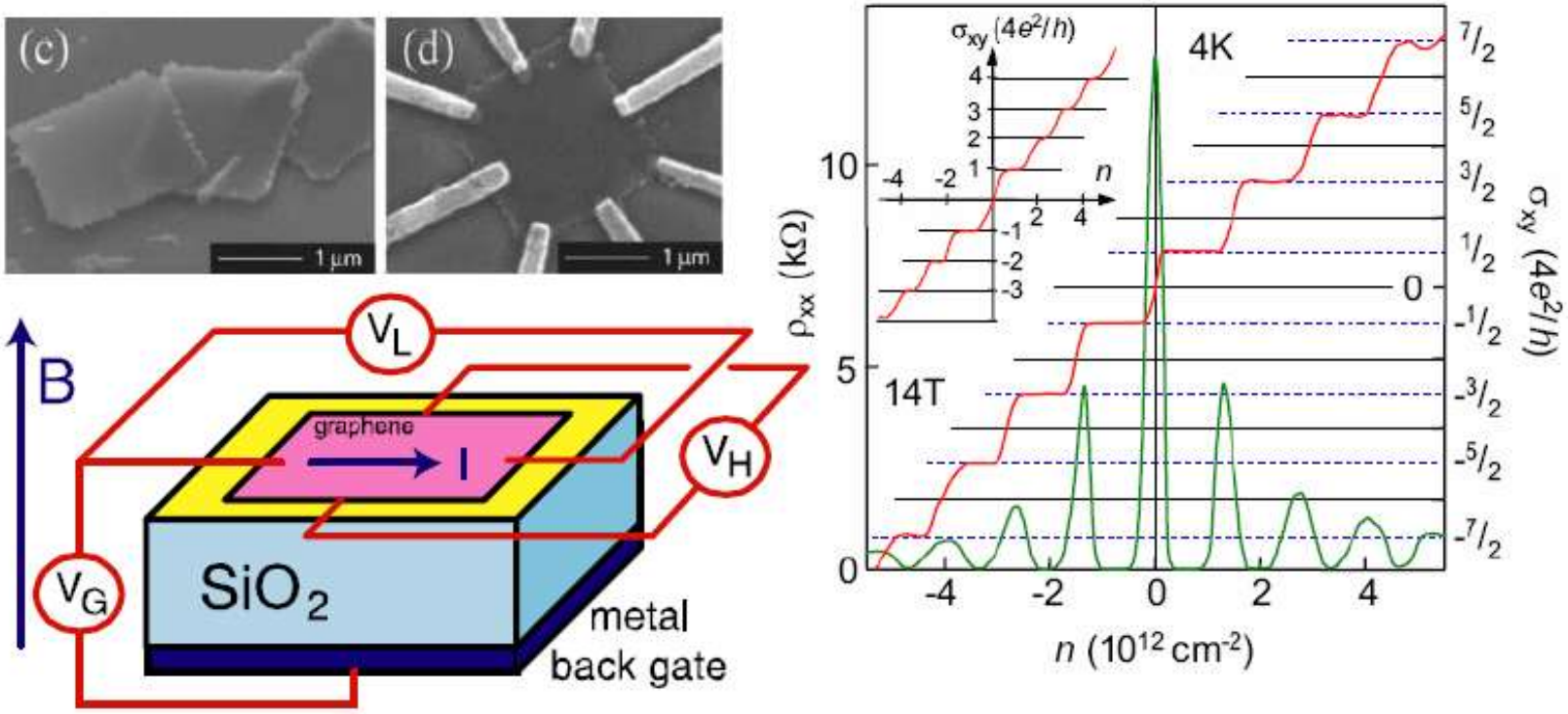

- Gate voltage controls charge n on graphene (parallel plate capacitor)

½ integer quantum hall effect showing massless nature of charge carriers in graphene ($c \Leftrightarrow v_F$)

Geim, Novoselov and Kim, Zhang (2005)

ambipolar behavior
(FET geometry)

Novoselov et al.

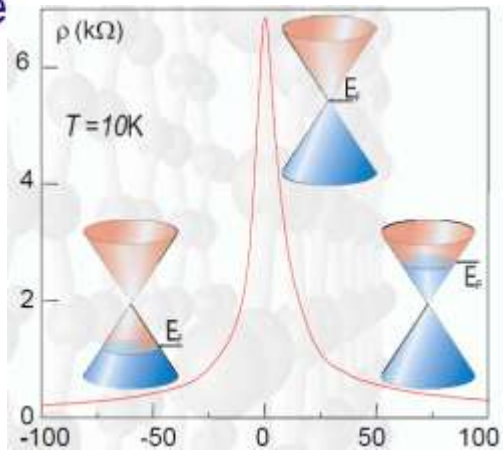

Kane, Princeton